The Thesis Committee for Apostolos Psaros Andriopoulos
Certifies that this is the approved version of the following thesis:

Seismic Retrofit of RC Columns with FRP Composites and Anchorage System

APPROVED BY
SUPERVISING COMMITTEE:

Supervisor:

James Jirsa

Trevor Hrynyk

Seismic Retrofit of RC Columns with FRP Composites and Anchorage System

by

Apostolos Psaros Andriopoulos, M.Eng.

Thesis

Presented to the Faculty of the Graduate School of

The University of Texas at Austin

in Partial Fulfillment

of the Requirements

for the Degree of

Master of Science in Engineering

The University of Texas at Austin

May 2015

Dedication

To my friends, including my brother

“Friendship is a single soul dwelling in two bodies”

Aristotle

Acknowledgements

I would like to express my sincere gratitude to Professor James O. Jirsa for his guidance and insight throughout this study. His valuable comments and constant encouragement have helped me to strengthen my capacity for critical and creative thinking. Separate thanks go to Professor Trevor Hrynyk for the time he spent reviewing this material.

Furthermore, I would like to thank the people that stood by me, especially in the last two years of my life. Special thanks go to my close friends, both in Greece and in the United States, to my parents and also to my brother.

Last but not least, I would like to express my appreciation for the financial support throughout my studies at The University of Texas at Austin to “Andreas Mentzelopoulos Scholarships – University of Patras”.

Abstract

Seismic Retrofit of RC Columns with FRP Composites and Anchorage System

Apostolos Psaros Andriopoulos, MSE

The University of Texas at Austin, 2015

Supervisor: James O. Jirsa

Research on the use of composite materials in structural applications started more than 30 years ago but still remains active. The challenges that accompany those applications are diverse and seem to increase as the variety of applications grows. There are several fiber-reinforced polymer (FRP) systems that have been introduced through the years for strengthening reinforced concrete (RC) structures. Those systems focus on strengthening of slabs, beams and columns.

The present study pertains to seismic retrofit of rectangular RC columns. The typical FRP materials used in structural applications are introduced, as well as, how FRP materials become an integral part of the force-resisting system. In addition, analysis work pertaining to a series of strengthened RC columns was conducted and the results were compared to the experimental data. Moreover, deficiencies of typical material models were highlighted. Design guidelines are discussed and recommendations about current design practices are provided. Finally, research gaps and future research recommendations are identified.

Table of Contents

List of Tables x

List of Figures xi

Chapter 1: Introduction 1

1.1 Composite Materials and FRP 1

1.1.1. Composite Materials 1

1.1.2. Types of FRP 2

1.1.3. Use of FRP materials in strengthening of RC structures 3

1.2 Limitations of FRP composite wraps for RC members 4

1.3 Summary of the Present Study 5

Chapter 2: Mechanics of FRP-Confinement 6

2.1 Summary of the chapter 6

2.2 Confinement in general 6

2.3 Confinement with FRP 8

2.4 Mechanics of FRP-confinement (Part A) 9

2.5 FRP confining pressure 11

2.6 Mechanics of FRP-confinement (Part B) 16

2.7 Confinement Effectiveness Coefficient 17

2.8 Shape factor k_h 18

2.9 Comparison of the shape factors.....20

2.10 Combination of Steel and FRP 21

2.11 Equivalent diameter 25

2.12 Corner Radius 26

2.13 Geometry of the cross-section 31

2.14 Size of the column 35

2.15 Concrete Strength.....36

2.16 Jacket thickness.....40

2.17 FRP ultimate strain 49

2.18 Confinement efficiency.....55

2.19 Minimum amount of FRP to achieve sufficient confinement.....60

Chapter 3: Anchorage System – Current Advances 62

3.1 Summary of the chapter.....62

3.2 Anchorage System: Definition & Importance 62

3.3 Behavior of Anchors.....66

3.4 Effect on Confinement.....67

3.5 Strengthening Poorly-Detailed RC Columns.....71

3.6 Design Guidelines & Recommendations.....75

Chapter 4: Analysis Investigation and Examples 84

4.1 Summary of the chapter 84

4.2 Analysis Tool: OpenSees 84

4.3 Experimental Program By Ozcan Et Al. (2010) 85

4.3.1 Experimental Program Description 85

4.3.2 Concrete 88

4.3.3 FRP-Confined Concrete 90

4.3.4 Response Comparison of computed results and experimental response 94

4.3.5 Type-2 Curves 109

4.3.6 Discussion 114

4.3.7 Example 117

Chapter 5: Summary, Conclusions and Recommendations 124

5.1 Summary and Conclusions 124

5.2 Recommendations 125

5.3 Future Research 125

Bibliography 127

Vita 132

List of Tables

Table 1.1: Mechanical properties for the most common types of fibers (Brigante 2013) . 2

Table 2.1: Different formulas for k_h 20

Table 2.2: Calculation of the equivalent diameter (Csuka and Kollár 2012) 25

Table 2.3: Mean compressive strengths and corresponding f'_{cc}/f'_c (Wang and Wu 2008) 28

Table 2.4: Confinement criteria for acceptable behavior..... 58

Table 2.5: Minimum thickness according to the sufficient confinement criteria 61

Table 3.1: Experimental investigations with FRP jackets and anchorage systems 64

Table 3.2: Summary of lap splice conditions suitable for rehabilitation (Kim 2008) 76

Table 4.1: Specimen Details 87

Table 4.2: Peak loads in experiment (average values) and analysis 94

Table 4.3: Effect of anchor dowels in confinement of specimen S5 119

Table 4.4: Minimum thickness required for specimen S5 123

List of Figures

Figure 1.1: Composite materials 1
Figure 1.2: Typical FRP and mild-steel stress-strain curves (Benzaid and Mesbah 2013) 3
Figure 2.1: Stress-strain curves for Steel-, FRP-confined and unconfined concrete (Harajli 2006) 10
Figure 2.2: Confinement pressure on square columns (Wu et al. 2006) 13
Figure 2.3: Contours of confining pressure for columns with different corner radius ratio (Wu et al. 2006) 15
Figure 2.4: Stresses in an FRP-confined circular section 16
Figure 2.5: Stresses in an FRP-confined rectangular section 16
Figure 2.6: Effective lateral confining pressure for FRP-reinforced cross-sections (Campione and Miraglia 2003) 17
Figure 2.7: Stress-strain curves for FRP-confined concrete specimens with different shapes of the cross-section (Campione and Miraglia 2003) 18
Figure 2.8: Variation of effective confinement area ratio with aspect ratio (Lam and Teng 2003) 19
Figure 2.9: Variation of shape factor with aspect ratio 20
Figure 2.10: a) Entire column confined by FRP, b) core column confined by Steel, c) confined and unconfined portions of a square column. 22
Figure 2.11: Different confined zones of rectangular sections (Montuori et al. 2013) ... 22
Figure 2.12: Axially loaded strengthened RC column (Koksal and Doran 2011) 24
Figure 2.13: Definition of equivalent diameter. Figure by Csuka and Kollár (2012) 26
Figure 2.14: Corner radius variations of the columns and CFRP rupture at r=0 (Wang and Wu 2008) 27

Figure 2.15: Effect of corner radius on confinement (Wang and Wu 2008) 28
Figure 2.16: Variation in effective stress in FRP with r/b (r/b=0.5 indicates circular column) (Campione and Miraglia 2003)..... 29
Figure 2.17: Comparisons between test results and existing confinement models for C30 concrete (f'_c=4.35 ksi) (Wang and Wu 2008)..... 30
Figure 2.18: Comparisons between test results and existing confinement models for C50 concrete (f'_c=7.25 ksi) (Wang and Wu 2008)..... 31
Figure 2.19: Aspect ratios of column (Wu and Wei 2010)..... 32
Figure 2.20: Strength gain of confined concrete versus aspect ratio. (Wu and Wei 2010) 32
Figure 2.21: Ultimate and peak strains versus aspect ratio (Wu and Wei 2010)..... 34
Figure 2.22: Stress concentration factor (Yang et al. 2004) 35
Figure 2.23: Normalized ultimate strength versus (L/D) ratio (Mirmiran et al. 1998).... 36
Figure 2.24: Effect of unconfined strength on concrete confinement efficiency (vertical axis is f'_{cc}/f'_c in all three graphs) (Mandal et al. 2005)..... 38
Figure 2.25: Effect of unconfined strength on peak strains (Mandal et al. 2005) 39
Figure 2.26: Effect of unconfined concrete strength on a) strength enhancement, b) axial strain at peak strength, and c) hoop strain at peak strength (Bisby et al. 2012) 40
Figure 2.27: Effect of jacket's thickness on the strengthening ratio (Maalej et al. 2003)41
Figure 2.28: Example of FRP thickness's influence (Constitutive law by Spoelstra and Monti (1999)). Figure by (Montuori et al. 2013)..... 43
Figure 2.29: Example of FRP thickness's influence (Constitutive law by Montuori et al. (2012)). Figure by Montuori et al. (2013)..... 43

Figure 2.30: Gain in concrete compressive strength versus number of confining layers (Chaallal et al. 2003) 44
Figure 2.31: Relationship between f'_{cc}/f'_c and f_l/f'_c for square columns with cross-section dimension from 4 to 36 in., confined with CFRP (R is the corner radius and B is the cross-section dimension) (Faustino et al. 2014) 45
Figure 2.32: Dilation ratio versus number of CFRP confining layers (Chaallal et al. 2003) 46
Figure 2.33: Transverse strains versus number of CFRP confining layers (Chaallal et al. 2003) 46
Figure 2.34: Gain in compressive strength versus CFRP jacket to column stiffness ratio (Chaallal et al. 2003) 48
Figure 2.35: Gain in ductility versus number of CFRP confining layers (Chaallal et al. 2003) 48
Figure 2.36: FRP strength test methods (Chen et al. 2011) 50
Figure 2.37: Prefabricated steel moulds with various corner radii (Wang and Wu 2008) 50
Figure 2.38: Failure modes of CFRP-confined concrete specimens (Wang and Wu 2008) 51
Figure 2.39: Ultimate strain distribution in CFRP (Wang and Wu 2008) 52
Figure 2.40: FRP strains at peak stress. The solid line denotes the C30 concrete grade (4.35 ksi) and the dashed line denotes the C50 concrete grade (7.21 ksi) (Wang and Wu 2008) 53
Figure 2.41: FRP measured lateral strain versus modified confinement ratio for all test results (Mirmiran et al. 1998) 54

Figure 2.42: FRP lateral strain predictions and measure test results versus FRP volumetric ratio for 25 MPa (3.625 ksi) concrete (Hassan and Chaallal 2007) 55
Figure 2.43: Typical stress-strain curves of FRP-confined concrete (Hu 2013) 56
Figure 2.44: Ultimate strength ratio versus (2R/D)(f_l/f'_c) ratio (Mirmiran et al. 1998) .. 57
Figure 2.45: Performance of the proposed criterion (Hu 2013) 59
Figure 2.46 Performance of the proposed model with results reported in 14 test programs (Hu 2013) 60
Figure 3.1: a) CFRP anchor, b) GFRP anchor, c) CFRP jackets with CFRP anchors 63
Figure 3.2: Preparation of anchors (Zhang et al. 2012) 65
Figure 3.3: Installation of anchors (Zhang and Smith 2012) 65
Figure 3.4: Typical adhesive anchor failure modes 66
Figure 3.5: Effective confined area without and with anchors 67
Figure 3.6: Effective confined area without and with anchors 68
Figure 3.7: FRP strain distribution along column height (Galal et al. 2005) 69
Figure 3.8: Energy dissipation of cyclically loaded columns (Energy dissipation versus cumulative drift ratio) (Wu et al. 2008) 70
Figure 3.9: Confinement effect of CFRP jackets and CFRP anchors (Kim 2008) 72
Figure 3.10: Layout of the CFRP jackets and CFRP anchors, specimen 6-C-R20-C (Kim 2008) 73
Figure 3.11: Envelope of cyclic response, specimen 5-C-R20-C (Kim 2008) 74
Figure 3.12: Envelope of cyclic response, specimens 5-C-R20-C & 6-C-R20-C (Kim 2008) 75
Figure 3.13: Shear friction mechanism for a typical specimen (Kim 2008) 79

Figure 3.14: Suggested spacing between CFRP anchor and lap spliced bars (Kim 2008) 81
Figure 3.15: Component force vs deformation curves (FEMA 356, 2000) 82
Figure 3.16: Type-2 curves for different rehabilitation methods (Kim 2008) 83
Figure 4.1: Specimen Details (Ozcan et al. 2010) 86
Figure 4.2: (a) CFRP anchorage configurations for 8-pinned and (b) 16-pinned type, (c) CFRP anchor dowel detailing (Ozcan et al. 2010) 87
Figure 4.3: Displacement-controlled loading protocol 88
Figure 4.4: Constitutive law for unconfined concrete for all specimens 89
Figure 4.5: Constitutive law for steel-confined concrete for all specimens 90
Figure 4.6: Constitutive law for CFRP-confined concrete for all specimens 91
Figure 4.7: Comparison between FRP- and steel-confined concrete 93
Figure 4.8: Experimental response comparison for specimens S1, S2 & S5 95
Figure 4.9: Experimental normalized response comparison for specimens S1, S2 & S5 95
Figure 4.10: Experimental response comparison for specimens S1, S3 & S4 96
Figure 4.11: Experimental normalized response comparison for specimens S1, S3 & S4 97
Figure 4.12: Experimental response comparison for specimens S1, S3 & S5 97
Figure 4.13: Experimental normalized response comparison for specimens S1, S3 & S5 98
Figure 4.14: Experimental response comparison for specimens S1, S2 & S3 98
Figure 4.15: Experimental normalized response comparison for specimens S1, S2 & S3 99
Figure 4.16: Analytical response comparison for specimens S1, S2 & S5 99

Figure 4.17: Analytical normalized response comparison for specimens S1, S2 & S5. 100
Figure 4.18: Analytical response comparison for specimens S1, S3 & S4. 100
Figure 4.19: Analytical normalized response comparison for specimens S1, S3 & S4. 101
Figure 4.20: Analytical response comparison for specimens S1, S3 & S5. 101
Figure 4.21: Analytical normalized response comparison for specimens S1, S3 & S5. 102
Figure 4.22: Analytical response comparison for specimens S1, S2 & S3. 102
Figure 4.23: Analytical normalized response comparison for specimens S1, S2 & S3. 103
Figure 4.24: Test-Analysis response comparison for specimen S1 . 104
Figure 4.25: Test-Analysis normalized response comparison for specimen S1 . 104
Figure 4.26: Test-Analysis response comparison for specimen S2 . 105
Figure 4.27: Test-Analysis normalized response comparison for specimen S2 . 105
Figure 4.28: Test-Analysis response comparison for specimen S3 . 106
Figure 4.29: Test-Analysis normalized response comparison for specimen S3 . 106
Figure 4.30: Test-Analysis response comparison for specimen S4 . 107
Figure 4.31: Test-Analysis normalized response comparison for specimen S4 . 108
Figure 4.32: Test-Analysis response comparison for specimen S5 . 108
Figure 4.33: Test-Analysis normalized response comparison for specimen S5 . 109
Figure 4.34: Type-2 curve for specimen S1 (Reference specimen). 110
Figure 4.35: Type-2 curve for specimen S2 (16-pinned). 111
Figure 4.36: Type-2 curve for specimen S3 (8-pinned). 112
Figure 4.37: Type-2 curve for specimen S3 (No-pinned). 113
Figure 4.38: Type-2 curve for specimen S5 (16-pinned). 113
Figure 4.39: Type-2 curves for the retrofitted columns . 114
Figure 4.40: Test-Analysis normalized response comparison for specimen S2 . 116

Figure 4.41: Arching action in square column.....117
Figure 4.42: Concrete arching action for 16-pinned type anchor configuration.....119
Figure 4.43: Experimental normalized response comparison for specimens S2 & S4..120
Figure 4.44: Constitutive law for FRP- and steel-confined concrete of specimen S5...121
Figure 4.45: Analytical normalized response for S5 with and without anchors.....122

Chapter 1: Introduction

1.1 Composite Materials and FRP

1.1.1. Composite Materials

Often some of the greatest advances in science come from the study and use of what already exists in abundance in Nature. A composite material is defined as a system made out of two or more materials (phases) with different properties. Composite materials are an evolution of material science since they combine the best mechanical properties of the materials. The composites used for structural purposes are usually made out of continuous fibers that build the frame of the material and convey stiffness and resistance in the direction of the fibers.

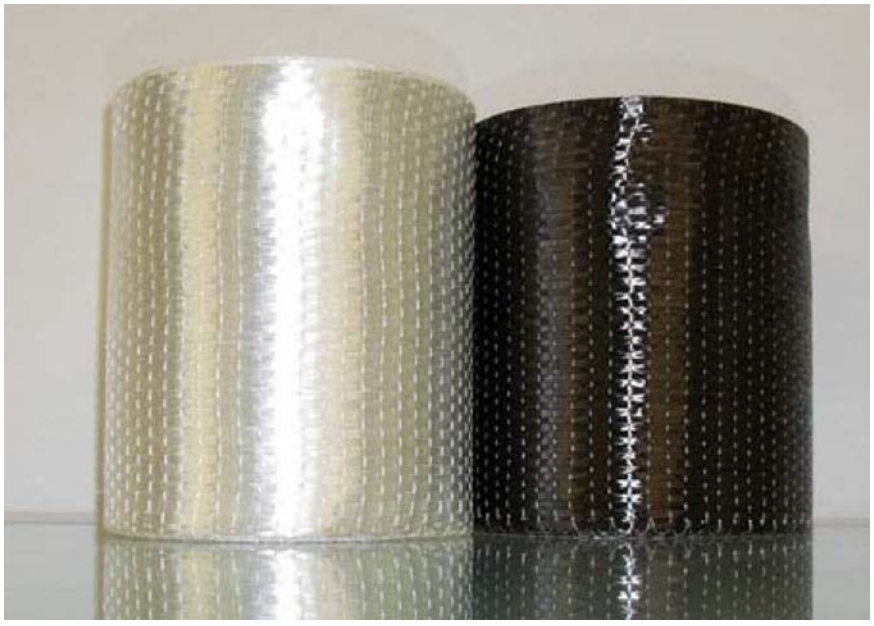

Figure 1.1: Composite materials

1.1.2. Types of FRP

Fiber reinforced polymer (FRP) composites are made of three necessary components: fibers, polymers and additives (such as plasticizers, heat stabilizers and others). The layers of FRP composite materials are called *laminates* and can be oriented in different angles depending on the scope.

The types of FRP used for structural purposes can be sorted according to the type of fibers used. The most popular fibers used in composites in structures are glass and carbon fibers. Table 1.1 summarizes some of the important mechanical properties of the basic types of fibers.

Table 1.1: Mechanical properties for the most common types of fibers (Brigante 2013)

	Properties				
Fiber	Stiffness E (DaN/mm^2)	Strength σ_{max} (DaN/mm^2)	Density δ (g/cm^3)	Specific stiffness (E/δ) (10^8 mm)	Specific strength (σ/δ) (10^6 mm)
E-glass	7,000	300	2.5	28	120–160
S-glass	8,000	450	2.5	32	180
Carbon HM	38,500	200	1.9	202	105
Carbon HS	26,000	250	1.9	136	131
Carbon M	20,000	250	1.8	111	138
Boron	42,000	240	2.4	175	139
Aramid	12,000	220	1.5	80	88
Steel	21,000	250	7.8	26	32
Tungsten	35,000	250	19	18	13
Beryllium	31,500	130	1.8	175	72

As seen in Table 1.1 glass fibers (GFRP) have higher strength compared to carbon fibers (CFRP) but CFRPs are considerably stiffer (higher Young's modulus) than GFRPs. These are significant properties that are always taken into account during retrofit design. In addition, the cost of material depends on the type of fiber used, the weight per area and the distribution of the fibers in the plane (uniaxial, biaxial, or multi-axial). GFRP is the

most economic material, while CFRP seems to be the most expensive. The cost of CFRP strongly depends on its elastic modulus. For example, to double the elastic modulus of a CFRP, the cost requirements may become three or four times greater (Brigante 2013). A typical stress-strain curve for CFRP and GFRP materials is compared with a typical steel response in Figure 1.2. Note that strength of GFRP is usually higher than strength of CFRP, even though this information is not illustrated in Figure 1.2.

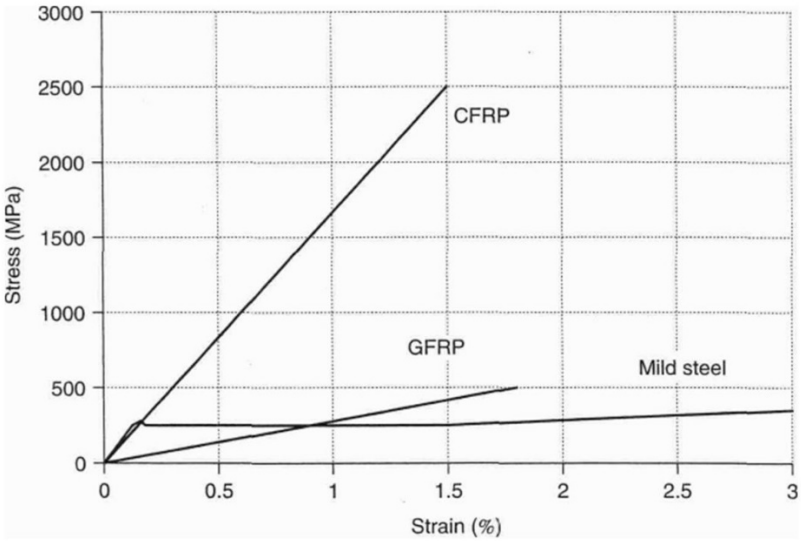

Figure 1.2: Typical FRP and mild-steel stress-strain curves (Benzaid and Mesbah 2013)

1.1.3. Use of FRP materials in strengthening of RC structures

In steel-reinforced concrete structures, concrete and steel cooperate in a manner such that the performance benefits of one material compensate for the limitations of the other. This process is explained in detail in Chapter 2. Externally-bonded FRP wraps, as summarized by GangaRao et al. (2006), act as reinforcement in tension, provide protection to the concrete surface and the reinforcing steel from chemical and moisture ingress, and

enhance the flexural strength and stiffness of the structural element. For these reasons FRP-strengthening of reinforced concrete members in seismic areas can be effective in achieving one or more of the goals listed below (Brigante 2013):

- Enhance flexural capacity or combined bending and axial capacity,
- Increase shear capacity,
- Enhance the ductility of plastic hinges,
- Prevent buckling of longitudinal bars,
- Increase the tensile capacity of the panels of beam-column joints.

In the present study, the effectiveness of FRP in retrofitting reinforced concrete columns that are vulnerable to seismic damage will be investigated.

1.2 LIMITATIONS OF FRP COMPOSITE WRAPS FOR RC MEMBERS

The application of FRP composite wrap technology has been found to be extremely useful in retrofitting existing structural members but some limitations exist. In fact, there are cases where the use of FRP materials is restricted if the application has not been verified through tests or successful previous applications. There are several limitations that usually cause problems, such as the uncertainties about the long-term performance of FRPs and the concerns about their fire resistance. In addition, there are other more specific concerns, such as the shear-lag phenomenon when the number of fiber composite wrap layers is increased. However, the findings in this present study are in light of the limited knowledge of the material properties and the application procedures.

Several questions have to be answered during the design of an FRP-retrofit, such as what the thickness of the FRP jacket should be, how the concrete column should be prepared to be able to accommodate the presence of the jacket, or how the behavior of the

retrofitted column could be assessed. Deficiencies of current modeling techniques are highlighted and examples and methods to accommodate such deficiencies are discussed.

1.3 SUMMARY OF THE PRESENT STUDY

Chapter 2 serves as a review of the mechanics of retrofitting reinforced concrete columns with FRP. The basic principles of the FRP-confinement are explained, as they are important in understanding the fundamental behavior of the system. The main parameters that affect the behavior of the retrofitted column and how retrofit design influences behavior are summarized. For each parameter presented there is a review of the experimental studies found in the literature that relate to the findings.

In Chapter 3, anchorage systems and their impact on retrofit procedures are introduced. There is a quick review of positive effect of anchors on confinement. The findings of Kim (2008) related to confinement for reinforcement of splices are discussed and recommendations on how the findings apply to design are presented.

In Chapter 4, the experimental study of Ozcan et al. (2010) is presented and an analytical method to predict the behavior of FRP-retrofitted columns is illustrated. The experimental and analytical results are discussed and compared. In addition, the deficiencies of current stress-strain models are highlighted with an illustrative example. Finally, some of the findings of Chapter 2 and Chapter 3 are incorporated in the example of Chapter 4.

In Chapter 5, the findings of the study are summarized. Current advances related to FRP-retrofit of reinforced concrete columns are discussed and recommendations for future research are presented.

Chapter 2: Mechanics of FRP-Confinement

2.1 Summary of the chapter

The purpose of this chapter is to introduce and explain the mechanics of confinement using FRP jackets. At the beginning, there is a review of the widely known confinement theory of concrete with transverse steel reinforcement and the fundamental principles that govern the confinement of circular cross-sections with FRP jackets are described. In addition, the clear difference between confinement in a circular section and in a rectangular section is stated, and an approximate method, which is often used in the research community, for modeling the confinement in a rectangular section is introduced.

Researchers all over the world have tried to explain the behavior of the confined rectangular columns and have proposed relationships and parameters to describe the behavior; parameters that can be implemented in conventional stress-strain models. Due to the fact that the aforementioned approximate method is not the most accurate, but is convenient for design purposes, a complete review of factors that affect the behavior of the retrofitted rectangular column is done. There has not been any other review in the literature that accounts for all the factors that affect the behavior and also compares the opinions of a number of researchers.

An introduction to the quantification of confinement is proposed. Factors and parameters that affect behavior, the expressions provided by the researchers, and the confinement efficiency are fundamental topics that are discussed in detail. Lastly, further knowledge gaps that future research should fill are addressed throughout the chapter.

2.2 Confinement in general

Even though there are significant differences between confinement provided by steel hoops and stirrups and by FRP jackets, there are some core principles that one should

always keep in mind while researching the behavior of FRP-confined concrete. For this reason, this section serves as an introduction to the confinement mechanism that will be described later in this chapter. A complete summary of the behavior of confined concrete has been presented by Li (2004) and will be outlined next.

In general confining pressure can be provided to the concrete by transverse reinforcement in the form of spirals, circular hoops or ties. When a column is subjected to pure axial compression or both axial compression and bending moment, initially the longitudinal strains, and hence the transverse strains generated by the Poisson's effect in the core concrete are small. The transverse reinforcement is barely stressed and the lateral pressure is negligible. Consequently, the concrete behaves as unconfined concrete. At higher compressive strains the concrete will attempt to expand in the radial direction due to progressive internal micro-cracking. For the confined core concrete such lateral expansion is reduced as a result of restraint provided by the transverse reinforcement which exerts lateral passive confining pressure to the core. Thus, at this stage the core concrete is no longer loaded in a uniaxial manner, but is under a triaxial state of stress. Therefore the tendency of concrete to dilate after cracking and the radial stiffness of the transverse reinforcement to restrain concrete dilation, are two important factors affecting concrete confinement. It is widely accepted that this mechanism can enhance the axial compressive strength of the core concrete and typically results in ductile behavior. In contrast to the core, cover concrete will spall as only the core concrete is restrained from lateral expansion and the cover concrete is not.

It has been found that circular hoops and spirals can confine concrete much more effectively than square or rectangular ties because under transverse strains the circular hoops are placed in hoop tension and can apply a continuous circumferential confining

pressure, while ties are mainly effective in confining concrete at the corners of the ties. The sides of ties have a tendency to bend outwards under high lateral strains and as a consequence, rectilinear ties exert a non-uniform confining pressure to the concrete that depends on the tie bending stiffness. This is an important topic that will be covered in following sections in more detail. Finally, there are some fundamental principles that govern the concrete confinement by transverse steel and also apply to confinement by FRP jackets:

- Strength and ductility of confined concrete depend on the volumetric ratio of transverse reinforcement, which means that a higher transverse reinforcement ratio results in a higher transverse confining pressure.
- In rectangular columns confined by rectilinear ties, the area of the effectively confined concrete and the distribution of the pressure provided, have a noticeable effect on the effectiveness of confinement.
- The constitutive law of the lateral reinforcement defines the way the confining pressure will be applied to the concrete. Using a material like steel that yields at a certain point, no additional restraint can be expected as the hoop strain increases after lateral steel reaches the yield plateau, while the situation is different when FRP is used.

2.3 CONFINEMENT WITH FRP

Currently, FRP jacketing has appeared as a popular retrofitting technique to provide confinement to existing columns. An advantage of it compared to common retrofitting systems like reinforced concrete or steel jacketing, is that with FRP jackets the confining layer is very thin, flexible, and can be easily used for any column shape.

Furthermore, the FRP jackets can be painted to produce the desired aesthetic finish, owing to the fact that they are corrosion resistant.

Despite the fact that steel and FRP confinement mechanisms are similar in some aspects, there are also some major differences that must be pointed out. For steel-confined concrete, the confinement of concrete core begins at relatively low axial load levels due to the high modulus of steel. Also, the confining pressure remains constant when steel is in its yield plateau and the concrete experiences a slight softening before it reaches the maximum strength, after which it follows a gradual post-peak descending branch. However, for most FRP-confined concrete, the FRP provides confining pressure under larger axial strains, largely due to its low modulus. However, this is not the case for some carbon fiber reinforced polymers that have a high modulus of elasticity (up to 84,000 ksi). Lastly, FRP-confined concrete is not sensitive to small lateral expansion, but when the lateral strain increases, the FRP jacket will be activated and apply continuously increasing lateral confining pressure to the concrete until the fibers fracture (Li 2004).

2.4 MECHANICS OF FRP-CONFINEMENT (PART A)

Understanding the mechanics of confinement is the most important task prior to any modeling attempt. The confinement mechanism of FRP-confined concrete is based on a material that would provide enough tensile strength in the hoop direction to restrain the increase in the transverse strain under compression loading to the column. In fact, that strain is produced by loading a concrete column in the axial direction, which results in a radial concrete expansion due to Poisson's effect. The confining material must be selected and designed to provide a more ductile column (Figure 2.1) and to meet serviceability requirements.

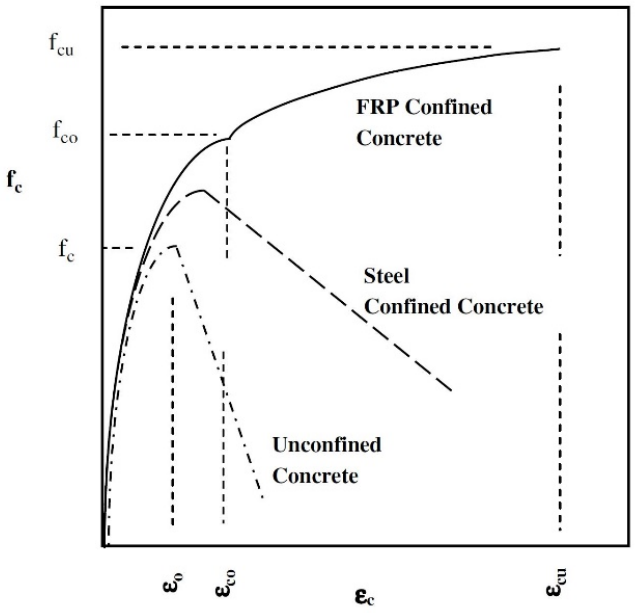

Figure 2.1: Stress-strain curves for Steel-, FRP-confined and unconfined concrete (Harajli 2006)

As described before for steel confinement, under low levels of longitudinal strain, the concrete behaves nearly elastically and the transverse strain is related proportionally to the longitudinal strain by Poisson's ratio. When the transverse strain is very small, the confinement action does not affect its behavior. As the axial load increases and the value of longitudinal stress reaches 75% to 80% of f'_c, cracks start to form which result in large increases in the transverse strain. This necessitates the use of confining materials in the form of an external jacket capable of restraining the dilation of the core concrete.

If the behavior described above for steel confined concrete based on the mechanics of confinement that presented in the previous section, then the question that arises is why FRP confinement should be treated differently? As explained before, the Young's modulus of FRP (depending on its type) is different than the one of steel and the

confinement is activated earlier or later (usually later than steel). In addition FRP does not yield but is elastic, which completely changes the way the confinement is applied to the concrete. More specifically, steel yields at some point and in effect stops providing confinement to the concrete as effectively as before. On the other hand, FRP wraps provide confinement until their rupture.

According to the explanation by Youssef (2003) on the mechanism of confinement by FRP jackets, the first assumption that has to be made is the deformation compatibility. In compliance with that, the lateral (radial) strain of the confined specimens is equal to the strain in the FRP jacket. Secondly, the confinement provided by an external jacket, regardless of its type, is of the passive type, which means that confining pressure is developed only after the surrounding member undergoes hoop elongation (Mirmiran and Shahawy 1997). By wrapping the concrete with an external continuous FRP jacket, the fibers in the hoop direction, resist the transverse expansion of the concrete providing a confining pressure. At low levels of longitudinal stress, the transverse strains are so small that the FRP jacket induces little confinement, if any. However at higher longitudinal stress levels, the increase in transverse strains activates the FRP jacket and the confining pressure becomes significant. The general confining pressure creates a tri-axial state of stress in the concrete, similar to the one acquired using transverse steel reinforcement.

2.5 FRP CONFINING PRESSURE

The fundamental problem in rectangular jacketing is the lack of understanding of the mechanism of confinement. As described before, the lateral confining stress f_j, is applied to the concrete when the loading to the column is such that the concrete starts to dilate and expand laterally. The geometric shape of the column was shown by several researchers to provide large variation in the amount of confinement achieved and thus the

confining pressure depends on the geometry of the cross-section. In fact, by confining a circular member, the FRP jacket provides a uniform confining stress around the perimeter resulting in a great improvement in member's behavior under loading. However, confining square or rectangular members tends to produce confining stress concentrated around the corners of such members. The scope of this section is to give a greater insight into this matter.

The confinement pressure produced by a rectangular jacket is not uniform across the cross-section and this non-uniformity of the confinement stress significantly reduces the confinement effect and greatly complicates the problem. To gain a fundamental insight into the confinement provided by a square jacket, Wu et al. (2006) considered the idealized experiment shown in Figure 2.2. It is based on the assumption that the jacket is made of a membrane material that can only provide resistance in tension (i.e. no flexural resistance) and that the material of the concrete column is linear elastic. For a column cross-section without a jacket and subjected to a uniform axial strain ε, the transverse concrete strain in both transverse orthogonal directions will have a constant value of v times ε, where ν is the Poisson's ratio (represented by the symbol μ in Figure 2.2) and ε is the axial compressive strain (taken as positive) of the column. Because of the uniform transverse strain across the cross-section, the cross-sectional shape of the dilated column must be exactly the same as the original shape but with an increased side length of $(1+v \cdot \varepsilon)b$.

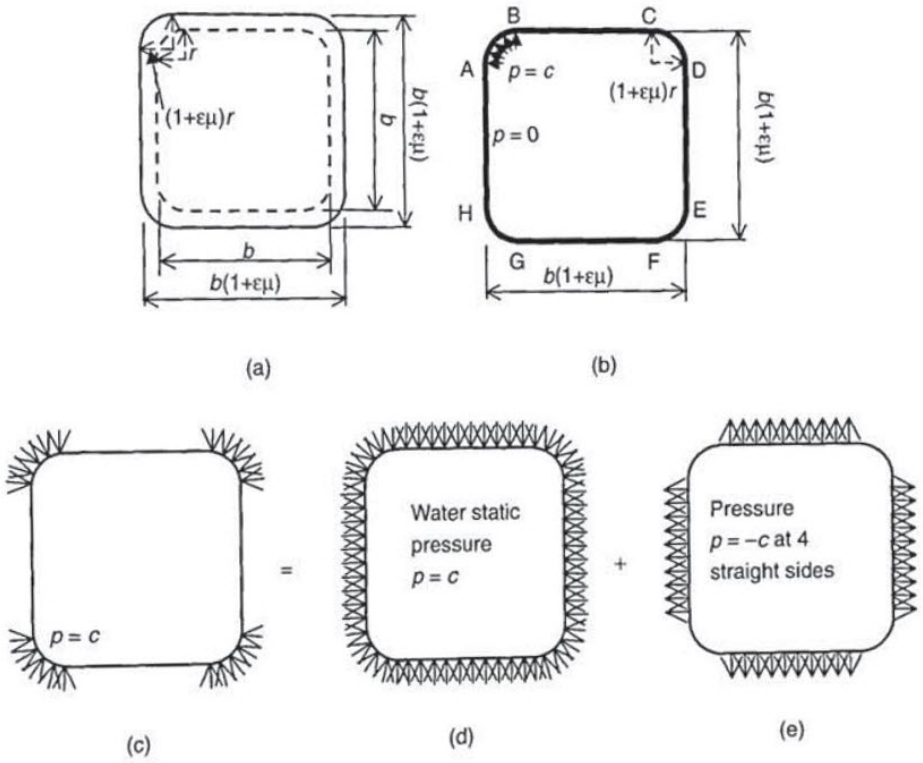

Figure 2.2: Confinement pressure on square columns (Wu et al. 2006)

As noted in the paper, for a membrane jacket to maintain the original shape, the only possible pressure distribution is a uniform radial pressure *p* in the four corners and a zero pressure at the four straight sides. Based on the action and reaction law, the confinement pressure exerted on the concrete column must be equal and opposite of that. Next, they introduce a parallelism of the confinement pressure on the column that is visualized as the superposition of a water static pressure on the whole surface of the column as in Figure 2.2d and a uniform negative pressure $p=-c$ at the four straight sides. The water static pressure in Figure 2.2d provides a uniform confinement that can only produce a uniform transverse stress field without variation across the cross section. Therefore, the variation of transverse stress field induced by the external pressure in

Figure 2.2 represents the variation of the superimposed transverse stress field of Figure 2.2d and Figure 2.2e, and hence the equivalent case of Figure 2.2c. In other words, the variation of transverse stress shown in Figure 2.2c portrays the confinement stress field distribution caused by a rectilinear jacket.

In addition, Wu et al. (2006) performed a linear elastic finite element analysis and found that the magnitude of the confining pressure will not change the shape and variation of the stress field distributions, but will only change the magnitudes of the transverse stresses. Apart from that, the constant negative pressure at the four straight sides in Figure 2.2e produces transverse stress distributions (contour of confinement pressure) as shown in Figure 2.3. It can be seen that the distribution approaches a uniform field when the corner radius approaches zero. This can be also mathematically explained: when the corner radius approaches zero, the water static pressure of Figure 2.2d and the negative pressure of Figure 2.2e cancel out, resulting in a zero external pressure and zero confinement stress in the cross-section as in Figure 2.3a. Apparently, this is why Mirmiran et al. (1998) recommended that a sharp corner (zero corner radius) offers no confinement, although some other researchers do not agree on that. In contrast, when the straight sides approach zero a circular section is obtained and a uniform confinement field is achieved as in Figure 2.3h.

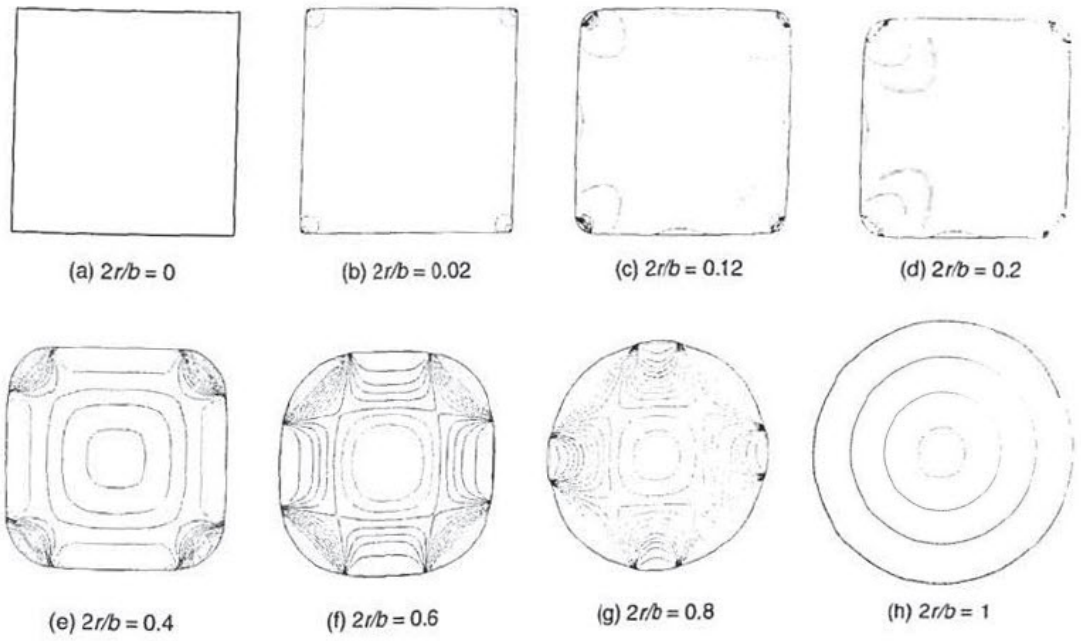

Figure 2.3: Contours of confining pressure for columns with different corner radius ratio (Wu et al. 2006)

Both the theoretical analysis depicted in Figure 2.2 and the numerical results in Figure 2.3 show that the proportion of the well confined zone relative to the whole cross-sectional area is decided by the ratio of corner radius to the half width of the column, i.e. r/0.5b. Thus, when this parameter equals zero a sharp corner is obtained and no confinement is provided; when it equals one, a circular section is obtained, which consequently gives the most effective confinement.

2.6 MECHANICS OF FRP-CONFINEMENT (PART B)

Circular cross-section

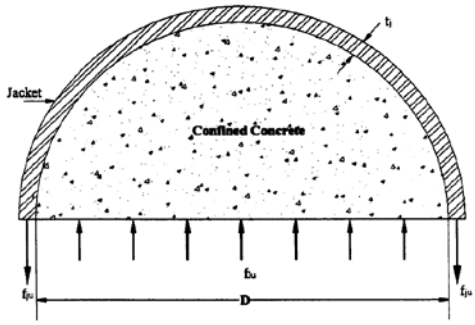

Figure 2.4: Stresses in an FRP-confined circular section

As shown above in the free body diagram of the circular cross-section of a plain concrete member confined with an FRP jacket, the pressure acting on the concrete is caused by the jacket. It can be shown that the confining stress due to the FRP jacket is:

$f_l = \frac{1}{2}\rho_j f_j$ (2.1), where $\rho_j = \frac{4t_j}{D}$

The effective lateral confining stress is $f'_l = k_f f_l$ (2.2), where k_f is the confinement effectiveness coefficient. Figure 2.6 illustrates stress distribution according to the cross-sectional shape.

Rectangular cross-section

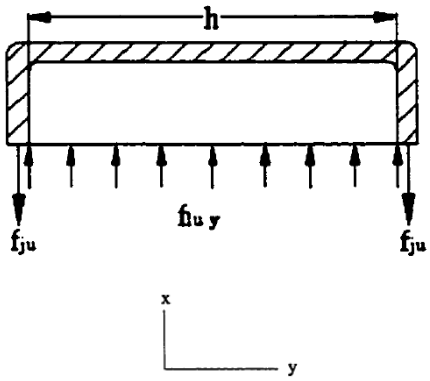

Figure 2.5: Stresses in an FRP-confined rectangular section

The pressure acting on the concrete in the y direction is

$f_{l,y} = \frac{2f_j t_j}{h}$ (2.3)

and similarly the confining stress in the x direction is

$f_{l,x} = \frac{2f_j t_j}{b}$ (2.4)

The need for an average confining stress is apparent, in order to construct a simpler design-oriented constitutive law.

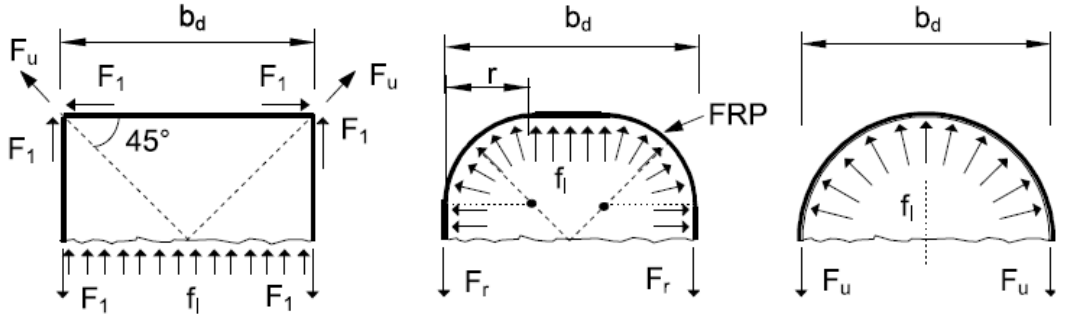

Figure 2.6: Effective lateral confining pressure for FRP-reinforced cross-sections (Campione and Miraglia 2003)

2.7 CONFINEMENT EFFECTIVENESS COEFFICIENT

An important topic in the process of understanding the mechanics of confinement is the quantification of the effectiveness of the confinement provided by FRP. According to Pellegrino and Modena (2010), the effectiveness coefficient can be the product of three individual factors, one that expresses the vertical efficiency, the shape factor that expresses the horizontal efficiency and the factor k_a that is used when fibers are spirally installed with an angle α with respect to the member cross section. The factors can be described as follows:

$$k_v = (1 - \frac{p'_f}{2 \cdot d_{min}})^2 \text{ , } k_a = \frac{1}{1+tan^2 a} \text{ and } k_h = \frac{A_g - A_{eff}}{A_g} \quad (2.3)$$

Where p'_f is the net distance between two subsequent wraps and d_{min} is the minimum cross section of the member, α is the angle of the fibers (0 if they are horizontal), A_g is the gross area of the cross-section (defined later in detail) and A_{eff} is the effectively confined area. For RC confined members with continuous FRP wrapping, k_v=1 is assumed. k_f is the coefficient of efficiency of the confinement and can be computed as the following product of coefficients: $k_f = k_v \cdot k_a \cdot k_h$ (2.4).

2.8 SHAPE FACTOR K_H

As noted by Csuka and Kollár (2012), for a concentrically loaded circular cross-section, the entire section is uniformly confined, while for rectangular cross-sections the confinement is higher at the corners and at the center of the cross section and lower at the midpoints of the sides. At this point, a complete review of the several shape factors that have been suggested by the researchers will be done.

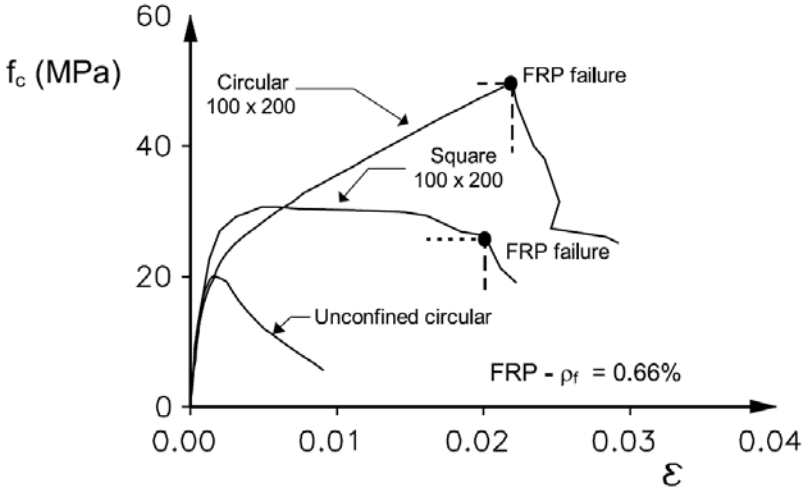

Figure 2.7: Stress-strain curves for FRP-confined concrete specimens with different shapes of the cross-section (Campione and Miraglia 2003)

Along with other factors for the model that Lam and Teng (2003) produced, they suggested a shape factor that can be written in terms of a ratio of the effectively confined area by the area of the cross-section:

$$k_h = \frac{A_{eff}}{A_c} = \frac{1-\frac{\left(\left(\frac{b}{h}\right)(h-2r)^2+\left(\frac{h}{b}\right)(b-2r)^2\right)}{3A_g}-\rho_{sc}}{1-\rho_{sc}} \tag{2.5}$$

where ρ_{sc} is the cross sectional area ratio of the longitudinal steel reinforcement, r is the corner radius and A_g is the gross area of the cross-section that can be evaluated as:

$$A_g = bh - (4 - \pi)r^2 \tag{2.6}$$

The effect of the aspect ratio, as defined by Lam and Teng (2003), is illustrated in the following graph, where R_c is the corner radius.

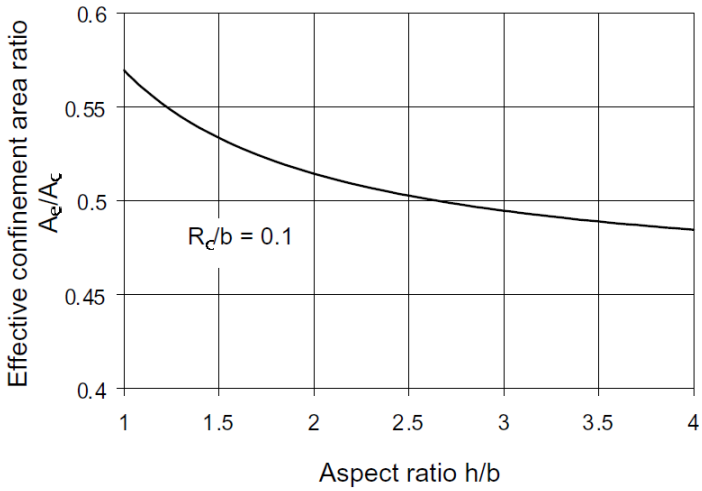

Figure 2.8: Variation of effective confinement area ratio with aspect ratio (Lam and Teng 2003)

The factors suggested by the other researchers use similar parameters. The following table summarizes the expressions found in the literature.

Table 2.1: Different formulas for k_h

Reference	Shape factor k_h
Mirmiran et al. (1998)	$\frac{2r}{h}, (h \geq b)$
Lam and Teng (2003)	$\frac{1-\frac{\left(\left(\frac{b}{h}\right)(h-2r)^2+\left(\frac{h}{b}\right)(b-2r)^2\right)}{3A_g}-\rho_{sc}}{1-\rho_{sc}}$
Harajli (2006) & Youssef et al. (2007)	$1-\frac{\left((h-2r)^2+(b-2r)^2\right)}{3bh}$
ACI 440 & Al-Salloum (2007)	$1-\frac{\left((h-2r)^2+(b-2r)^2\right)}{3A_g}$
Ozcan et al. (2010)	$(1-\frac{\left(\left(\frac{b}{h}\right)(h-2r)^2+\left(\frac{h}{b}\right)(b-2r)^2\right)}{3bh})\sqrt{\frac{h}{b}}$
Toutanji et al. (2009)	$(\frac{2r}{D})^{0.1}(\frac{b}{h})^{0.13}, D=\frac{2bh}{b+h}$
Wu and Wei (2010)	$(\frac{h}{b})^{-1.7}, (h \geq b)$

2.9 COMPARISON OF THE SHAPE FACTORS

The factors described before are applied to a typical cross-section with width 12 inches and corner radius 4 inches. As it is illustrated in Figure 2.9, as the aspect ratio (h/b) increases the shape factor and in effect the ratio of the effectively confined area decreases. It is worth to be noted that some of the models of Table 2.1 are similar to some others and are not presented in Figure 2.9.

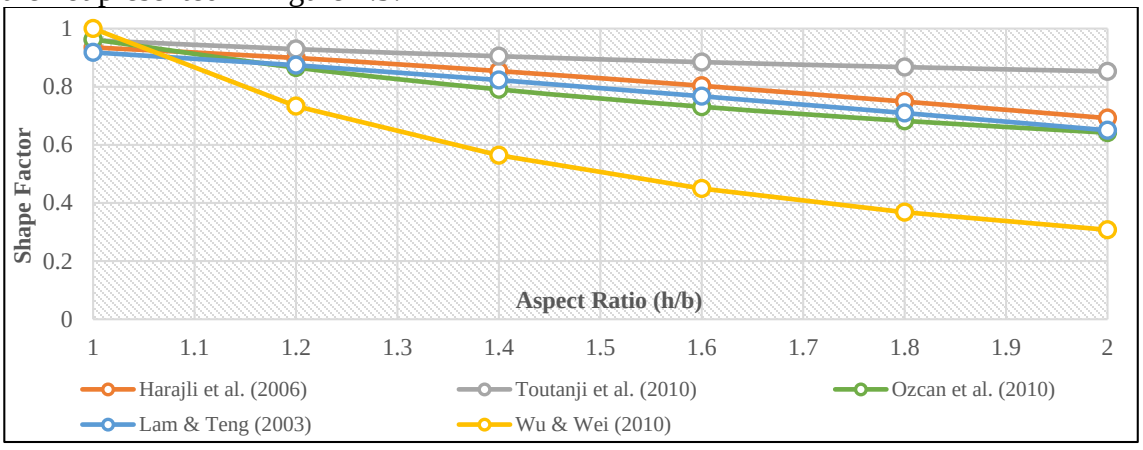

Figure 2.9: Variation of shape factor with aspect ratio

Another useful finding from Figure 2.9 is that four of the five researchers use almost identical shape factors, while Wu and Wei (2010) seem to use a more conservative expression. Although, it doesn't mean that they use an inaccurate shape factor, one could point out that they use an expression where the corner radius and the aspect ratio are independent. For example, they do not take into account the case where the aspect ratio might be too large but the corner radius is also large enough that it counteracts the negative effect of the large aspect ratio. A more in-depth description of the corner radius and its effect on the performance will be given later in this chapter.

2.10 COMBINATION OF STEEL AND FRP

Another important topic that has to be clarified is the treatment of individual areas inside the cross-section that have different material properties. To be more specific, the cross section can be divided into three discrete regions, each one of which is characterized by a different constitutive law:

a. The area where the concrete is unconfined.
b. The area that is surrounded by the transverse steel reinforcement, or in other words, the core concrete, which is confined by both the FRP jacket and the transverse steel.
c. The area outside the transverse steel reinforcement, but inside the jacket, also known as the cover concrete, which is confined only by the FRP jacket.

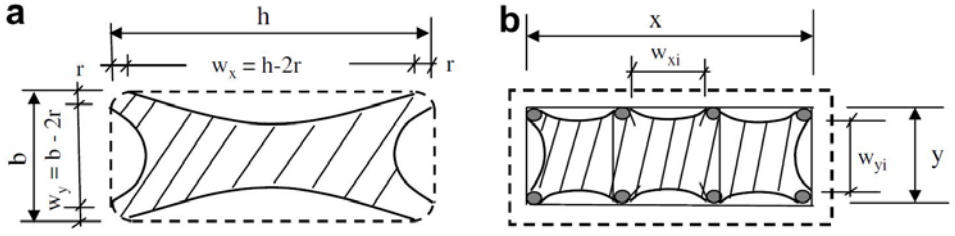

Figure 2.10: a) Entire column confined by FRP, b) core column confined by Steel, c) confined and unconfined portions of a square column.

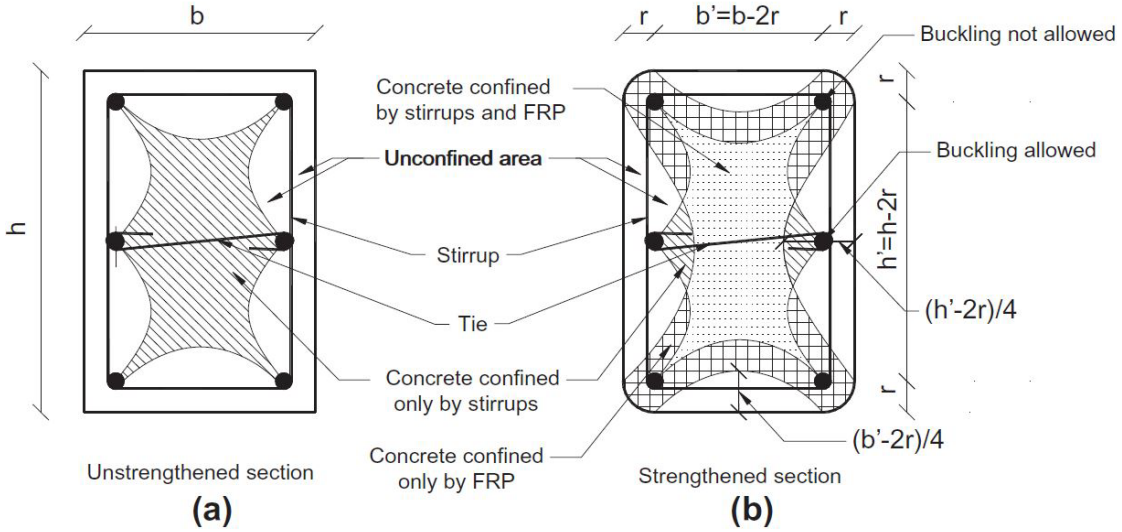

Figure 2.11: Different confined zones of rectangular sections (Montuori et al. 2013)

These discrete regions were presented by Wang and Restrepo (2001) and can be calculated using the following:

a. The region where the concrete is unconfined is the area that is not highlighted in Figure 2.10a.

$$A_1 = \sum \frac{w^2}{6} \tag{2.7}$$

b. The highlighted area of Figure 2.10b.

$$A_2 = \left(xy - \sum \frac{{w_i}^2}{6}\right)\left(1 - \frac{s'}{2x}\right)\left(1 - \frac{s'}{2y}\right) - A_s \quad (2.8)$$

c. The area of the column minus the above defined areas, or

$$A_3 = bh - (4r^2 - \pi r^2) - A_1 - A_2 \quad (2.9)$$

where:

A_s is the area of the longitudinal steel reinforcement

b is the small side of the cross-section,

h is the large side of the cross-section,

w (w_x and w_y) are the clear distances that define the FRP-confined and unconfined regions as shown in the first picture,

w_i (w_{xi} and w_{yi}) are the clear distances that define the Steel-confined and unconfined regions as shown in the second picture,

x and y are the sides that define the location of the transverse steel reinforcement and

r is the corner radius of the column

It is clear that the only region of the cross-section that is completely unconfined is defined by the area A_1 and depends directly on the clear distance between the corners of the column. This subject is of a great interest in the upcoming sections. In accordance to Wang and Restrepo (2001) the compressive load carried by the concrete, P_c results from the loads sustained by those three distinct regions:

$$P_c=P_{c1}+P_{c2}+P_{c3} = F_{c0}*A_1+ F_{cc,j,s}*A_2+F_{cc,j}*A_3 \quad (2.10)$$

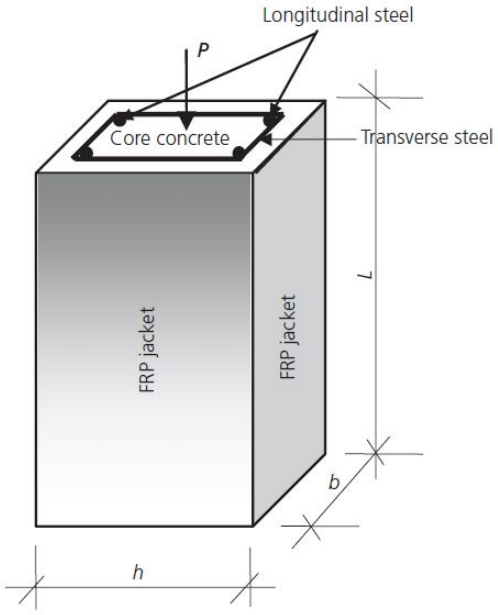

Figure 2.12: Axially loaded strengthened RC column (Koksal and Doran 2011)

where P_{c1} is the load carried by the unconfined concrete, P_{c2} is the load carried by the effective area of concrete confined by both the FRP jacket and the steel hoops and P_{c3} is the load carried by the area of concrete confined by the FRP jacket. F_{c0}, $F_{cc,j,s}$, $F_{cc,j}$, and are the compressive stresses in the regions A_1, A_2 and A_3 respectively. Finally, it has to be pointed out that $F_{cc,j,s}$ is simply the sum of the effects of the lateral stress provided by the jacket and the lateral stress provided by the transverse steel, or

$$F_{cc,j,s}=F_{l,j}+F_{l,s}=F_{cc,j}+F_{cc,s} \quad (2.11)$$

In conclusion, the above defined regions and compression forces are important for the understanding of the behavior and the analysis of an FRP-retrofitted column. The complexity that comes along with them dictates the use of a simple model for the FRP-confined region, which can be the average stress of the aforementioned stresses $f_{l,x}$ and $f_{l,y}$

in Equations (2.3) and (2.4). However, as described below, the average stress is not always the average value of the two stresses and there are several ways to calculate this average stress.

2.11 EQUIVALENT DIAMETER

Most of the formulas for determination of the confining pressure provided by the FRP jacket and eventually the stress-strain model were produced for circular cross-sections and all of them included the diameter of the circular section as a parameter in the calculations. When researchers began reporting test results for retrofitted rectangular columns, a need for a model similar to the ones produced for circular columns arose. Here is where the equivalent diameter of the rectangular column comes into play. In fact, most of the models for non-circular cross-sections are actually modifications of the ones for circular columns and the first parameter that required refinement was the diameter. More specifically, the Equations (2.3) and (2.4) will be converted to an equivalent equation identical to Equation (2.1). Table 2.2 summarizes the main approaches that have been suggested by the researchers through the years, as presented by Csuka and Kollár (2012). The expressions of Table 2.2 are also illustrated in Figure 2.13.

Table 2.2: Calculation of the equivalent diameter (Csuka and Kollár 2012)

Reference	**Equivalent Diameter (D)**
a) Mirmiran et al. (1998)	$h, (h \geq b)$
b) ACI 440, Harajli (2006) & Lam and Teng (2003), Youssef et al. (2007)	$\frac{2bh}{b+h}$
c) Al-Salloum (2007)	$\sqrt{2}b - 2r(\sqrt{2} - 1)$, can be used only for square columns
d) Lam and Teng (2003)	$\sqrt{b^2 + h^2}$

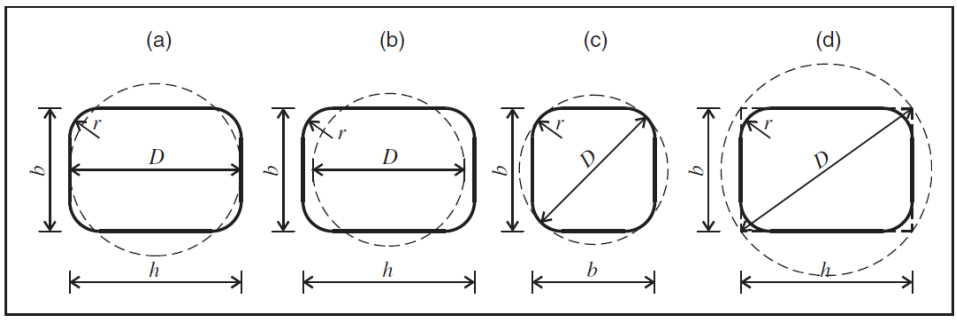

Figure 2.13: Definition of equivalent diameter. Figure by Csuka and Kollár (2012)

2.12 CORNER RADIUS

The external FRP laminates are usually bent when they are wrapped around columns, in order to achieve better confinement. Although this is common practice, the effect of this approach is not well understood or analyzed. Bending certainly affects the performance and efficiency of the FRP jacket and the confinement action depends on the curvature of the corners. The tests that have been published have established that the corner radius has a notable impact on the confinement effectiveness. In this section, the work done by Mirmiran et al. (1998), Campione and Miraglia (2003), Wang and Wu (2008), Hassan and Chaallal (2007), Ilki et al. (2008), Ozcan et al. (2010) and Pham and Hadi (2013) is reviewed.

The parameter that is conventionally used in the literature for the corner radius is the ratio of the corner radius to half the smallest side of the column, or 2r/b. It should be noted that for a square column 2r/b equals 1.0 means that the column cross-section has become circular. In the work of Wang and Wu (2008) a total of 108 CFRP-confined concrete columns were tested and the results indicated, as expected, that corner radius is of great importance in relation to the efficiency of confinement. More specifically, they found out that the strength of the FRP-confined concrete is in direct proportion to the

corner radius ratio, independently of the concrete grades they used. In contrast, the effective confinement of columns with sharp corners is incapable of increasing the strength of the columns. It is sufficient, though, to increase the ductility of the columns, after the peak load is achieved. Figure 2.14 shows the way an FRP-retrofitted column with sharp corners fails.

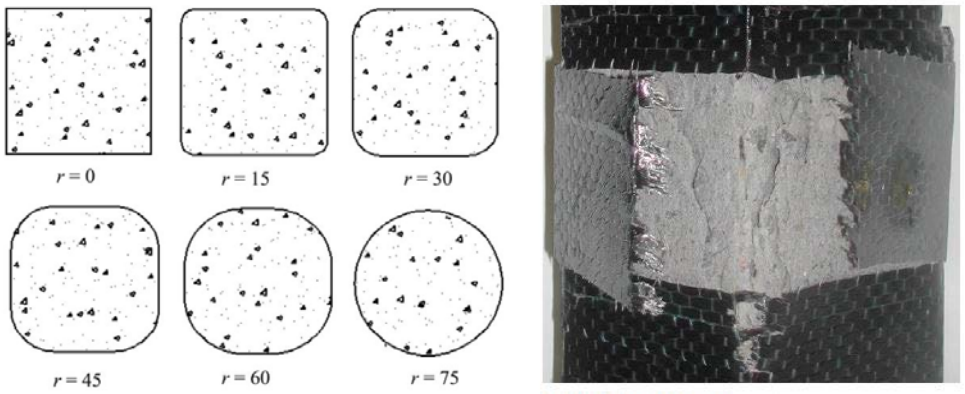

Figure 2.14: Corner radius variations of the columns and CFRP rupture at r=0 (Wang and Wu 2008)

The following table summarizes the results of Wang and Wu (2008) for C30 (30 MPa) concrete (f'_c around 4.5 ksi) for both one and two layers of CFRP laminates. The strength enhancement for the sharp columns is definitely negligible and can become almost three times the strength of unconfined concrete for 2-ply CFRP jackets with 2r/b equal to 1.0. The results are presented in Table 2.3 and Figure 2.15 illustrates these results graphically.

Table 2.3: Mean compressive strengths and corresponding f'_{cc}/f'_c (Wang and Wu 2008)

Corner radius ratio 2r/b	C30 concrete (f'_c=4.35 ksi)				
	Unconfined (f'_c)	With 1-ply (f'_{cc})	f'_{cc}/f'_c	With 2-ply (f'_{cc})	f'_{cc}/f'_c
0	31.7	32.2	1.02	32.2	1.02
0.2	31.9	33.6	1.05	42.2	1.32
0.4	32.3	39.8	1.23	56.5	1.75
0.6	30.7	43.7	1.43	68.0	2.22
0.8	31.8	50.0	1.57	78.9	2.48
1	30.9	55.8	1.80	84.8	2.74

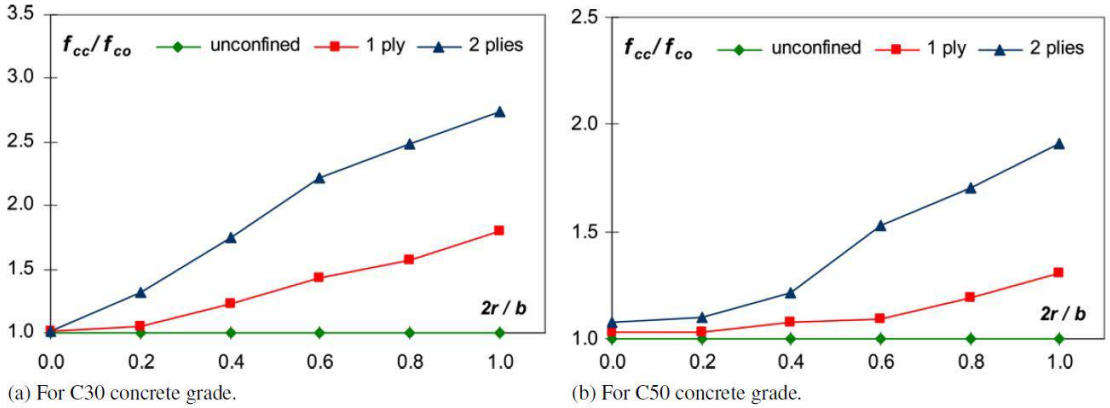

Figure 2.15: Effect of corner radius on confinement (Wang and Wu 2008)

It is interesting to note that Campione and Miraglia (2003) arrived at similar conclusions and also realized that the relation between 2r/b and the strength enhancement is linear (Figure 2.16).

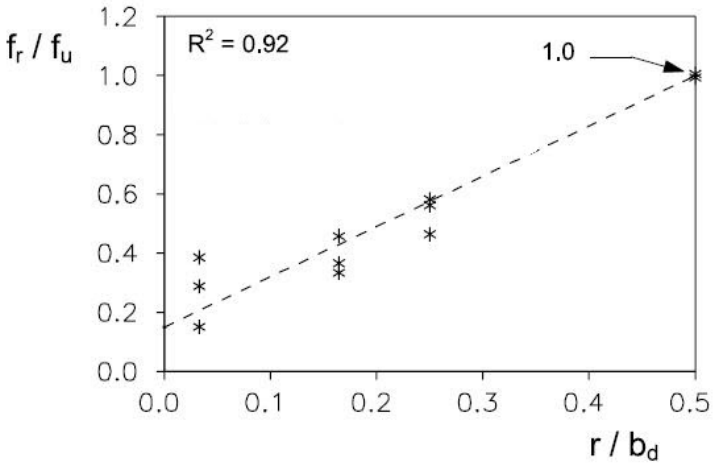

Figure 2.16: Variation in effective stress in FRP with r/b (r/b=0.5 indicates circular column) (Campione and Miraglia 2003)

Almost identical conclusions were drawn by Ilki et al. (2008), who also observed that there was no significant difference between axial strains in specimens with different corner radii. However, according to the tests of Ozcan et al. (2010), the response that was observed implied that reducing the corner radius not only decreased the CFRP-confined region, but also reduced the displacement and curvature ductility. More specifically, there was a specimen with reduced corner radius that showed deficient behavior in energy dissipation terms. Finally, reducing the corner-rounding had an insignificant effect on lateral strength and on secant-stiffness degradation responses. Hassan and Chaallal (2007) pointed out that it is not always feasible to increase corner radius on columns because of the reinforcing steel bars close to the corners of them.

At this point, the author would like to mention that a more sophisticated model to connect the parameter 2r/b with both the strength and ductility enhancement of the FRP-confined columns is needed. It can be seen in Figure 2.17 and Figure 2.18 produced by

Wang and Wu (2008), that the current models do not predict the FRP-confined concrete strength in a conservative manner when corner radius of the column varies.

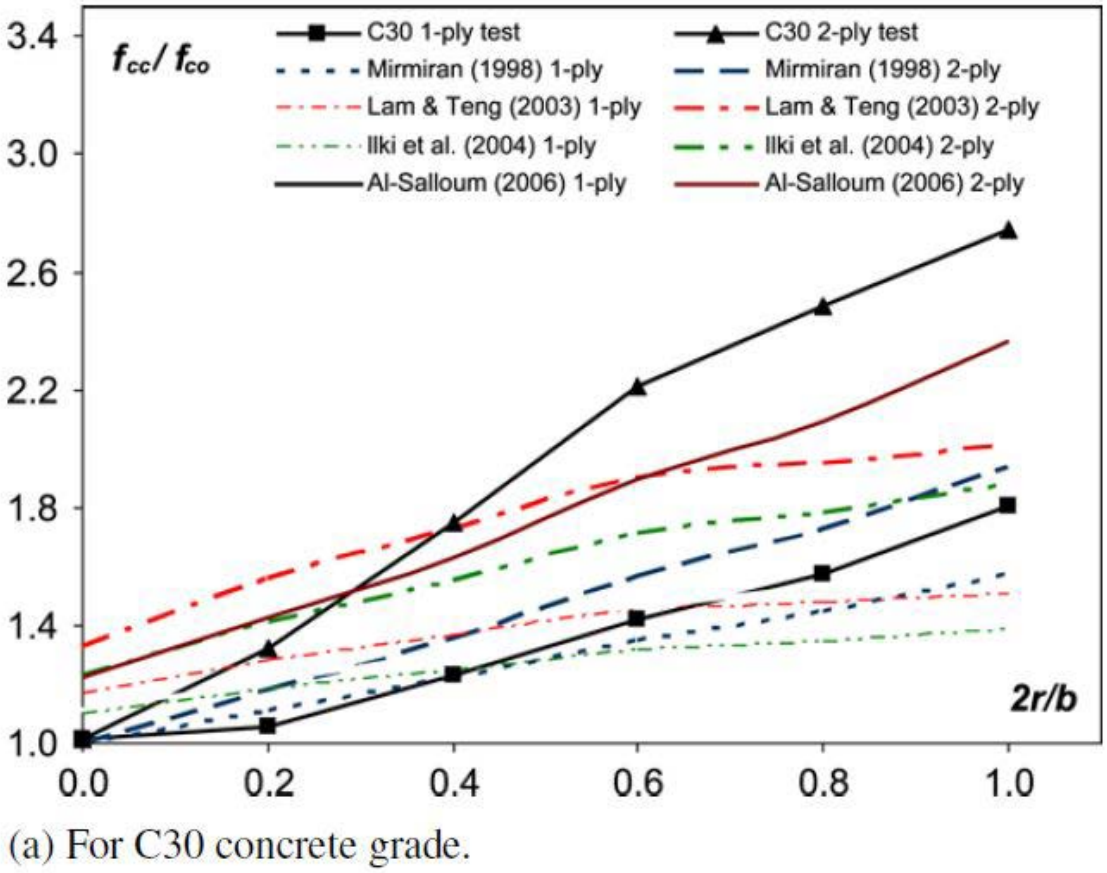

Figure 2.17: Comparisons between test results and existing confinement models for C30 concrete (f'_c=4.35 ksi) (Wang and Wu 2008)

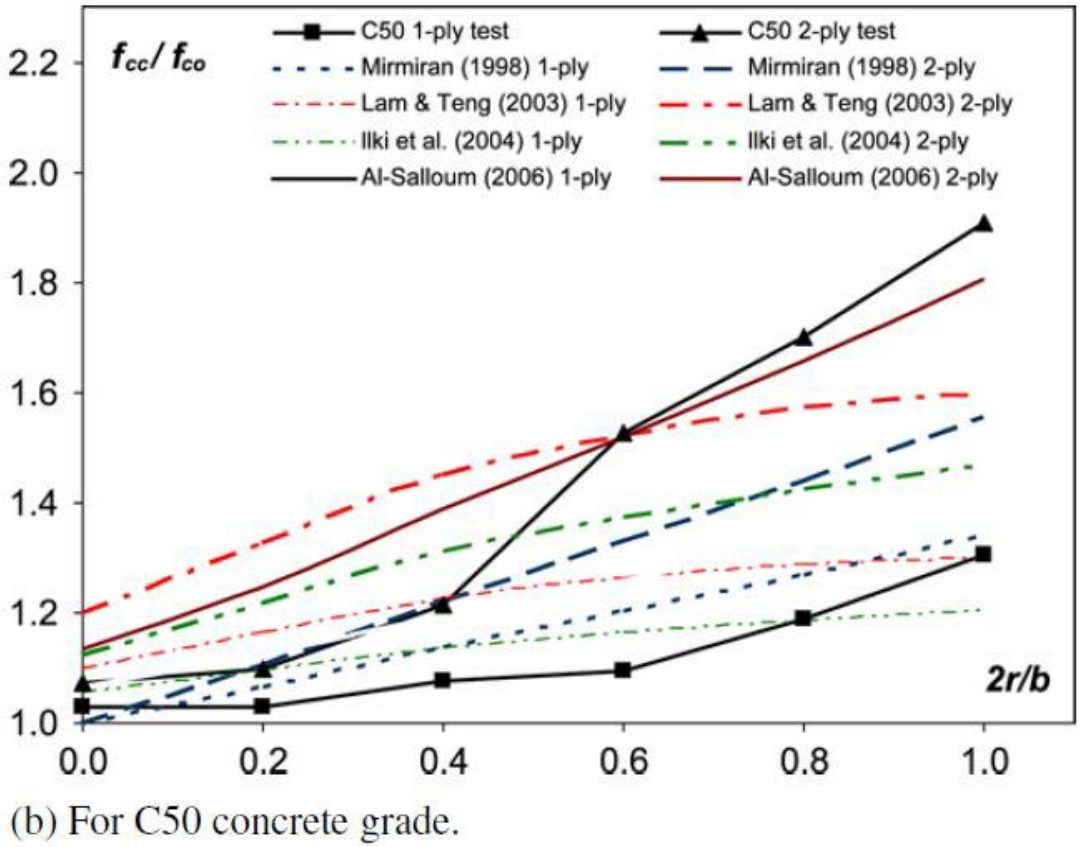

(b) For C50 concrete grade.

Figure 2.18: Comparisons between test results and existing confinement models for C50 concrete (f'_c=7.25 ksi) (Wang and Wu 2008)

2.13 GEOMETRY OF THE CROSS-SECTION

The research on FRP strengthening of columns has primarily concentrated on characterizing the performance of circular FRP-retrofitted columns. Some publications in the literature propose models for several cross-sectional geometries, but the data for rectangular columns with changing aspect ratio is scarce. The main purpose of this section is to qualitatively and quantitatively explain the behavior of rectangular columns with aspect ratios varying from 1.0 to 2.0. It is widely accepted that enhancement of the compressive strength and the ductility of both square and rectangular columns can be

achieved, but not to the level seen in circular columns. Research has shown that the strength gain of confined concrete depends on the aspect ratio of the cross section and, more specifically, decreases when the aspect ratio increases. It is remarkable that there is almost no strength enhancement for columns with an aspect ratio of 2.0 (typical aspect ratios used in practice presented in Figure 2.19).

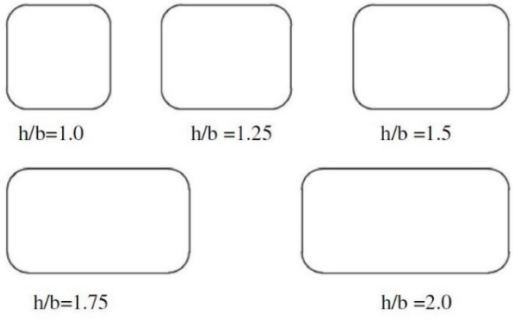

Figure 2.19: Aspect ratios of column (Wu and Wei 2010)

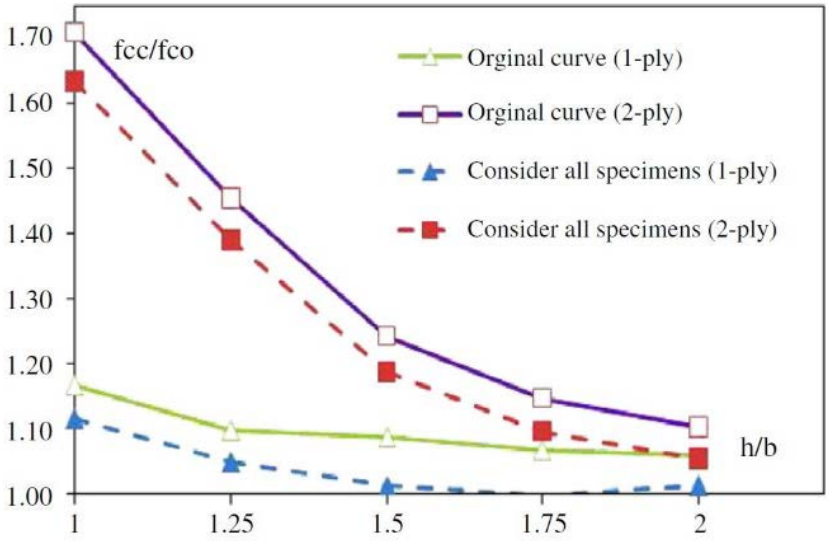

Figure 2.20: Strength gain of confined concrete versus aspect ratio. The original curves do not include the disregarded as unusual test data but the curves with all the specimens do include them. (Wu and Wei 2010)

It is apparent from Figure 2.20 that the aspect ratio influences the behavior of the confined column and this is the reason why most design guidelines limit the aspect ratio to 1.5 or less. There are two main explanations that have been proposed in the literature. Firstly, the aspect ratio, as it has been described earlier, directly affects the effectively confined area of the column, and most researchers have noted that the effective area is of great importance for the quantification of the strength and ductility gain of FRP-strengthened columns. Additionally, the confining pressure is concentrated at the corners of the columns due to the membrane action in the transverse sides of the FRP wrap, while at the other points the pressure depends on the flexural rigidity of the FRP jacket and hence the thickness of it. For example, a large number of FRP layers with high modulus of elasticity should be used to counteract this negative effect and to achieve significant strength gain. However, this technique would not be cost effective and has not been verified with experimental data.

The effects of the cross-sectional aspect ratio that have been presented by Wu and Wei (2010) illustrate the importance of the topic. They actually noticed that if the retrofit design is not correct, the aspect ratio would have a negative effect on the performance and the whole strengthening process would be unsuccessful. They also pointed out that the peak and ultimate strain variation should be of interest. More specifically, as shown in Figure 2.21, there has been a descending branch in the stress strain response of some columns (unsuccessful retrofit) and the strains at the peak loads were different from those at the ultimate failure. In general, the value of the ultimate lateral strains on the shorter side of the column increases as the aspect ratio increases and those on the longer side tend to decrease. In general the ultimate axial strains of the column decrease as the aspect ratio increases, a finding that shows the effect of aspect ratio on the ductility of the column.

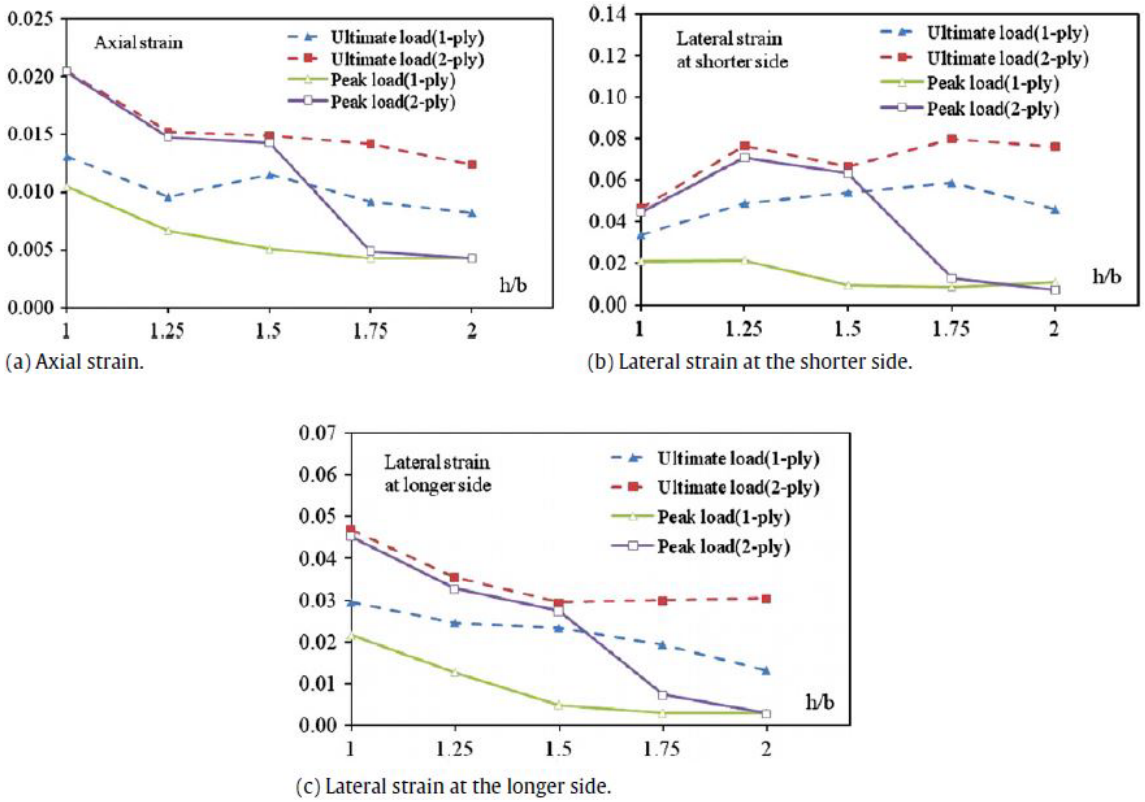

Figure 2.21: Ultimate and peak strains versus aspect ratio (Wu and Wei 2010)

Finally, Yang et al. (2004) showed that the aspect ratio and corner radius should be correlated because the ratio of these two parameters defines the final behavior of the concrete. As expected, as the ratio of corner radius to the size of the column decreases, the stress concentration increases causing a decrease of the confinement efficiency (Figure 2.22). In this figure, “radius” is the equivalent diameter and “corner insert” is the corner radius.

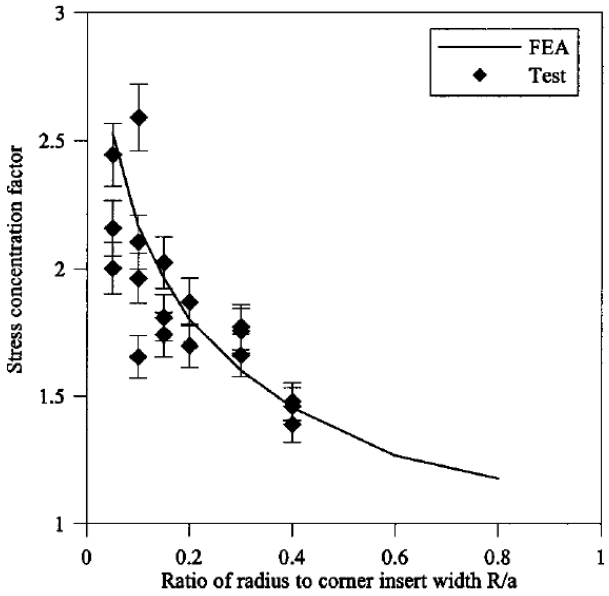

Figure 2.22: Stress concentration factor (Yang et al. 2004)

2.14 SIZE OF THE COLUMN

Although there is not much information concerning the effect of size (length and cross-sectional size) of the column, it has been shown that it is important. Mirmiran et al. (1998) investigated the length effect, by testing columns with varying length to diameter ratio (up to 5:1) and pointed out noticeable discrepancies in behavior. However, note that even the longest columns used would still qualify as short columns. Even though the experimental data used was limited to short columns, they noted some *insignificant decrease* in strength and deformation capacity enhancement, for which they proposed an expression. Figure 2.23 compares their experimental data with the analytical model they proposed. The size of the column is a parameter that should be investigated in more detail in the future because the use of existing models has been limited to small short columns. The purpose of such an investigation should be the testing of columns of different sizes

with FRP wraps in a portion of the length of the column. More specifically, the next topics have not been extensively investigated and need clarification:

- The limits of current design guidelines in terms of size of the cross section, aspect ratio and length.
- The behavior of columns with length to diameter ratio greater than 5:1.
- The behavior of partially wrapped columns.

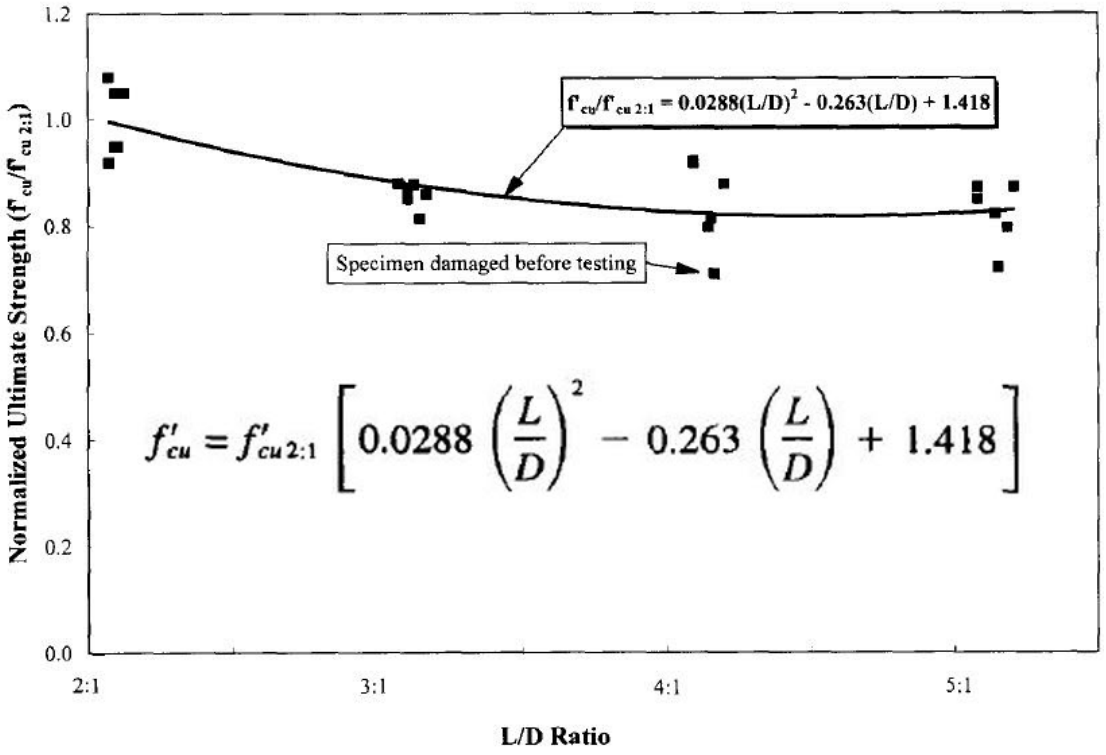

Figure 2.23: Normalized ultimate strength versus (L/D) ratio (Mirmiran et al. 1998)

2.15 CONCRETE STRENGTH

It has been suggested in the literature that a parameter that possibly influences the effectiveness of the FRP jackets on confining concrete columns is the original strength of

the unconfined concrete of the column. The strength of the unconfined concrete (f'_c) is used in all models that predict the behavior of FRP-retrofitted columns, but it has been shown that the accuracy of those models is limited to the commonly used unconfined strengths. There has not been a sophisticated model that relates the experimental results with the explanations that researchers have proposed. As described by Hassan and Chaallal (2007) the current models and guidelines relate the confined concrete strength (f'_{cc}) to the FRP volumetric ratio (ρ_j) which indirectly relates the strength enhancement to f'_c. The main trend that has been observed in laboratory tests is that the FRP confinement efficiency decreases when f'_c increases and this observation is reasonable. This can be attributed to the small dilatancies of high-strength concrete, which directly makes the FRP wrap less effective, because as described before the FRP jacket is activated only when concrete expands in the hoop direction. In general, the FRP jackets can be more efficient and cost effective in the case of low strength concrete. Figure 2.24 shows the aforementioned reduction in confinement efficiency when f'_c increases, as presented by Mandal et al. (2005) for circular columns. It has been experimentally shown by Ilki et al. (2008) that the same reduction applies to rectangular columns as well. As illustrated in Figure 2.24, the stress-strain models found in the literature grossly overestimate the strength enhancement of columns where concrete with f'_c larger than 5 ksi was used.

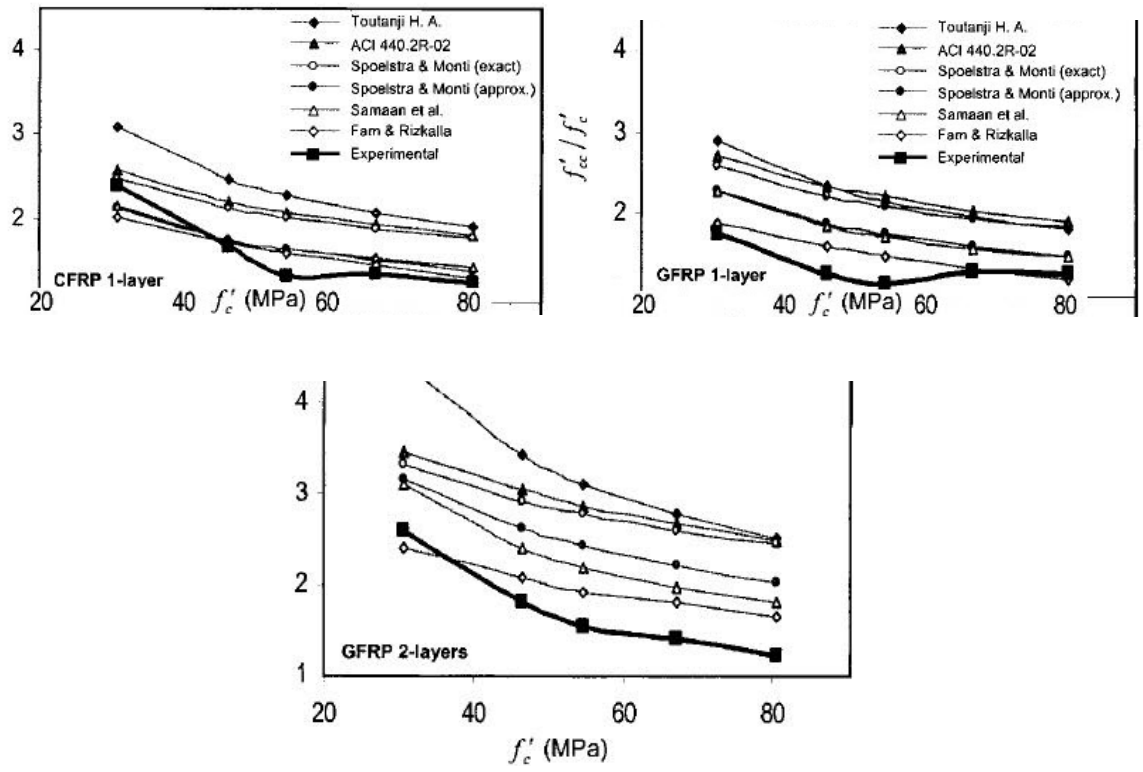

Figure 2.24: Effect of unconfined strength on concrete confinement efficiency (vertical axis is f'_{cc}/f'_c in all three graphs) (Mandal et al. 2005)

Ilki et al. (2008) noticed that the transverse FRP hoop strains were lower for high-strength concrete compared to low and medium. The same observation was made by the comparative study of Mandal et al. (2005) as illustrated in Figure 2.25. It was also indicated that the ductility was reduced when higher strength concrete was used. Again, the models for prediction of the hoop strain at maximum load predicted the trend but were not accurate. As explained by Bisby et al. (2012) this might be due to the well-known low deformability of high-strength concrete compared to low-strength and the aforementioned reduction in confinement effectiveness.

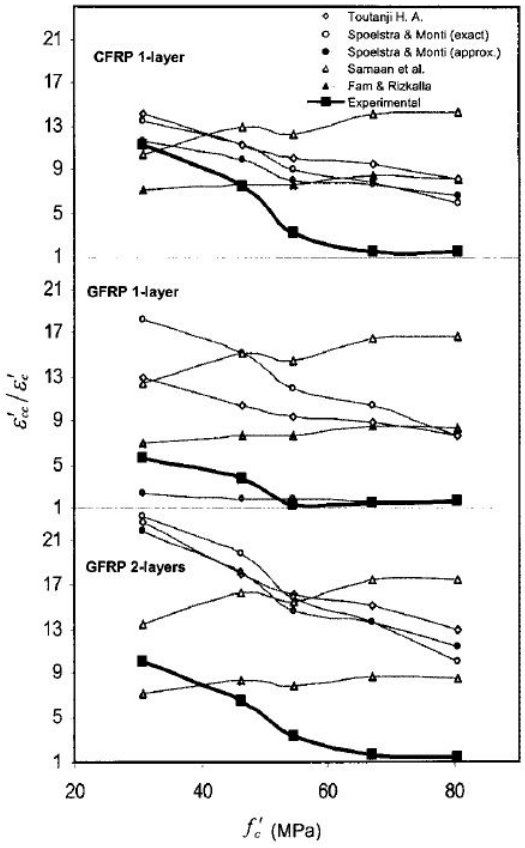

Figure 2.25: Effect of unconfined strength on peak strains (Mandal et al. 2005)

Figure 2.26 shows the results of Bisby et al. (2012) and gives a better picture of which parameters are affected and to what degree. It is worth stating that most researchers agree that both strength and deformation capacity highly depend on the strength of unconfined concrete in both circular and rectangular columns. Additionally, it is remarkable that all other parameters for which there is evidence suggesting that they influence the behavior of the FRP-retrofitted columns, do not significantly affect the behavior of columns with high f'$_c$. For example, it is commonly accepted that increasing the modulus of elasticity (E_{frp} or E_j), the thickness (t_j) or the strength of the FRP jacket can increase the strength of the confined-concrete. However, this is not the case with high-strength concrete, since tests have shown that only marginal increases in concrete strength can occur.

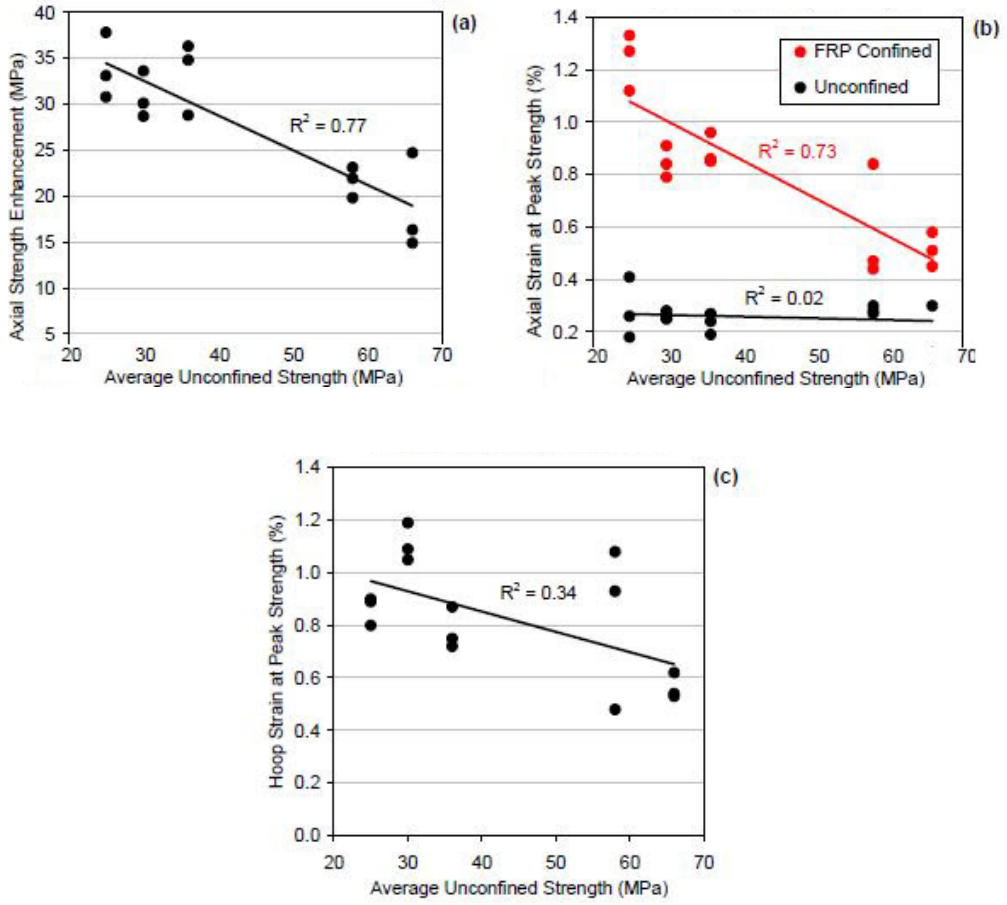

Figure 2.26: Effect of unconfined concrete strength on a) strength enhancement, b) axial strain at peak strength, and c) hoop strain at peak strength (Bisby et al. 2012)

2.16 JACKET THICKNESS

One of the most important parameters in the design of column retrofit is the thickness of the FRP wrap, which is equivalent to the stiffness of the jacket. In general, as explained earlier in the confinement mechanics section, the confining pressure is directly related to the thickness of the jacket (t_j) and this is also confirmed by the design expressions and the experimental results in the literature. In this section, this relation of

the confining stress with the thickness will be explained in more detail and the effect of the thickness on several aspects of behavior will be investigated.

Since the beginning of the investigations on the behavior of FRP-encased concrete as a structural material in 1982 (Fardis and Khalili 1982) the wrap thickness was the main parameter involved in the calculation of the strength and ductility gain by the FRP-retrofit. As illustrated in Figure 2.27, the obvious trend is that the strength of the confined concrete increases when the number of FRP-layers (equivalent to the increase in the thickness) increases.

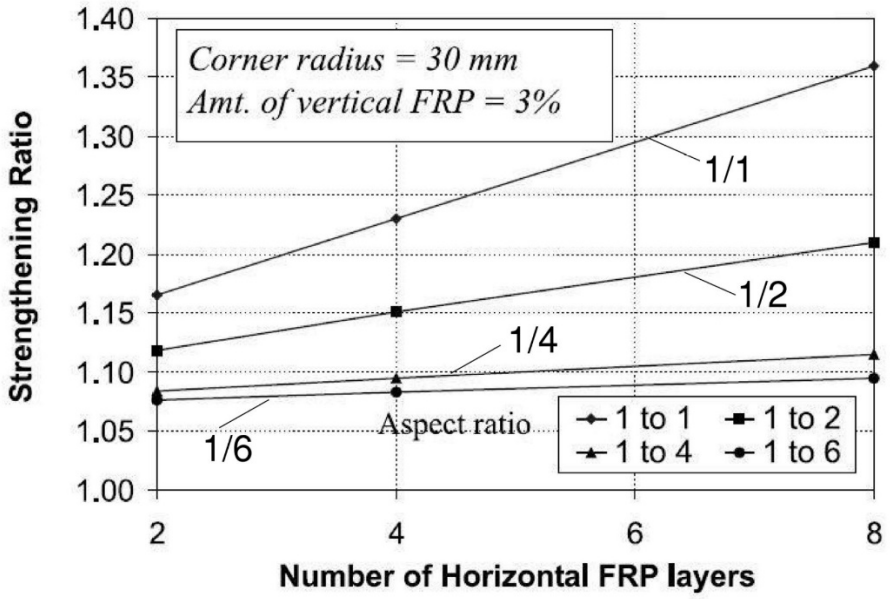

Figure 2.27: Effect of jacket's thickness on the strengthening ratio (Maalej et al. 2003)

Seible et al. (1997) proposed design expressions for FRP-strengthening of reinforced concrete columns, to achieve shear, flexural and lap-splice gain. It is important to state the main parameters that affected the calculation of the minimum t_j needed in that design expression, as this expression was one of the first expressions that the research

community trusted and used for many years. Seible et al. (1997) suggested that the thickness should be proportional to the size of the column, the target strength and deformation capacity but inversely proportional to the confining pressure and the ultimate strain of the FRP jacket. All these relations are reasonable, because as explained in earlier sections, the confinement efficiency increases as the size of the column decreases and/or the confining pressure and the ultimate FRP strain increases. As the FRP permits the concrete to dilate without rupture of the column both the strength and deformation capacity grow.

One way or another, all of the models take t_j into account in terms of the number of plies (layers) n_j, an example of which is shown in Figure 2.28 (stress-strain curves under axial loading). As it is pointed out by Montuori et al. (2013), the adoption of an alternative stress-strain law would yield similar results regarding the effect of the number of FRP layers. It is true though that most constitutive laws do not have a sophisticated model that could correlate the thickness with the dilation properties of the concrete described before and the transverse strain of the FRP. Apparently, the increase in both ductility and strength is remarkable (more than 100% increase from 1 to 6 sheets). However, the growth in bending moment is negligible (Figure 2.28 and Figure 2.29).

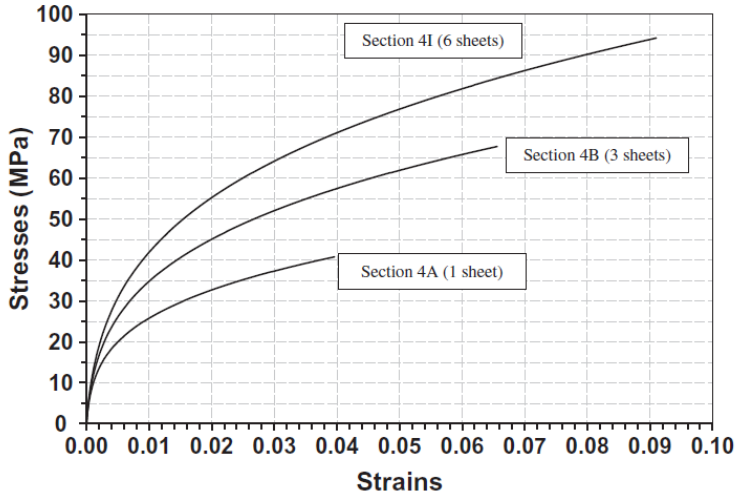

Figure 2.28: Example of FRP thickness's influence (Constitutive law by Spoelstra and Monti (1999)). Figure by (Montuori et al. 2013)

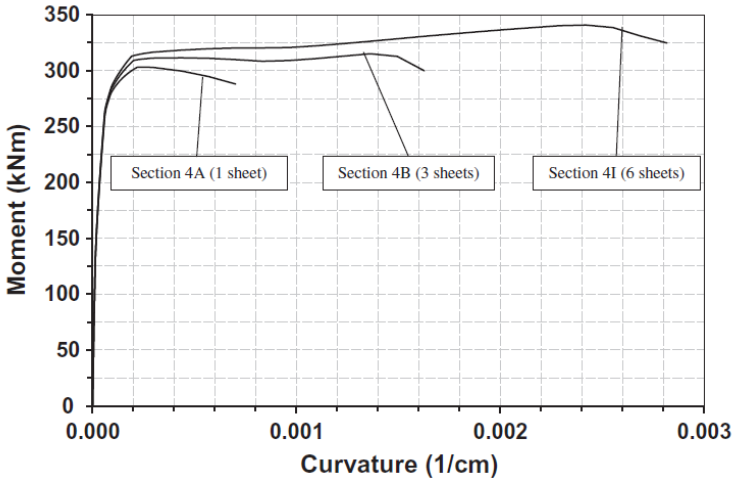

Figure 2.29: Example of FRP thickness's influence (Constitutive law by Montuori et al. (2012)). Figure by Montuori et al. (2013)

The next topic that needs more in-depth investigation is whether this apparent enhancement is affected by other parameters. As shown in Figure 2.27 the enhancement

due to FRP thickness increase highly depends on the aspect ratio, as it is obvious that for aspect ratio more than 2:1 the enhancement is insignificant. Figure 2.30 illustrates the dependence on the strength of unconfined concrete. It was described in a previous section, that concrete strength is a parameter that lacks investigation and thus the constitutive laws provided in the literature should be used more carefully for medium- and high-strength concrete. In this particular case, the gain accompanying the increase in the layer number is negatively affected by the use of higher strength concrete.

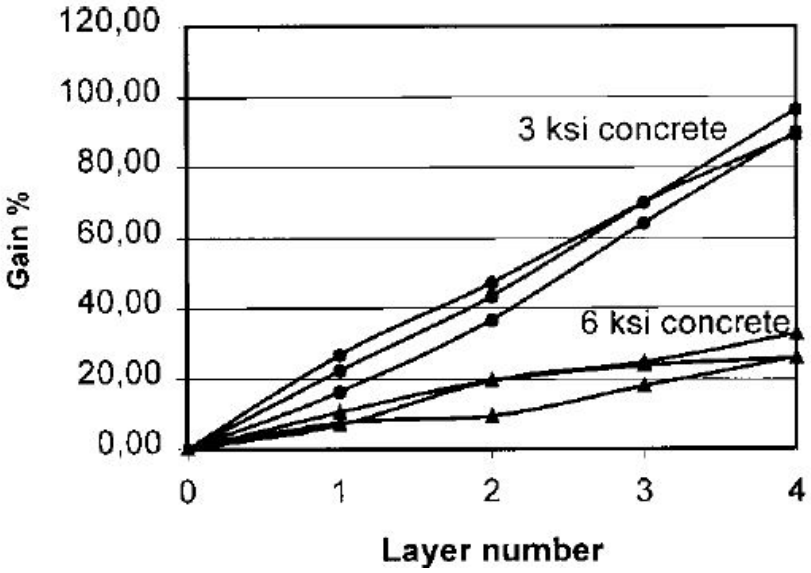

Figure 2.30: Gain in concrete compressive strength versus number of confining layers (Chaallal et al. 2003)

The unconfined strength of the concrete is also used in the ratio $(2r/b)*f_l/f'_c$ and was described before. It is a common parameter which is used for comparison of the confinement effectiveness of concrete columns. It seems that a large number of experimental results agrees that the strength enhancement is at least linearly proportional to $1/f'_c$ (Figure 2.31).

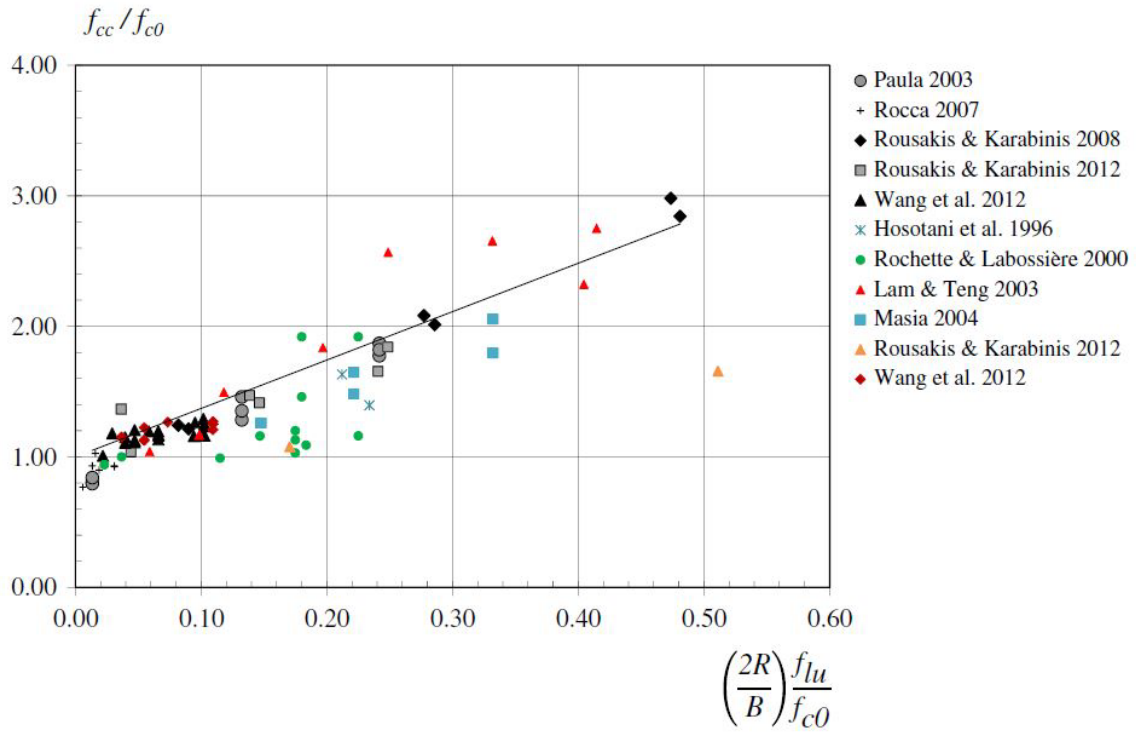

Figure 2.31: Relationship between f'_{cc}/f'_{c} and f_l/f'_{c} for square columns with cross-section dimension from 4 to 36 in., confined with CFRP (R is the corner radius and B is the cross-section dimension) (Faustino et al. 2014)

Although, the aforementioned experimental results and investigations agree that an increase in the jacket thickness has only advantages for the column retrofit, a more profound investigation is needed to explain the behavior of the strengthened column. Figure 2.32 and Figure 2.33 and the next comments will attempt to relate the stiffness of the FRP wrap with the dilation properties of the concrete. The number of layers used in the experimental study of Chaallal et al. (2003) is within the limits encountered in practice.

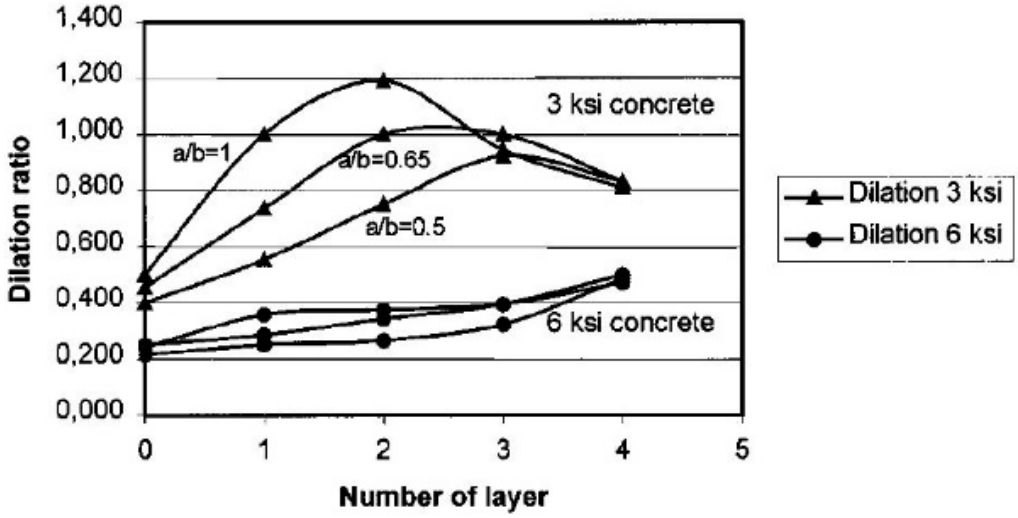

Figure 2.32: Dilation ratio versus number of CFRP confining layers (Chaallal et al. 2003)

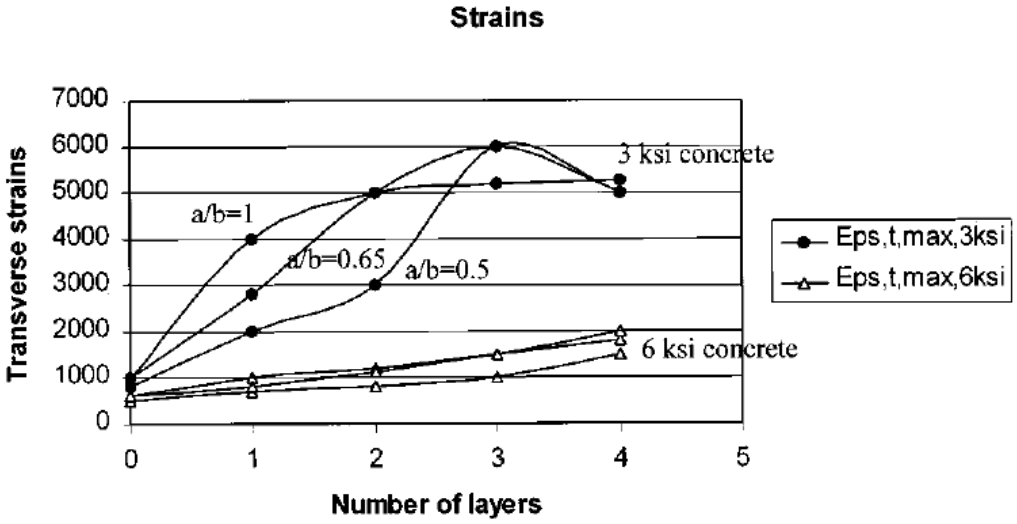

Figure 2.33: Transverse strains versus number of CFRP confining layers (Chaallal et al. 2003)

Figure 2.32 demonstrates the aforementioned connection. In all cases, it was observed that increasing the number of layers of FRP led to strength gain and ductility

increase. It is shown, however, that the transverse strains and the dilation ratio of the concrete reach a certain peak and then decrease independently of an increase of the number of layers. This finding suggests that increasing the stiffness of the jacket can lead to growth of the transverse strains and permit more ductility growth, but this increase seems to peak at a certain point. After that point, any strength and ductility enhancement is attributed only to the increase of the FRP lateral stiffness. This particular observation is of great importance, because it means that alternative ways should be found to increase the strength and/or ductility, since increasing only the thickness of the column could prove to be cost-ineffective. There is an alternative design method presented by Pantelides and Moran (2012) to account for the change in dilation properties in relation to the stiffness of the jacket. In a few words, this is the most sophisticated model for calculation of the required thickness of the jacket and is based on the needed stiffness of the jacket to improve the performance of an existing column. On the other hand, the model is quite difficult to be used in design. Alternative methods are presented in section 2.19 of the present study.

In conclusion, as also shown in the next two figures (Figure 2.34 and Figure 2.35), the increase in strength and ductility is directly related to the increase of the thickness (equivalent to stiffness) of the FRP jacket, and the effect is remarkable. However, the constitutive laws, suggested by the researchers, and the design considerations should start taking into account the dilation properties of the concrete and the increase in the ultimate transverse strains that accompany an increase to the stiffness of the jacket. Apart from that, the parameter “rigidity ratio” should be used instead of the number of layers in order to quantify the need of an increase to the jacket thickness. As explained by Chaallal et al.

(2003), the ratio of the FRP stiffness in the lateral direction to the column axial stiffness E*A is the “rigidity ratio” that is used in the horizontal axis of Figure 2.34.

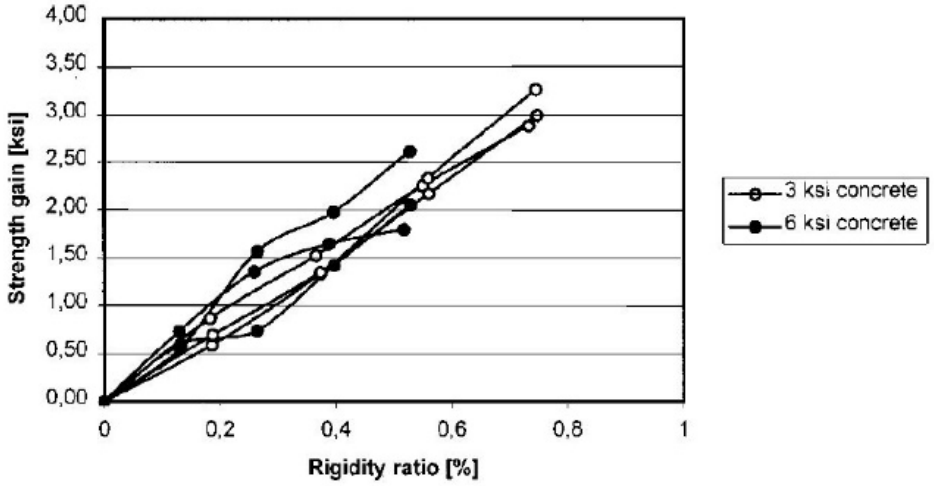

Figure 2.34: Gain in compressive strength versus CFRP jacket to column stiffness ratio (Chaallal et al. 2003)

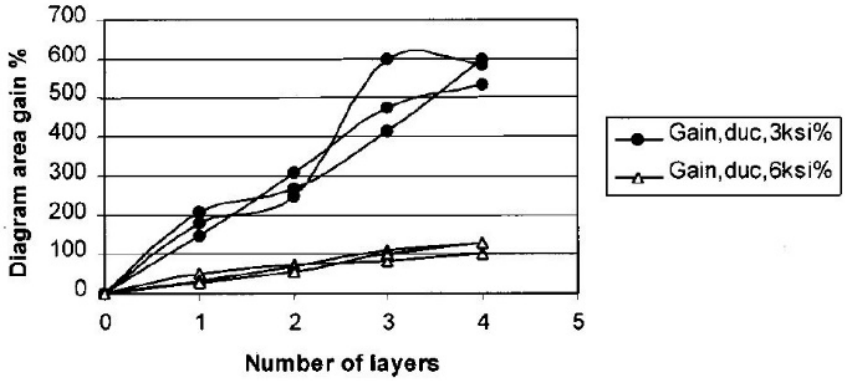

Figure 2.35: Gain in ductility versus number of CFRP confining layers (Chaallal et al. 2003)

2.17 FRP ULTIMATE STRAIN

Failure of a fiber reinforced polymer (FRP) composite wrapped concrete is usually governed by rupture of the FRP in the hoop direction, and the designer consequently needs to know the strain or stress at which rupture of the FRP will occur. The strain in the FRP jacket at failure is an important parameter for the determination of the maximum passive confining pressure acting on the rectangular column, which, in turn, directly influences the confined concrete strength. Although some researchers found that the rupture strain can reach 95% of the value given by the manufacturer, most investigations showed that the rupture strain is usually 30-50% lower. Two material test methods are usually used in the literature to obtain the hoop strength and rupture strain of FRP composites used in common applications: tensile tests of flat coupons and split-disk tests. In addition, it has been reported that the second type of tests, which is similar to the configuration of an FRP-wrapped column, yields smaller rupture strain. The paper of Chen et al. (2011) presents an investigation, using finite element (FE) analysis, into FRP hoop strains in the split-disk test with the aim of explaining possible reasons of the reduction of the FRP rupture strain in the test. Their FE results show that the local strains in an FRP ring in a split-disk test (Figure 2.36) are increased by the geometric discontinuities at the ends of the FRP and by circumferential bending of the FRP ring at the gap due to change of curvature there caused by the relative moment of the two half disks. The FRP ruptures once the strain at one of these locations reaches the FRP coupon rupture strain, leading to a lower apparent tensile strength than that obtained from flat coupon tests.

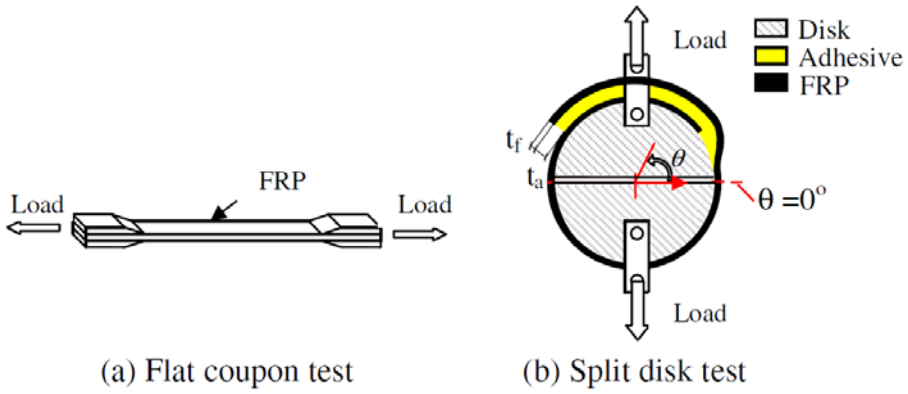

Figure 2.36: FRP strength test methods (Chen et al. 2011)

Another useful investigation on this matter has been conducted by Wang and Wu (2008).They studied the effect of the corner radius testing several columns with corner radii ranging from 0 to 75 mm (Figure 2.37). The 75mm column had a circular cross-section.

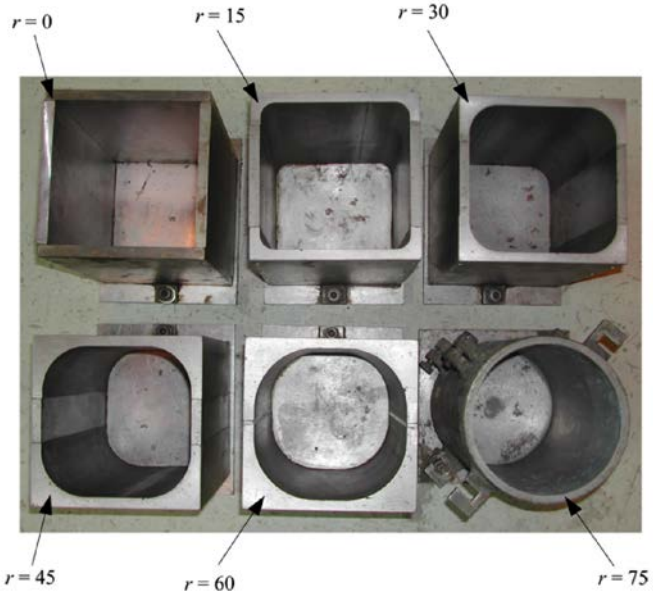

Figure 2.37: Prefabricated steel moulds with various corner radii (Wang and Wu 2008)

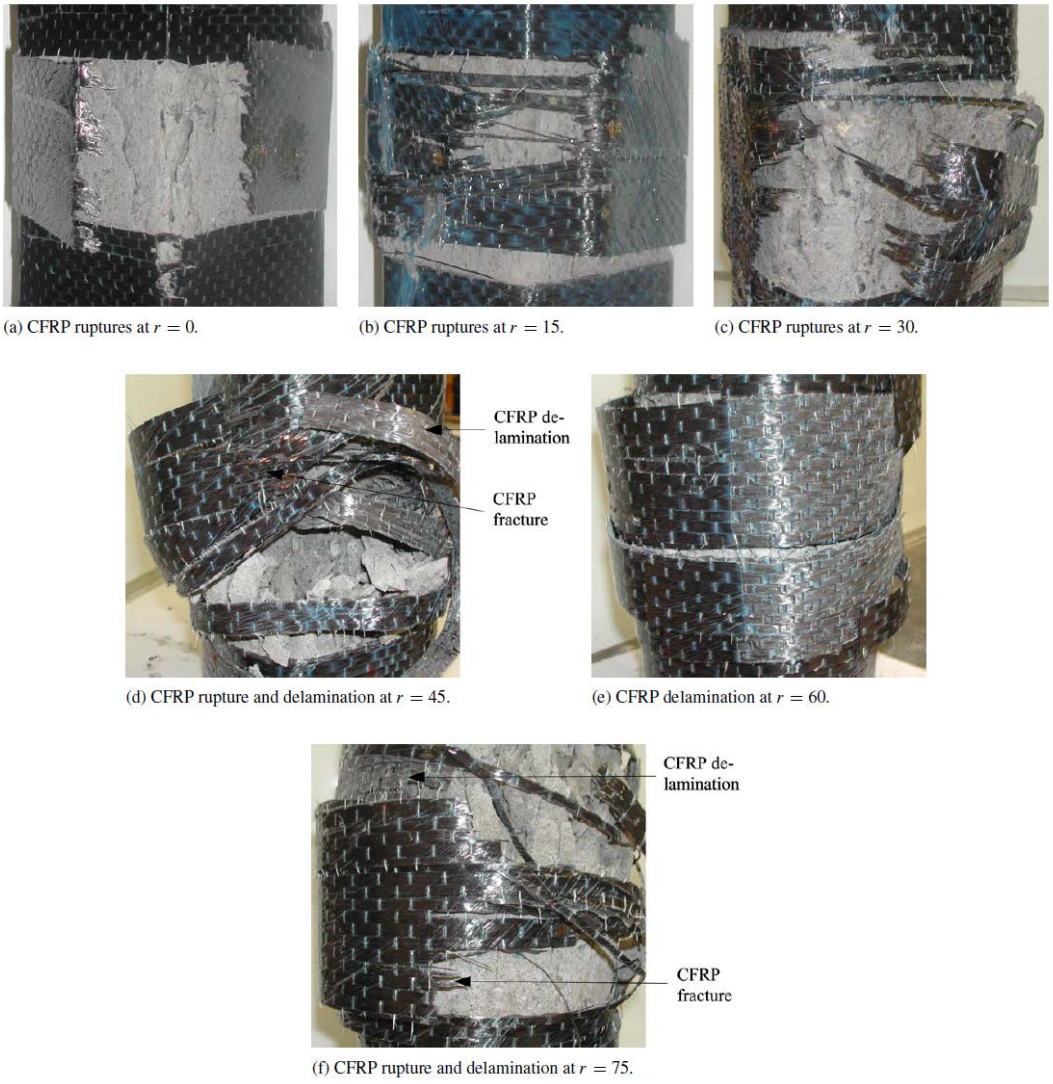

(a) CFRP ruptures at $r = 0$. (b) CFRP ruptures at $r = 15$. (c) CFRP ruptures at $r = 30$.

(d) CFRP rupture and delamination at $r = 45$. (e) CFRP delamination at $r = 60$.

(f) CFRP rupture and delamination at $r = 75$.

Figure 2.38: Failure modes of CFRP-confined concrete specimens (Wang and Wu 2008)

Two main causes have been suggested for the phenomenon of the early rupture of the FRP wrap: (i) non-uniform stress distribution in the FRP jacket due to deformation localization of the cracked concrete and thus, premature rupture of the FRP, and (ii) the curvature of the FRP jacket, especially at corners with a small corner radius. Figure 2.39 illustrates the CFRP strain distribution, where the solid and dashed lines refer to the single-

ply and two-ply CFRP-confined concrete specimens, respectively, with the maximum strain values marked at their locations. A quarter of the specimens is presented in the figure due to their symmetry. From this figure, it can be seen that the maximum tensile strain occurred at the middle of the side face or near the curvature changing point for the specimens with rounded corners, except for the specimens with a corner radius of 45 mm in the C30 series and 60 mm in the C50 series. For the columns with sharp corners, the maximum CFRP strains occurred near the corners of the section. The CFRP strain values of the confined columns with sharp corners indicate that the confining mechanism has not been fully activated at CFRP rupture.

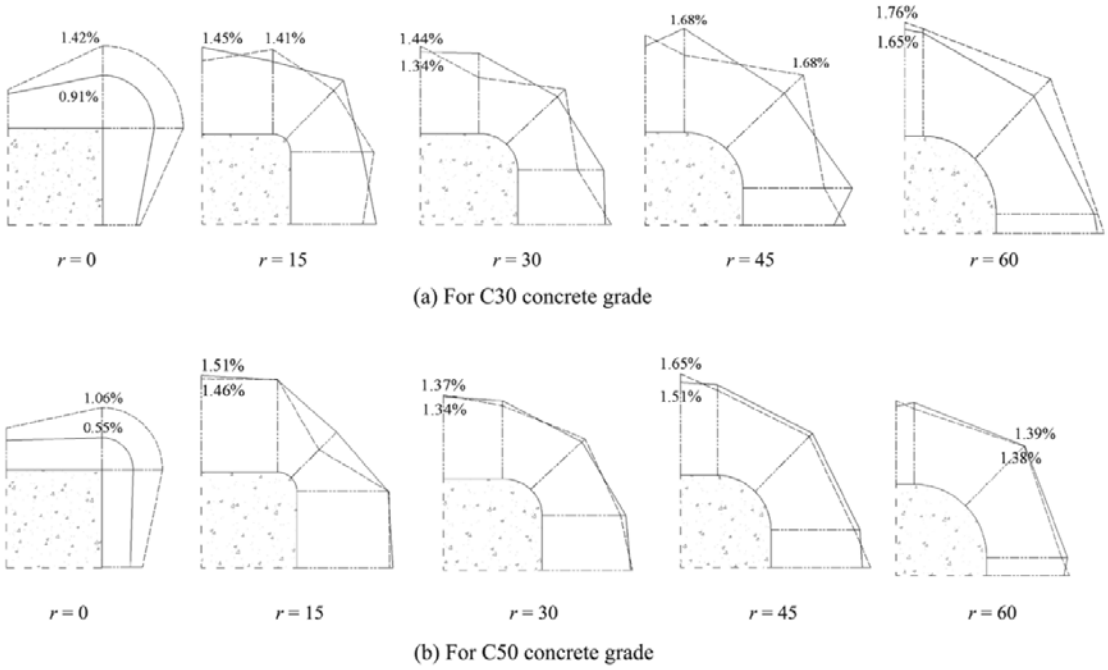

Figure 2.39: Ultimate strain distribution in CFRP (Wang and Wu 2008)

Figure 2.40 is a better representation of the conclusion drawn before, that the rupture strain of the composite increases as the factor 2r/b increases, or in other words as

the cross-section becomes circular. This is an important finding, because this is one of the most common mistakes made in practice.

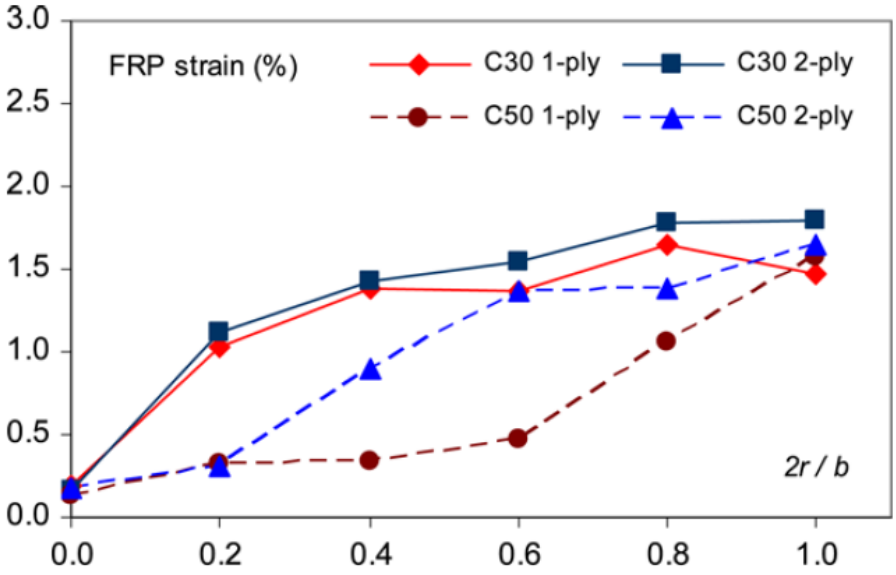

Figure 2.40: FRP strains at peak stress. The solid line denotes the C30 concrete grade (4.35 ksi) and the dashed line denotes the C50 concrete grade (7.21 ksi) (Wang and Wu 2008)

According to the model of Hassan and Chaallal (2007), the ultimate transverse strain $\varepsilon_{cc,t}$ of the confining FRP depends on the unconfined concrete strength f'_c and on the confinement coefficient k, as expressed by the next equation:

$$\varepsilon_{cc,t} = \frac{0.03+0.7k-1.4k^2}{f'_c},\ f'_c\ in\ MPa\ and\ k = \frac{E_j A_j}{E_{co} A_{co}} \qquad (2.12)$$

where E_j and E_{co} are the moduli of elasticity of the jacket and unconfined concrete respectively, while A_j and A_{co} are the areas of the jacket (per in: t_j x 1(in^2)) and the cross-section of the column respectively. The so-called modified confinement ratio (MCR),

which reflects the performance of the rectangular columns' confinement (Mirmiran et al. 1998), was calculated for the test specimens collected in the database and correlated to the FRP lateral strain. The MCR can be calculated using:

$$MCR = \frac{2r}{D}\frac{f_l}{f'_c} \tag{2.13}$$

where r is the corner radius, D is the long-side length dimension of the cross section, and f_l is the confining stress that can be calculated using Equation (2.1). All other terms are the same as previously defined. Figure 2.41 illustrates the relation between the ultimate FRP lateral strains and MCR considering all concrete strengths, FRP types, aspect ratios, and corner radii covered in the database. The general correlation (R^2) for a linear trend between the FRP lateral strains and MCR is 0.59. Correlations for more homogenous sub groups having similar concrete strength, FRP type, or aspect ratio could not be achieved given the lack of sufficient data.

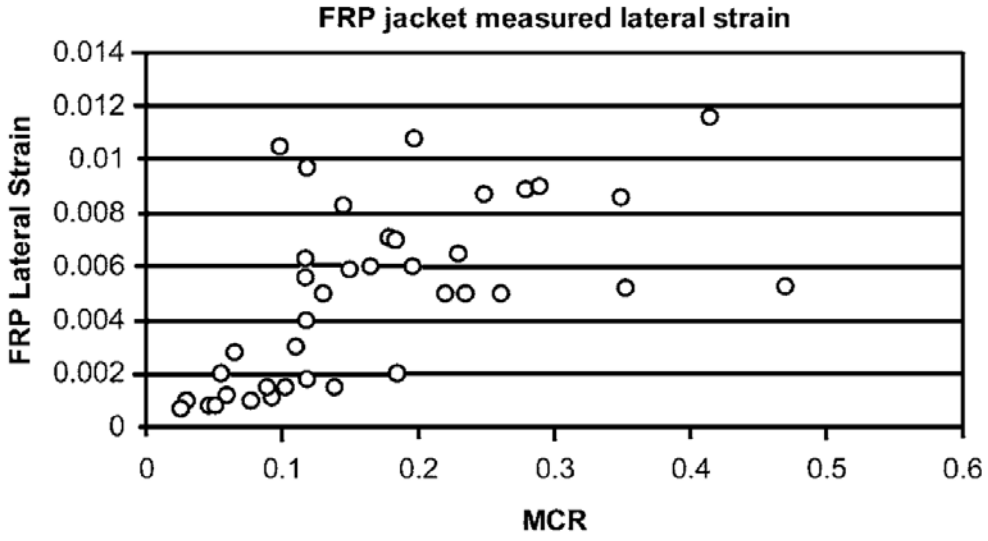

Figure 2.41: FRP measured lateral strain versus modified confinement ratio for all test results (Mirmiran et al. 1998)

Figure 2.42 presents the FRP lateral strains as a function of the FRP volumetric ratio as calculated according to the models of Wang and Restrepo (2001) and Chaallal et al. (2003).

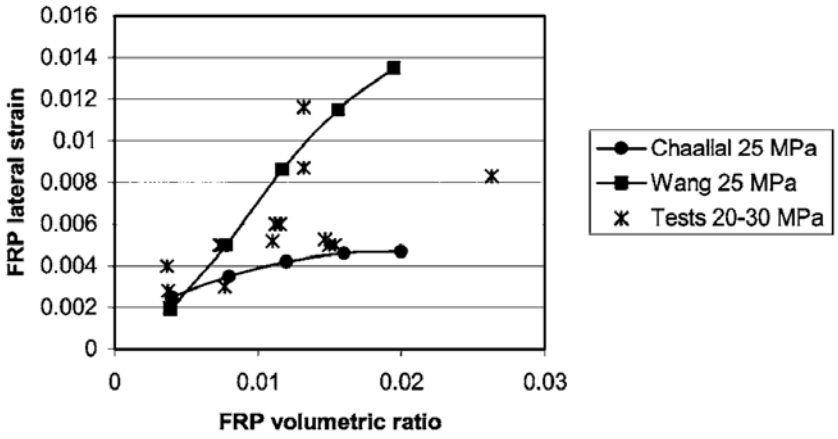

Figure 2.42: FRP lateral strain predictions and measure test results versus FRP volumetric ratio for 25 MPa (3.625 ksi) concrete (Hassan and Chaallal 2007)

Finally, another significant determination was made by Wu and Wei (2010) who found that the maximum strain of the FRP at rupture is unaffected by the aspect ratio. A reduction in FRP rupture strain was observed only for columns with sharp corners.

2.18 CONFINEMENT EFFICIENCY

The confinement efficiency is perhaps the most important aspect of FRP wrapping. Since the first experimental tests of FRP-strengthened rectangular columns presented in the literature, there have been columns that exhibited satisfactory behavior and others that did not. It can be quite subjective to determine whether the behavior of a column is sufficient or not, but most researchers have agreed that sufficient behavior is reached when the ultimate compressive strength of the column is at least larger than the strength of the unconfined concrete. In addition, there were some others that extended this theory and

consider the confinement provided by the FRP jacket successful only if the stress-strain law of the strengthened column showed strain hardening behavior, as shown in Figure 2.43. It is worth pointing out that even insufficient confinement (according to what is mentioned in this section) could still enhance the ductility of the column, at least in compressive axial loading as explained by Mirmiran et al. (1998).

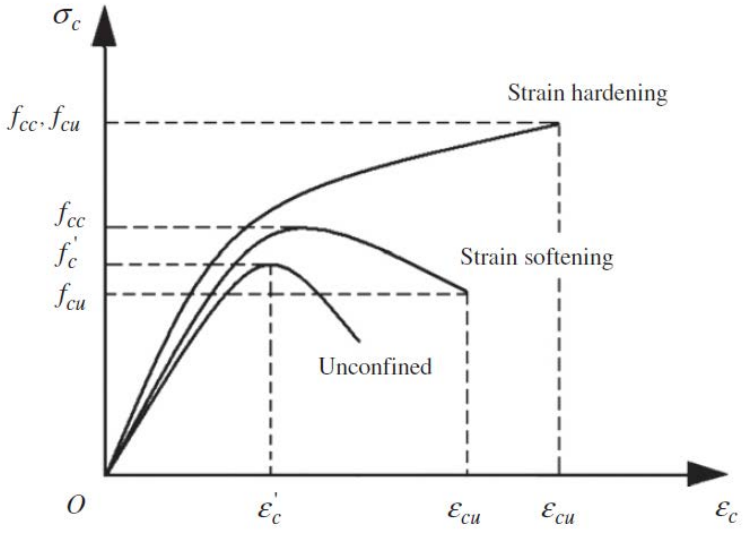

Figure 2.43: Typical stress-strain curves of FRP-confined concrete (Hu 2013)

Hu (2013) showed that the degree of strength and ductility gain largely depends on the confinement efficiency provided by FRP and that it is very important for the strengthening procedure to have a design tool in order to determine the sufficient/insufficient confinement accurately and easily. Before presenting the criteria for that determination, the “confinement efficiency” term should be explained. It was described in previous sections that the confining pressure depends on the FRP properties, the geometry of the cross-section and other parameters. In fact, the confinement pressure alone could be a parameter that quantifies the amount of confinement provided to the column. It would also be useful to compare this pressure (f_l) with the unconfined strength

of the concrete (f'_c), because for higher-strength concrete, higher confining stress is needed, as explained earlier in this chapter. Therefore, the ratio f_l/f'_c is a ratio that globally defines confinement effectiveness.

Additionally, the other parameters (geometry, corner radius, etc.) could also be included either using the effective confinement pressure, $f'_l=k_f*f_l$, in the numerator of the ratio, or multiplying the above mentioned ratio by a factor, for example 2r/D, where r is the corner radius and D the equivalent diameter of the column. Mirmiran et al. (1998) introduced the modified confinement ratio (MCR) that was defined as $2r/D*f_l/f'_c$, which, they found, is related to f'_{cu}/f'_{cc} in a logarithmic manner and D is the longer side length in the case of a rectangular section. More specifically, they proposed that if MCR is less than 15%, then the ultimate concrete stress (f'_{cu}) is going to be less than the peak stress (f'_{cc}) of the confined concrete column, which directly means that there is a descending branch in the stress-strain relationship.

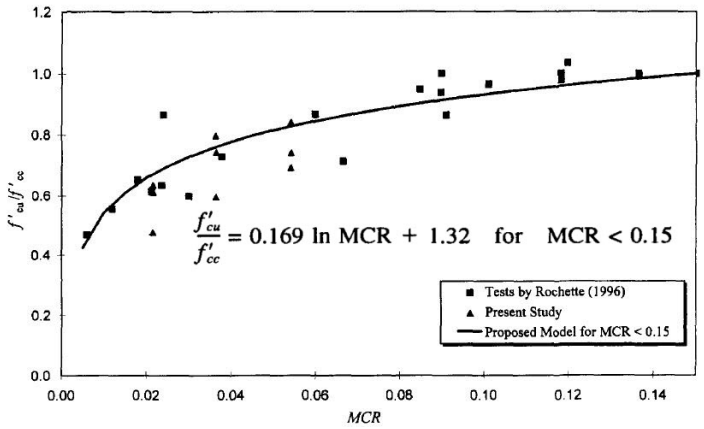

Figure 2.44: Ultimate strength ratio versus $(2R/D)(f_l/f'_c)$ ratio (Mirmiran et al. 1998)

It can be observed, that this relationship leads to an asymptote to the value of 1.0, which implies that after MCR becomes larger than 15% f'_{cu} is equal to f'_{cc}, or in other

words the second branch of the constitutive law is ascending. In contrast to that, in the widely used model of Lam and Teng (2003), that has been adopted with some modifications by the ACI 440.2R provisions, the confinement is considered successful if f'_{cu} is greater than f'_c, which implies that the second branch of the stress-strain law can be either ascending or descending. The criterion they use for judgment of the adequacy of the FRP material used is the ratio f'_l/f'_c to be greater than 7%. It is certainly a different criterion, where the effect of the corner radius is hidden in the shape factor (k_h same as k_f in most cases) in the effective confinement pressure $f'_l=k_h*f_l$.

Table 2.4 shows criteria that were proposed by several researchers to define the FRP confinement of a rectangular concrete column as sufficient or not. The criteria shown below define a parameter that has to be greater than a limit they use. Hu (2013) assessed all the previous models, for both circular and rectangular columns, and their expression is a result of a combination of the other criteria and revision of their boundary values. As stated in the publication, this improved criterion has extended accuracy and can be used for both circular and rectangular columns. Figure 2.45 and Figure 2.46 illustrate the performance of this model. Figure 2.45 correlates the ratio f_{cu}/f'_c to the confinement efficiency factor (χ) and illustrates the way the boundary value (BV) of 0.23 was found.

Table 2.4: Confinement criteria for acceptable behavior

Criterion		**Parameters**
Mirmiran et al. (1998)	$MCR=2r/D*\varphi_r \geq 0.15$	r: corner radius D: equivalent diameter φ_r: confinement ratio f_l/f'_c φ'_r: effective confinement ratio f'_l/f'_c f_{fu}: tensile strength of FRP k_h: shape factor ρ_f: volumetric ratio of FRP to concrete
Lam and Teng (2003)	$\varphi'_r \geq 0.07$	
Wu et al. (2006)	$\varphi_r \geq \lambda$, λ defined in paper	
Pantelides and Yan (2007)	$\varphi_r \geq 0.2$	
Wei et al. (2008)	$m=k_h\rho_f f_{fu}/f'_c \geq 0.2$	
Hu (2013)	$(2r/D)^{0.54}\varphi_r^{0.67} \geq 0.23$	

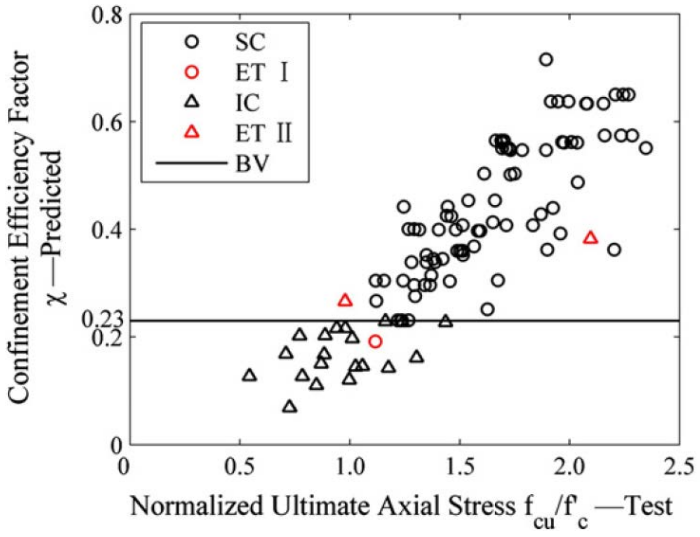

Figure 2.45: Performance of the proposed criterion (Hu 2013). Note: SC are the sufficiently confined specimens which are predicted correctly by the criterion; IC are the insufficiently confined specimens which are predicted correctly by the criterion; ET I denotes Error Type I (i.e. the error prediction that a sufficiently confined specimen by test is predicted as insufficiently confined by the criterion); ET II denotes Error Type II (i.e. the error prediction that an insufficiently confined specimen by test is predicted as sufficiently confined specimen by criterion): BV is the boundary value of the criterion; χ is the confinement efficiency factor: $(2r/D)^{0.54}\varphi_r^{0.67}$ (see Table 2.4) which Hu (2013) limited to 0.23.

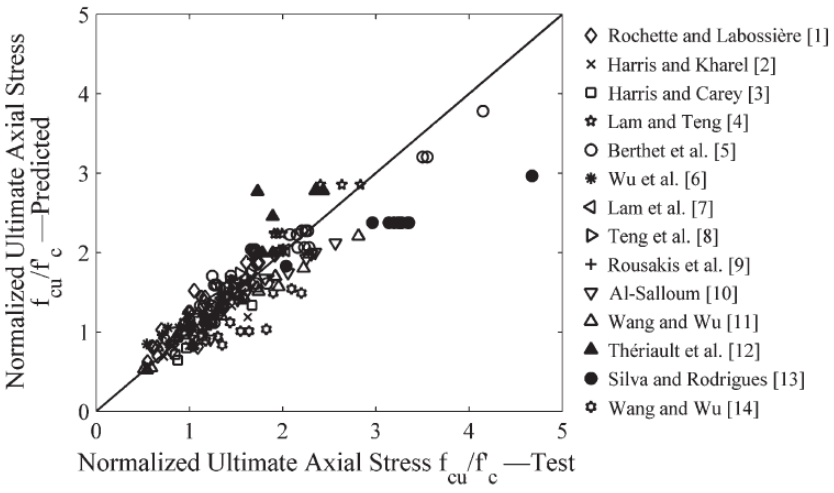

Figure 2.46 Performance of the proposed model with results reported in 14 test programs (Hu 2013)

2.19 MINIMUM AMOUNT OF FRP TO ACHIEVE SUFFICIENT CONFINEMENT

The above described expressions can be inverted in order to find the minimum amount of FRP, in terms of jacket thickness, that is needed to achieve adequate confinement. More specifically, the thickness needed can be calculated as

$$t_{j,min} = \frac{\varphi'_r D}{2 f_j k_h} \tag{2.14}$$

For example, according to the criterion of Lam and Teng (2003), where φ'_r has to be greater than 0.07, the minimum thickness can be expressed as $(0.07*D)/(2*f_j*k_h)$. In the same way, the other expressions can also be written with t_j as the unknown. This is the scope of the next table that gives an idea of what the thickness limit could be. These expressions combined with the thickness needed to provide adequate flexural strength can be the basis of the design of the retrofit. The tensile strength of FRP (f_{fu}) is the maximum value that f_j can take, which is $E_j\varepsilon_{h,rup}$. Finally, these criteria will be applied to an example in Chapter 4. ACI 440.2R (2008) suggests the criterion of Lam and Teng (2003) with the

limit 0.08 instead of 0.07, but as explained by Hu (2013) this criterion is not the most accurate.

Table 2.5: Minimum thickness according to the sufficient confinement criteria

Criterion	**$t_{j,min}$**	**Parameters**
Mirmiran et al. (1998)	$0.15(D/2r)Df'_c/2f_{fu}$	r: corner radius D: equivalent diameter φ_r: confinement ratio f_l/f'_c φ'_r: effective confinement ratio f'_l/f'_c f_{fu}: tensile strength of FRP k_h: shape factor ρ_f: volumetric ratio of FRP to concrete
Lam and Teng (2003)	$0.07Df'_c/2f_{fu}k_h$	
Wu et al. (2006)	$\lambda Df'_c/2f_{fu}$	
Pantelides and Yan (2007)	$0.2Df'_c/2f_{fu}$	
Wei et al. (2008)	$0.1bhf'_c/(b+h)f_{fu}k_h$	
Hu (2013)	$0.11(D/2r)^{0.80}Df'_c/2f_{fu}$	

Chapter 3: Anchorage System – Current Advances

3.1 SUMMARY OF THE CHAPTER

Anchorage systems have been shown to be useful in FRP-strengthening of reinforced concrete columns. FRP anchors are the focus of this chapter. However, there is limited experimental data and information about FRP anchors. The information found in the literature is reviewed and the findings of several investigations are discussed.

The first part of the chapter serves as an introduction to the use and advantages of anchors. Findings on the effectiveness of the anchors are reviewed. The second part describes in detail how the anchors help the column achieve better behavior. Two main advantages are shown: the effect on confinement and the effect on strengthening poorly detailed lap splices.

Finally, the design guidelines of Kim (2008) are described and there is some discussion on their findings. There are also some alternative methods that could be useful in design. Furthermore, current research gaps are identified and future research needs are outlined.

3.2 ANCHORAGE SYSTEM: DEFINITION & IMPORTANCE

The effectiveness of retrofitting reinforced concrete members with externally bonded FRP composites could be negatively affected by premature debonding of the FRP and therefore a way to delay this failure is of great importance. An anchorage system that could increase the efficiency and the reliability of FRP strengthening is required as the use of FRP systems in the retrofit industry becomes more prominent. Several ways to achieve this goal have been introduced in the literature and will be outlined later in this chapter. The most promising anchorage system though is the use of anchors made from FRP, which are attractive as they are non-corrosive and can be applied to a wide variety

of structural elements. There have been few investigations reported in the literature where FRP anchors were used. Table 3.1 summarizes the research conducted in the past years on column strengthening with FRP wraps and several types of anchors, such as CFRP anchors, GFRP, mechanical and steel rods.

Even though there are some differences in the behavior, the performance of strengthened columns with FRP anchors is similar to the behavior of columns with other types of anchors. However, this study mostly focuses on FRP anchors. Handmade anchors that are formed from bundles of fibers or commercially made FRP anchors that are available on the market can be inserted into predrilled epoxy filled holes in the concrete substrate. Figure 3.1 shows anchors before embedment and the column after insertion of the anchors.

Figure 3.1: a) CFRP anchor, b) GFRP anchor, c) CFRP jackets with CFRP anchors

Table 3.1: Experimental investigations with FRP jackets and anchorage systems

Research Name	Number of specimens	Names of specimens	Type of FRP jacket	Type of anchorage system
Tan (2002)	3	M22GPA, N02GA, N11GA	GFRP	GFRP
Galal, Arafa, and Ghobarah (2005)	1	SC2	CFRP	Mechanical
	1	SC3	CFRP	CFRP
	1	SC1R	GFRP	Mechanical
Ghobarah and Galal (2004)	1	SC2	CFRP	Steel Rods
	1	SC3	CFRP	CFRP
I. Kim (2008)	6	1-A-S8-M, 2-A-S8-M, 3-B-S10-M, 4-C-R20-M, 5-C-R20-C, 6-C-R20-C	CFRP	CFRP
P.-C. Chen, Lin, and Tsai (2008)	1	R06-RF2	CFRP	CFRP
Y.-F. Wu, Liu, and Wang (2008)	2	C4, C5	CFRP	GFRP
Ilki, Peker, Karamuk, Demir, and Kumbasar (2008)	5	LSR-R-1-1-40-a-A, LSR-R-2-1-40-a-A, NSR-R-2-175-5-40-A, LSR-R-1-1-40b-A, LSR-R-2-1-40b-A	CFRP	CFRP
Ozcan, Binici, and Ozcebe (2010)	3	S2, S3, S5	CFRP	CFRP
Ozcan, Binici, Canbay, and Ozcebe (2010)	4	S-NL-30, S-NL-10, R-NL-30, R-UL-30	CFRP	CFRP
Huaco Cardenas (2013)	1		CFRP	CFRP
TOTAL	**30**			

Figure 3.2 shows the required preparation of the anchors prior to their embedment in the column, while Figure 3.3 illustrates the installation process.

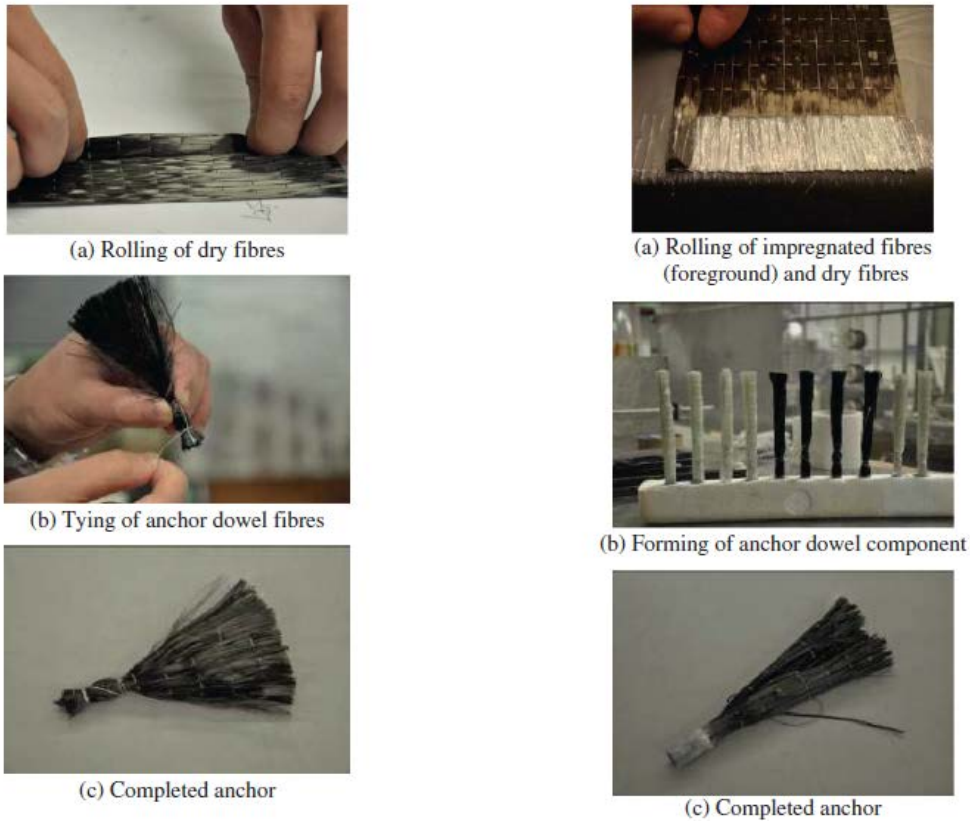

Figure 3.2: Preparation of anchors (Zhang et al. 2012)

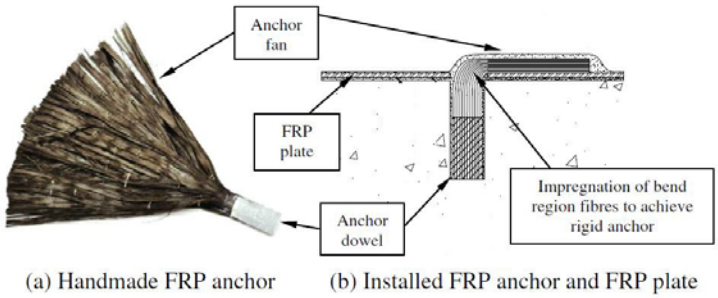

Figure 3.3: Installation of anchors (Zhang and Smith 2012)

3.3 BEHAVIOR OF ANCHORS

As explained by Smith (2009) and Kim and Smith (2009), anchors can fail in different ways depending mainly on their embedment length. For short embedment depths (h_{ef} less than 5d, where d is the anchor diameter), concrete cone failure is more likely to happen, while for larger lengths the failure mode is a combination of concrete cone and bond failure. Alternatively, anchors can fail by fracture.

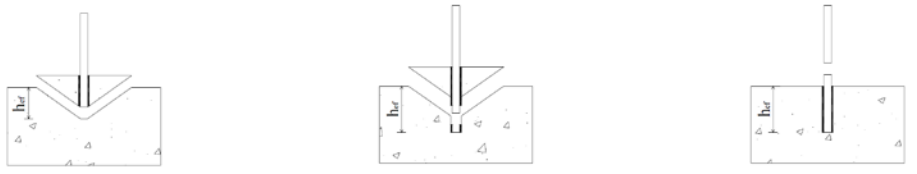

(a) Concrete cone failure (b) Adhesive-to-concrete, anchor-to-adhesive, or mixed interface failure (c) Anchor failure

Figure 3.4: Typical adhesive anchor failure modes

The following equations were proposed by Smith (2009) to calculate the maximum axial force that can be developed by the anchor (units in mm and MPa):

$$N_u = \min(N_{cc}, N_{cb}, N_{ar}) \tag{3.1}$$

$N_{cc} = 9.68 {h_{ef}}^{1.5} \sqrt{f'_c}$ (cone failure) (3.2)

$N_{cb} = 4.62\pi d_o h_{ef} \quad (f'_c < 20\ Mpa)$ (combined failure) (3.3)

$N_{cb} = 9.07\pi d_o h_{ef} \quad (f'_c \geq 20\ Mpa)$ (combined failure) (3.4)

$N_{ar} = 0.59 w_{frp} t_{frp} f_{frp}$ (anchor failure) (3.5)

Where N_u = pullout resistance of a single FRP anchor,

h_{ef} = effective embedment depth of the anchor,

d_o = diameter of the anchor hole,

w_{frp} and t_{frp} = width and thickness respectively of the fiber sheet in construction of the FRP anchor,

f_{frp} = tensile rupture strength of a flat FRP coupon.

3.4 EFFECT ON CONFINEMENT

In general, anchors improve the confinement effect of FRP wraps. In concrete columns with large faces, external FRP wraps have been shown to be inefficient, as explained in Chapter 2, and only marginally improve the capacity and ductility of wrapped columns. The fiber sheets are mainly active at the corners of a rectangular column and do not restrain the "bulging" of the FRP wraps away from the corners. The anchors (of all types, mechanical, steel rods and FRP) work as the key elements that reduce bulging and make the FRP jacket effective in confining the concrete enclosed.

It was shown in Chapter 2 that in rectangular columns with high cross-sectional aspect ratios, the effective confined area is only a small part of the actual cross-section. If anchors are applied to the fiber sheets and those sheets remain effectively bonded on the concrete column, the effectively confined area under the sheets increases. Thus, the wraps would not only be effective at the corners, but also at the locations where anchors are provided. However, there are still some unconfined areas inside the column, which form at the areas between the anchors, as shown in Figure 3.5. The aforementioned statement will be explained further with an example in Chapter 4.

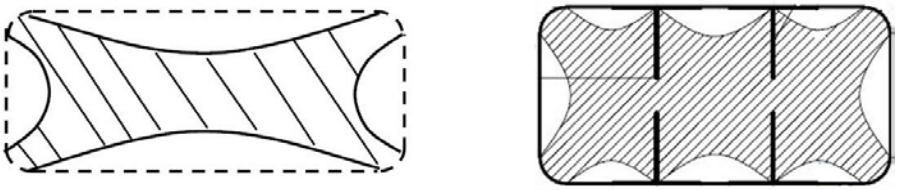

Figure 3.5: Effective confined area without and with anchors

Figure 3.6 illustrates how the effectively confined area can increase with the use of anchors. For calculation purposes Equation (2.7) was used, where (h-2r) was replaced by $\frac{(h-2r)}{number\ of\ anchors-1}$. Also, b/h and h/b were assumed equal to 1.0, because the arching

angle was assumed to be 45 degrees. Detailed information about the arching angle can be found in Chapter 4. As shown in Figure 3.6, the number of anchors on the large face of the column increase the effectively confined area so that it approaches asymptotically the confined area of a square column (h/b=1). For the purposes of this example, a typical column with b=12 in. and column depth varying from 12 in. to 24 in was considered. The corner radius was selected to be 4 in., so that b/2r=1.5. The corner radius selected was arbitrary and is not intended to be a recommendation for corner rounding.

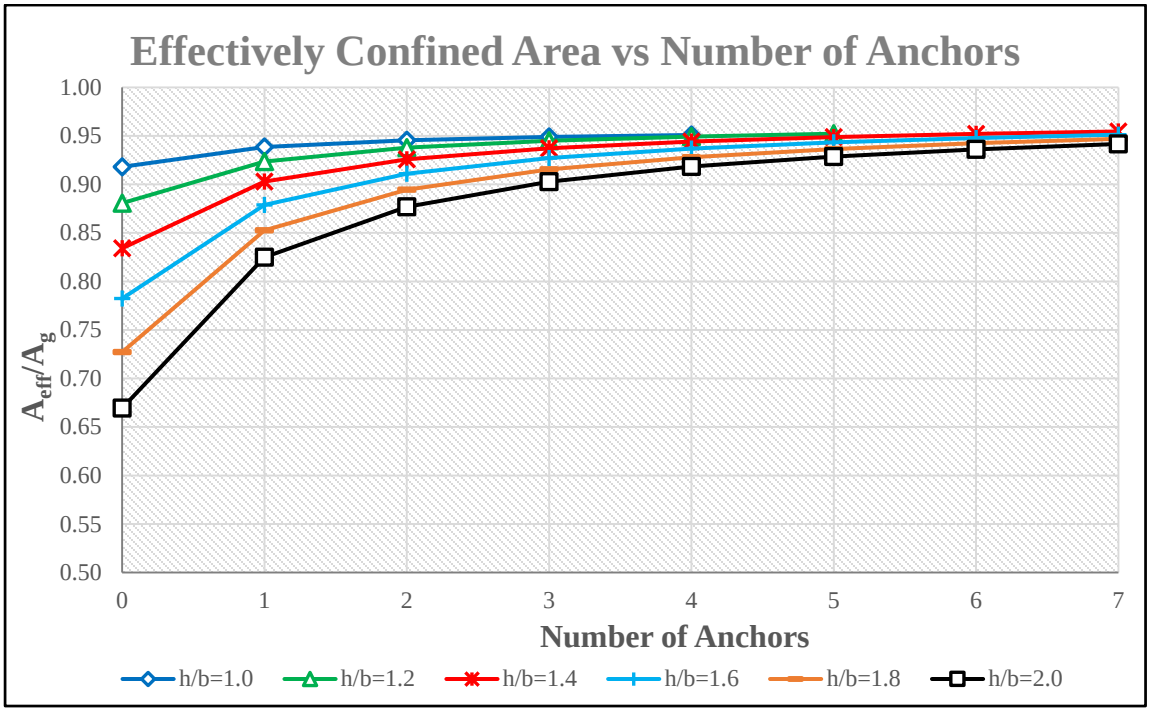

Figure 3.6: Effective confined area without and with anchors

The investigations that are outlined in Table 3.1 have concluded that such positive effects were seen in the experiments. In general, the experimental responses showed that elements that contained FRP anchors for confinement and shear strength (as in Figure

3.5), allowed ductile hinging at the column ends before column shear failure occurred. In addition, the improved confinement achieved with the use of anchors caused a more ductile response without a significant increase in lateral force resistance.

Another indication is that the anchors engage a larger portion of the jacket in confining the concrete. Thus the FRP strains should increase with the use of anchors. However, tests show that the FRP wrap was active and the strain along its perimeter was uniform. This delayed the fracture of the FRP because strains increased more gradually as the lateral drifts increased. The strains were not concentrated at the corners. The tests of Galal et al. (2005) (under lateral loading) illustrate this effect (Figure 3.7). The specimens with anchors are SC2, SC3 and SC1R, while SC2R has no anchors but has more strengthening at the top and bottom of the column.

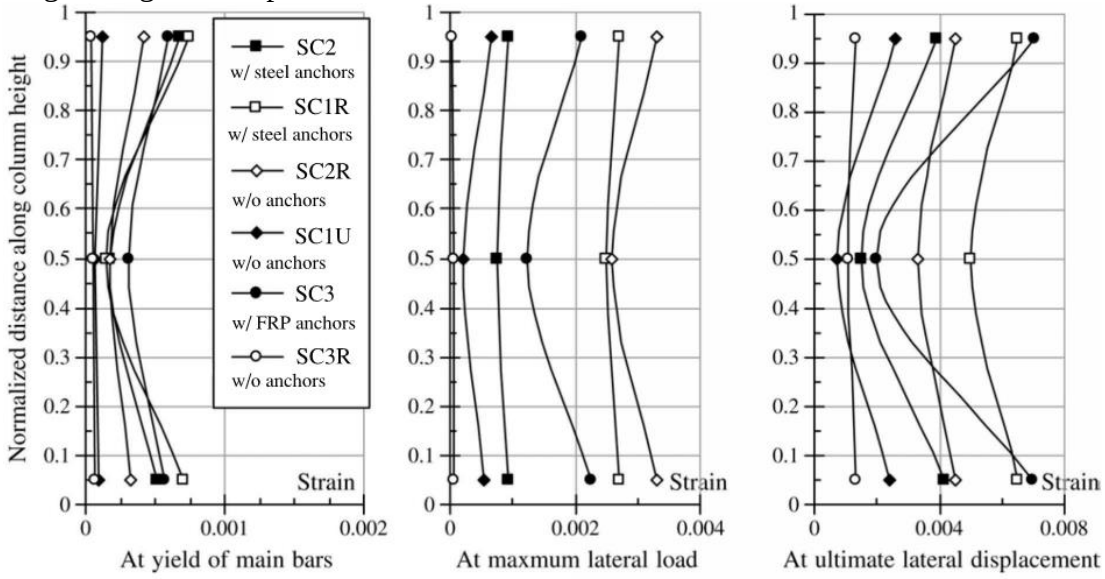

Figure 3.7: FRP strain distribution along column height (Galal et al. 2005)

Another important effect of the anchors on behavior has to do with energy dissipation. In Figure 3.8, Wu et al. (2008) show that columns with anchorage systems

(C4 and C5) dissipated more energy than the other specimens under cyclic lateral loading. Column C2 is the reference as-built column, C3 has only anchors but no jacket, C4 and C5 have jacketing and FRP anchors, while C6 has only jacketing. The cumulative energy dissipation is the area under the load-displacement curve, while the drift ratio is the lateral displacement divided by the height of the column. Anchors were effective in delaying concrete deterioration and preventing buckling of longitudinal reinforcement. This is why columns C4 and C5 continue to dissipate energy at large drift ratios, as seen in Figure 3.8. At the beginning columns C2 and C3 seem to be more "tough" and dissipate more energy at the same drift ratio compared to the other columns because there is more concrete cracking and crushing involved. On the other hand, C4 and C5 are still elastic at that point, but fail at much larger drifts.

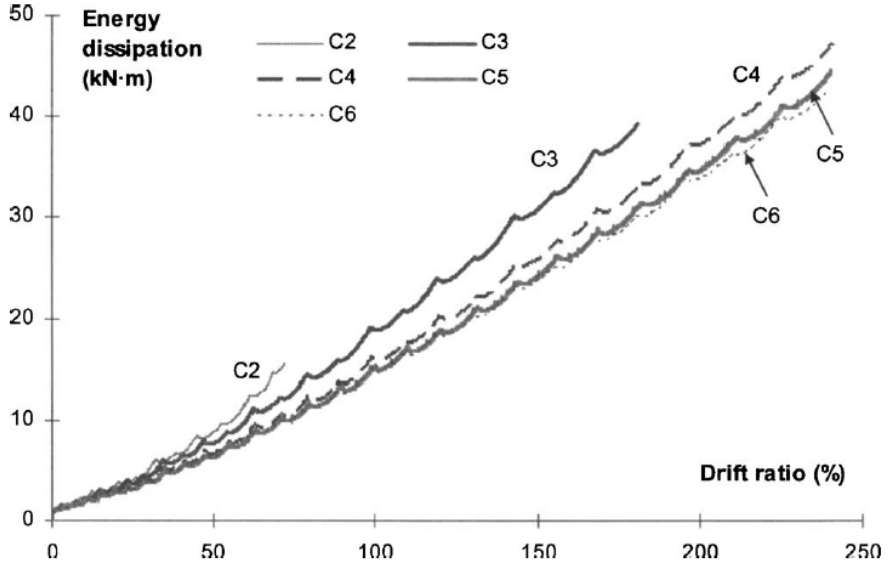

Figure 3.8: Energy dissipation of cyclically loaded columns (Energy dissipation versus cumulative drift ratio) (Wu et al. 2008)

Similar results were presented by Ghobarah and Galal (2004) and Galal et al. (2005). In conclusion, there is limited experimental data (Table 3.1) but clear evidence that anchorage systems increase the effectiveness of an FRP retrofit, as long as sufficient corner rounding is employed to avoid local fracture at sharp corners. More information about corner radii could be found in Chapter 2.

3.5 STRENGTHENING POORLY-DETAILED RC COLUMNS

Many reinforced concrete buildings are vulnerable to seismic damage, because the design did not consider earthquake events. Concrete columns with inadequate transverse reinforcement and/or inadequate lengths of lap splices are often seen. One reason such designs are observed in concrete structures built mainly before the 1970's is that lap splices in column longitudinal reinforcement were based on compression loads only. It is also widely accepted that the adequacy of a lap splice length depends basically on the amount of transverse reinforcement that confines that region. It could be said that the findings of the previous section could lead researchers to conclude that an anchorage system is also helpful in retrofitting poorly detailed lap splices in reinforced concrete columns.

Even though there is evidence of this, there is limited research on this topic so far. However, the investigations of Kim (2008) and Kim et al. (2011) provide some experimental data. Their investigations focused on poorly detailed concrete columns under extreme loading, such as earthquake loads or loss of a column support due to blast effect. Figure 3.9 summarizes the studies noted above. It shows how an anchorage system could be helpful in retrofitting an FRP-wrapped rectangular column. This was the primary motivation for their investigation.

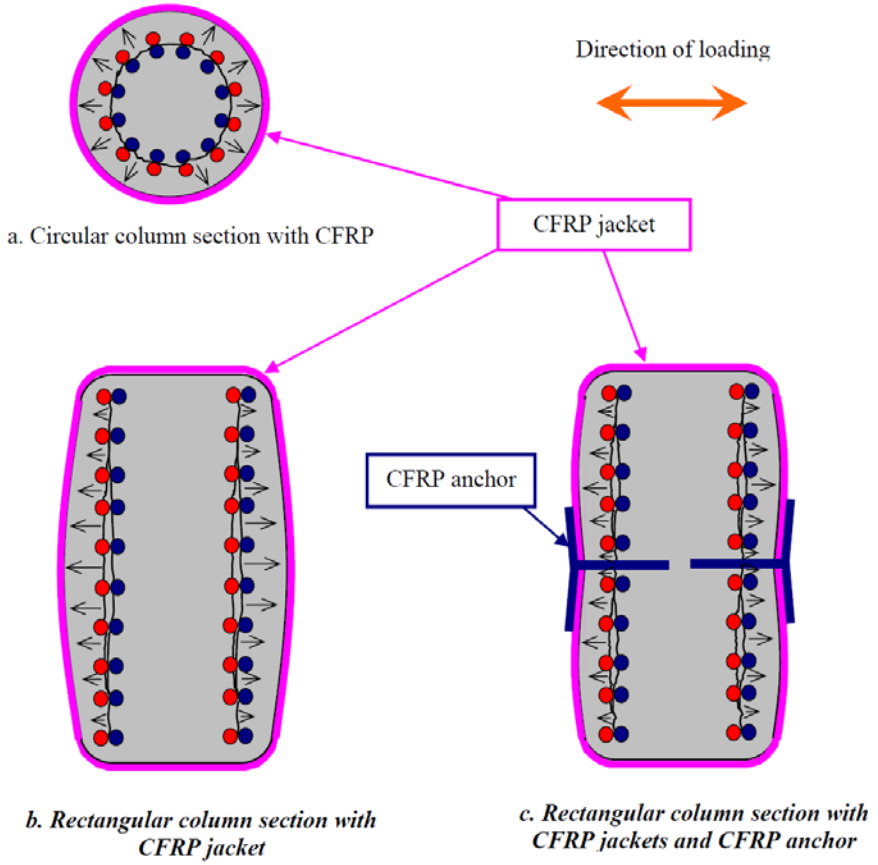

Figure 3.9: Confinement effect of CFRP jackets and CFRP anchors (Kim 2008)

The research project included both square and rectangular columns that were retrofitted using CFRP jackets only, CFRP anchors only, or a combination of CFRP jackets and anchors. The project included both damaged and undamaged columns. The effect of partial jacketing was also studied for cases where walls next to the column faces prevented continuous wrapping. This configuration is illustrated in Figure 3.10.

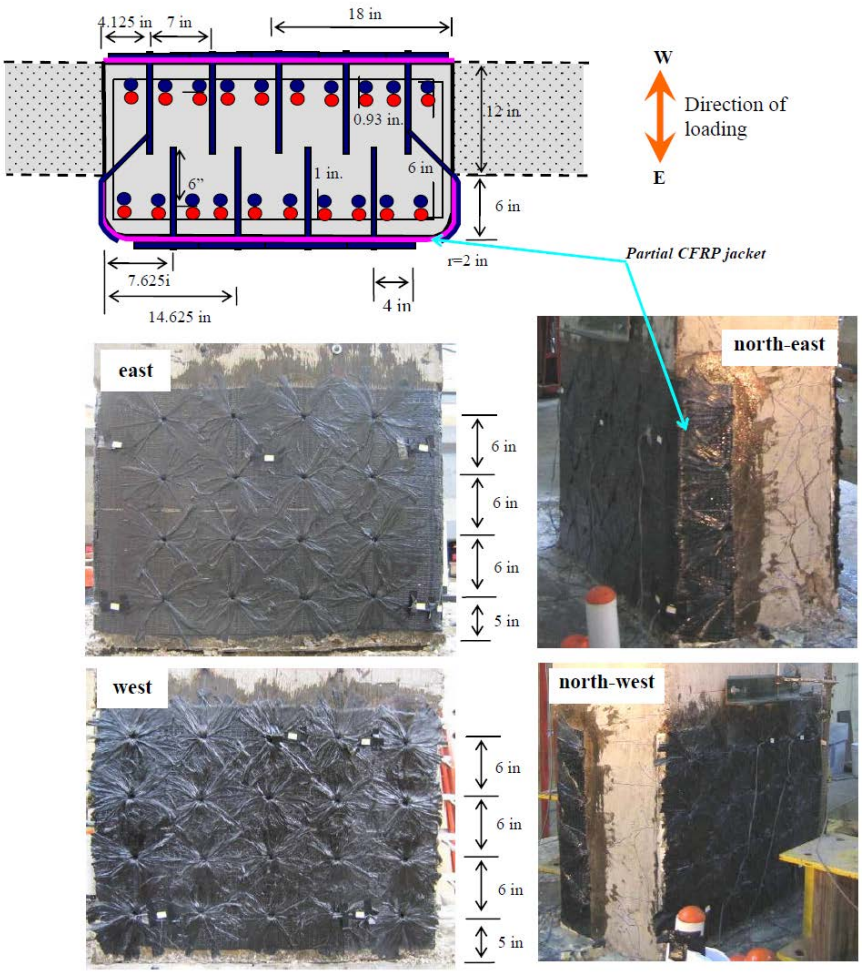

Figure 3.10: Layout of the CFRP jackets and CFRP anchors, specimen 6-C-R20-C (Kim 2008)

The following graph compares two specimens with different number of anchors (8-pinned and 16-pinned) and shows that the number of the anchors mainly influences the deformation capacity and not the strength (as discussed in the previous section).

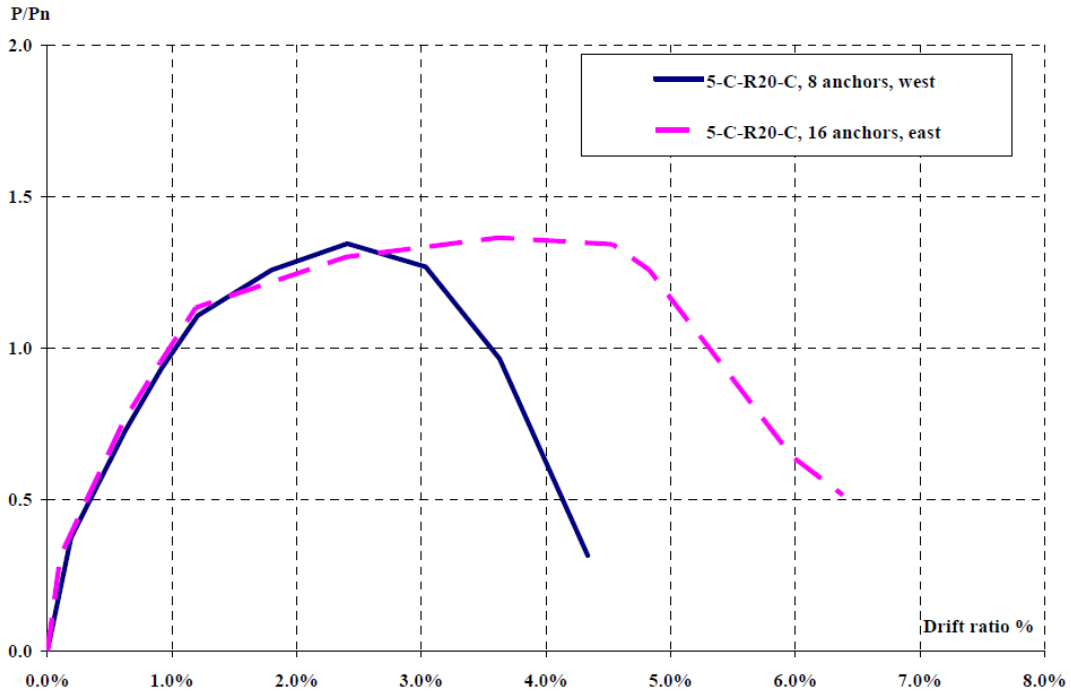

Figure 3.11: Envelope of cyclic response, specimen 5-C-R20-C (Kim 2008)

It was shown by Kim (2008) that the retrofit system (CFRP wraps and anchors) was not as effective in the rectangular columns as it was in square columns. In the case of the rectangular column, there was considerable increase of strength and deformation capacity, but not as much as observed in square columns. That actually implies that a retrofit design of a poorly detailed rectangular column with both FRP jacket and anchors can improve behavior but may not behave as well as a square retrofitted column.

For the partially wrapped column, it was found that the rehabilitation procedure can be as strong as a fully wrapped column with anchors but may not exhibit as much ductility, as illustrated in Figure 3.12.

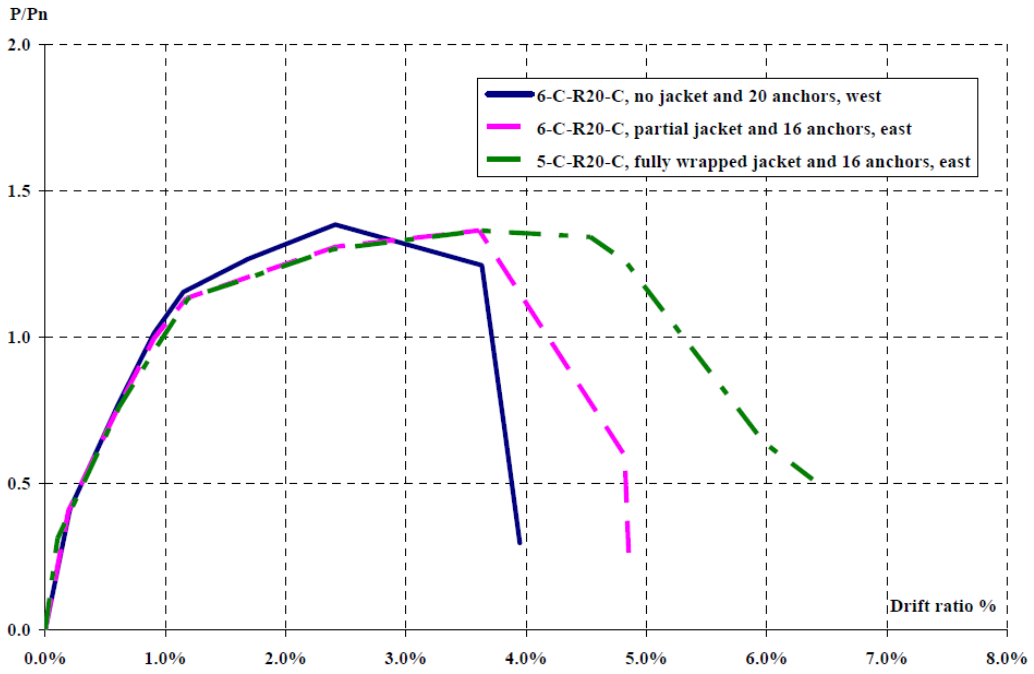

Figure 3.12: Envelope of cyclic response, specimens 5-C-R20-C & 6-C-R20-C (Kim 2008)

In conclusion, the findings of Kim (2008) showed that the same fundamental principles that were described in Chapter 2 apply to strengthening lap splice regions in columns. The main focus of such strengthening is to prevent brittle lap splice failure and to improve ductility through longitudinal reinforcement yielding. Corner radius, confinement effect and the shape of the cross-section are key parameters that have to be included in the design procedure.

3.6 DESIGN GUIDELINES & RECOMMENDATIONS

Design guidelines in international codes have been proposed for use of FRP confinement the past 15 years, but as it has been noted repeatedly, there is still much research to be done for large rectangular columns. A complete review of design

recommendations by five international design codes can be found in the paper of Tahir et al. (2013). In this section the design recommendations proposed by Kim (2008), developed from the experimental investigation, are discussed.

As explained previously, the column lap splices considered by Kim (2008) were designed following code provisions of ACI 318-63 and ACI 318-71. Strengthening of undamaged columns and repair of damaged columns was studied. Table 3.2 shows the recommendation for column strengthening/repair.

Table 3.2: Summary of lap splice conditions suitable for rehabilitation (Kim 2008)

Design code	ACI 318- 63		ACI 318- 71	
Number of spliced bars on a column face	Less than 5 spliced bars	Between 5 and 10 spliced bars	Less than 5 spliced bars	Between 5 and 10 spliced bars
Strengtheing (As-built column)	Yes	Yes	Yes	Yes
Repair (Damaged column)	Yes	Yes	Yes	No

The equation of ACI 318 for design of lap splices that limits the confinement factor to 2.5 was used to show that this factor for sufficiently CFRP-strengthened column can be larger. The confinement factor is $(c_b+K_{tr})/d_b$ and with a known l_d, was estimated to be between 3.2 and 4.4 in the test program. The estimated values indicate, that the actual effectiveness of the CFRP confinement can be larger than the code allows.

$$l_d = \left[\frac{3}{40}\frac{f_y}{\sqrt{f'_c}}\frac{\psi_t\psi_e\psi_s}{\left(\frac{c_b + K_{tr}}{d_b}\right)}\right]d_b \qquad \text{ACI 318-08 Section 12.2.3} \qquad (3.6)$$

l_d = development length for deformed bar in tension, in.

d_b = diameter of bar, in.

f'_c = compressive strength of concrete, psi

f_y = yield strength of reinforcement, psi

ψ_t, ψ_e, ψ_s = modification factor based on bar location, coating and size

c_b = a factor that represents the smallest of the side cover

K_{tr} = a factor that represents the contribution of confining reinforcement across potential splitting planes.

The above equation suggests the required lap splice length to avoid lap splice failure. Since splice failure was avoided in the tests, the above equation was used to estimate the confinement factor.

The number and the diameter of the FRP anchors must be determined in the design process. In the recommended design procedure of Kim (2008), shear friction was used. According to this design method (section 11.6 of ACI 318-11), the peak shear friction strength is the smallest of $0.2f'_cA_c$, $(480+0.08f'_c)A_c$ and $1600A_c$. A_c is the area of concrete section resisting shear transfer. Kim (2008) suggested that the shear friction strength should be greater than the expected tensile force in the spliced longitudinal bars ($T_b=1.25f_yA_s$), as illustrated in Figure 3.13.

The shear friction force developed by the tensile force in the CFRP wraps, anchors and the transverse steel needs to be larger than T_b. In the calculations of the forces developed in the anchors and the jacket, it was assumed that 1/3 of their ultimate strength can be developed, a conservative value derived from experimental results.

Other experimental investigations have shown that jackets can sometimes rupture and control the behavior of the column. Therefore, the nominal effective stress level in the FRP reinforcement can be alternatively calculated in accordance with Equations 3.7 and 3.8:

$$f_{fe} = 0.85E_f\varepsilon_{fe}, where\ \varepsilon_{fe} \leq \varepsilon_{fd} \quad (3.7)$$

$$\varepsilon_{fd} = 0.083\sqrt{\frac{f'_c}{n_f E_f t_f}} \leq 0.9\varepsilon_{fu} \quad (3.8)$$

These equations were suggested by ACI 440.2R (2008). The ε_{fd} term is the same as $\varepsilon_{h,rup}$ discussed by Lam and Teng (2003), who recommended a fixed value of $\varepsilon_{h,rup}=0.75\varepsilon_{fu}$. The parameter n_f is the number of FRP layers.

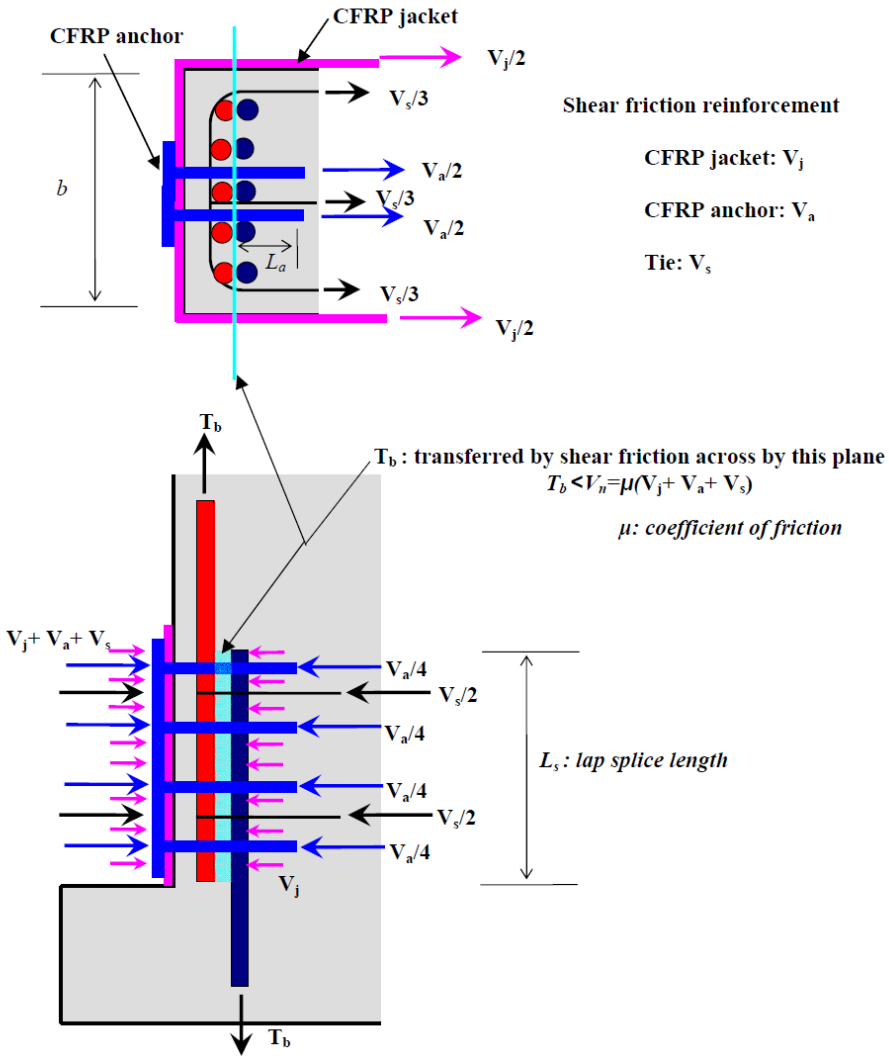

Figure 3.13: Shear friction mechanism for a typical specimen (Kim 2008)

Kim (2008) suggested that the following equations be used to calculate the required number and area of the anchors:

$$V_n = \mu(V_j + V_a + V_s) \geq T_b \quad (3.9)$$

$$V_j = (f_{fu}/3)t_f(2L_j) \quad (3.10)$$

$$V_a = n_a(f_{fu}/3)A_a \quad (3.11)$$

$$V_s = f_y A_{vf} \tag{3.12}$$

$$\frac{n_a A_a}{t_f} \geq \frac{1}{t_f}\frac{3}{f_{fu}}\left[\frac{T_b}{\mu} - \left(\frac{f_{fu}}{3}\right) t_f (2L_j) - f_y A_{vf}\right] \tag{3.13}$$

μ = coefficient of friction = 1.4 (ACI 318-08, 11.6.4.3)

V_n = nominal shear strength, lb

V_j = force perpendicular to shear plane contributed by CFRP jackets, lb

V_a = force perpendicular to shear plane contributed by CFRP anchors, lb

V_s = force perpendicular to shear plane contributed by transverse steel reinforcement, lb

f_{fu} = tensile strength of CFRP, psi

t_f = thickness of CFRP sheet, in.

L_j = width of CFRP jacket, in.

n_a = number of CFRP anchors

A_a = area of a CFRP anchor, in2

A_{vf} = area of steel shear-friction reinforcement, in2

$n_a A_a / t_f$ = effective width of total CFRP anchors, in2

Because the main topic of these design guidelines is lap splice strengthening, the maximum clear distance between the anchor and the spliced bars should be specified. Kim (2008) suggests that this clear distance should be less than 1.25 inches and there should be at least one anchor between no more than 2 longitudinal bars, excepting the corner bars of the column. Apart from the 1.25 in. clear spacing, the suggestion for at least an anchor between two bars is reasonable for typical seismic strengthening as well. The spliced bars tend to split the concrete cover. Thus, an anchor should restrict such deformation. The exact number of anchors between two longitudinal bars needs more research, because it depends on the effective area of the anchor, as shown in Figure 3.14. This effective region

is directly affected by the concrete cover and the distance between the two bars. For example, for larger distances, more than one anchor might be needed.

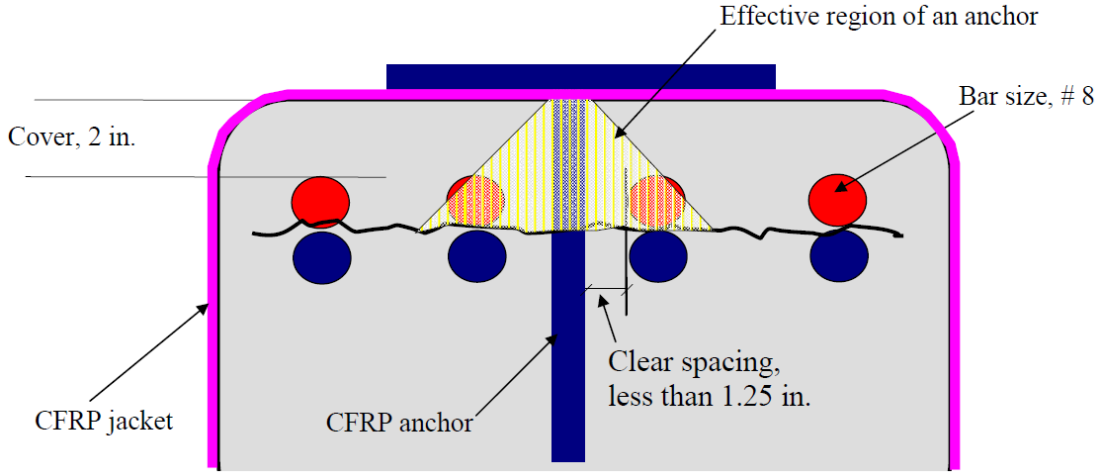

Figure 3.14: Suggested spacing between CFRP anchor and lap spliced bars (Kim 2008)

As for vertical spacing along the height of the jacket, the CFRP anchors should be at most 6 in. or ¼ of the lap splice length. Finally, the diameter and the depth of anchor hole to prevent bond failure of a CFRP anchor is discussed. In addition the area of the hole needs to be at least 40% larger than the area of the anchor for practical purposes. The maximum axial force that can be developed, was found in a previous section (N_u from equation (3.1)). Kim (2008) provided an alternative expression:

$$P_n = 4\sqrt{f'_c} \cdot h_c \cdot (d_c + h_c) \cdot \pi + 22\sqrt{f'_c} \cdot h_c \cdot (L_a - h_c) \quad (3.14)$$

P_n: tensile strength of CFRP anchor, lb

h_c: concrete cone depth, 2 in. (Ozdemir and Akyuz 2006)

d_h: diameter of anchor hole, in.

L_a: depth of anchor hole from the shear plane > 4 in. (Ozdemir and Akyuz 2006)

The recommendations of Kim (2008) are driven by experimental results where CFRP wraps and CFRP anchors were used. These design recommendations should be applied to all the test data that is available in the literature in order to conclude whether they compare well with other investigations.

Finally, apart from the anchors, design recommendations for the FRP jacket should be provided. As explained in Chapter 2, the thickness, or equivalent the number of FRP sheets, should be designed according to the minimum thickness equation of Hu (2013), the most recent criterion reported in the literature and one that tends to be conservative.

Kim (2008) suggests that if the aforementioned design guidelines are used, the behavior can be similar to typical reinforced concrete columns that are confined only by transverse steel reinforcement. More specifically, the backbone curves of FEMA 356 (Prestandard and Commentary for the Seismic Rehabilitation of Buildings, 2000) were compared to the experimental results.

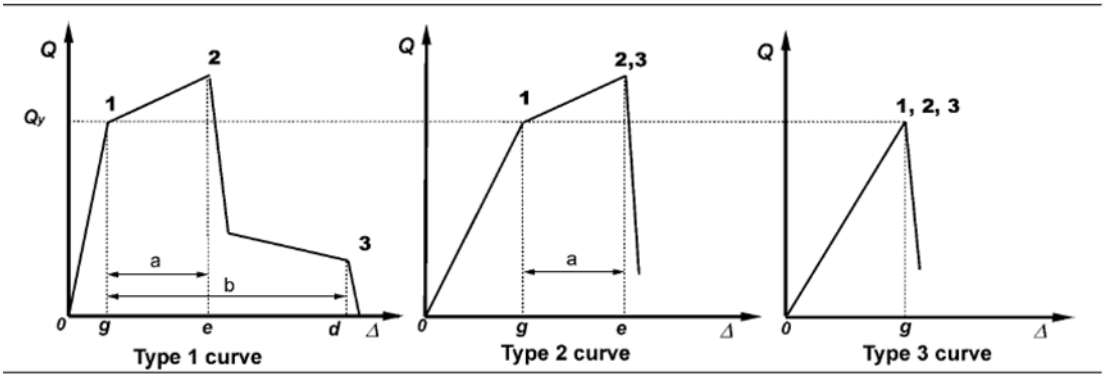

Figure 3.15: Component force vs deformation curves (FEMA 356, 2000)

It was shown that the Type-2 curve can be used, even though not much information exists regarding residual behavior. Also, the behavior of all the tested columns proved to be deformation-controlled. The interesting finding was that the column that had sufficient

number of anchors (16-pinned) had behavior similar to columns that are specified as “well confined” in the provisions (Conforming transverse reinforcement, for closely-spaced hoops). Furthermore, columns with partial jacketing or fewer anchors (8-pinned) exhibited slightly less satisfactory behavior. Figure 3.16 shows the trends for the different rehabilitation methods, with idealized curves developed according to the provisions of FEMA 356.

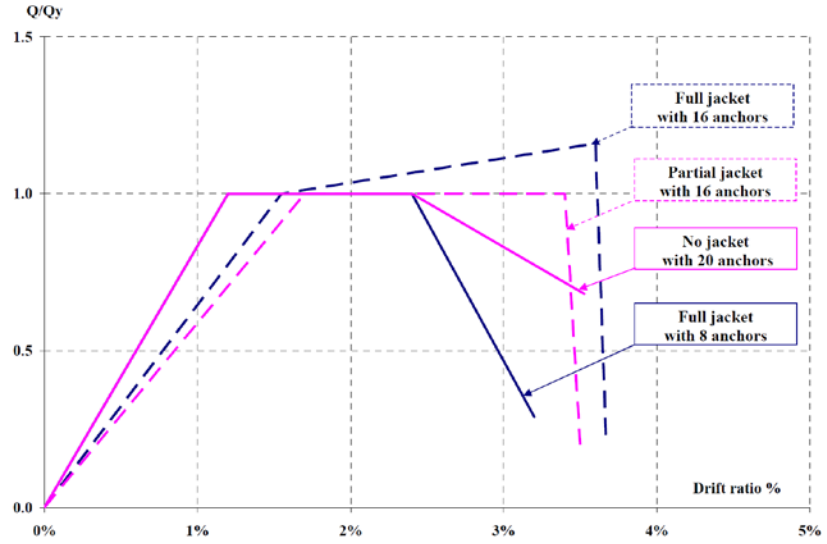

Figure 3.16: Type-2 curves for different rehabilitation methods (Kim 2008)

Similar Type-2 curves could be created for all the column tests available in the literature. Those curves should subsequently be compared to the FEMA 356 to draw useful conclusions. In this study, similar curves will be produced only for specimens of an experimental study discussed in Chapter 4.

Chapter 4: Analysis Investigation and Examples

4.1 Summary of the chapter

The topics discussed in the previous chapters will be investigated using an example from the literature. As explained in Chapter 2, the number of FRP plies, the concrete strength and the corner radius are some of the parameters that highly affect the behavior of an FRP-confined concrete column under uniaxial compression. In this chapter, the behavior under cyclic lateral loading of columns that are not fully but partially wrapped is examined. For this reason the experimental study of Ozcan et al. (2010), in which a representative example that included both CFRP wraps and CFRP anchors for the confinement of the columns is discussed. The experimental study is described and the analysis tools used are outlined. The experimental results are presented and discussed. Furthermore, the analysis results and the experimental results are compared and discussed. Finally, there is an example of how the analysis model can be used to accommodate the presence of CFRP anchors in one face of the column. Important parameters such as the shape factor that was defined in Chapter 2 will be adjusted and the effect of anchors will be illustrated comparing the analytical response before and after adding the anchors.

4.2 Analysis Tool: OpenSees

OpenSees is open source object-oriented software based on finite element computer applications. It is able to simulate structural response of systems subjected to earthquake motions (Mazzoni et al. 2006). OpenSees is widely-known scientific software with advanced capabilities that can be used for research and for analysis of structural and geotechnical simulations. Different from the typical commercial programs, OpenSees models are built by writing code in .tcl files, which contain the different characteristics of a simulation such as geometry, load patterns, recorders, and others. As part of the current

project, the experimental results of the study that will be described later are compared to an analytical model that was developed using OpenSees.

The OpenSees model built and tested in the current study is based on the example number 4, provided by the website of this open source software, in which a portal frame is analyzed under several loadings (including static reversed cyclic). The type of element used is the *Distributed Plasticity Element*, while for the cross-section, a *Fiber Section* is used. Lastly, the slip of the anchored reinforcing bars at the bottom of the column is also taken into account using the *BarSlip* uniaxial material at the base of the column. This material simulates the bar force versus slip response of a reinforcing bar anchored in a beam-column joint and also exhibits degradation under cyclic loading (Lowes et al. 2003).

4.3 EXPERIMENTAL PROGRAM BY OZCAN ET AL. (2010)

4.3.1 Experimental Program Description

The experimental study investigated in this chapter was conducted by Ozcan et al. (2010) and focuses on the confinement and ductility enhancement of flexure dominated reinforced concrete columns after strengthening with FRP wraps. The study consisted of five rectangular columns that have low concrete uniaxial compressive strength (1.3 to 2.2 ksi) and other seismic vulnerabilities, such as the use of plain bars and insufficient transverse reinforcement. Such deficiencies are often responsible for the collapse or extensive damage of buildings during earthquakes.

The effects of the parameters described in Chapter 2 in FRP-strengthened columns under cyclic loading will be investigated. More specifically, the effect of confinement provided by the means of FRP, the use of anchor dowels and the effect of the low strength concrete are the main topics that will be discussed in this chapter. The details of specimens tested by Ozcan et al. (2010) are illustrated in Figure 4.1. A more detailed description of

the features is given in Table 4.1, converted to imperial units. The poor-quality of the concrete used is obvious (details in Table 4.1) as well as the low transverse reinforcement provided for confinement. It is shown in the following sections that negligible strength enhancement was provided by the confinement of the transverse steel. Finally, Figure 4.2 shows the configuration of the anchors (pins) used (if any) in the four strengthened specimens. The number and the configuration of the anchors will be of great significance in the later sections. The corner radius was around 1.2 in. (30mm) in all cases.

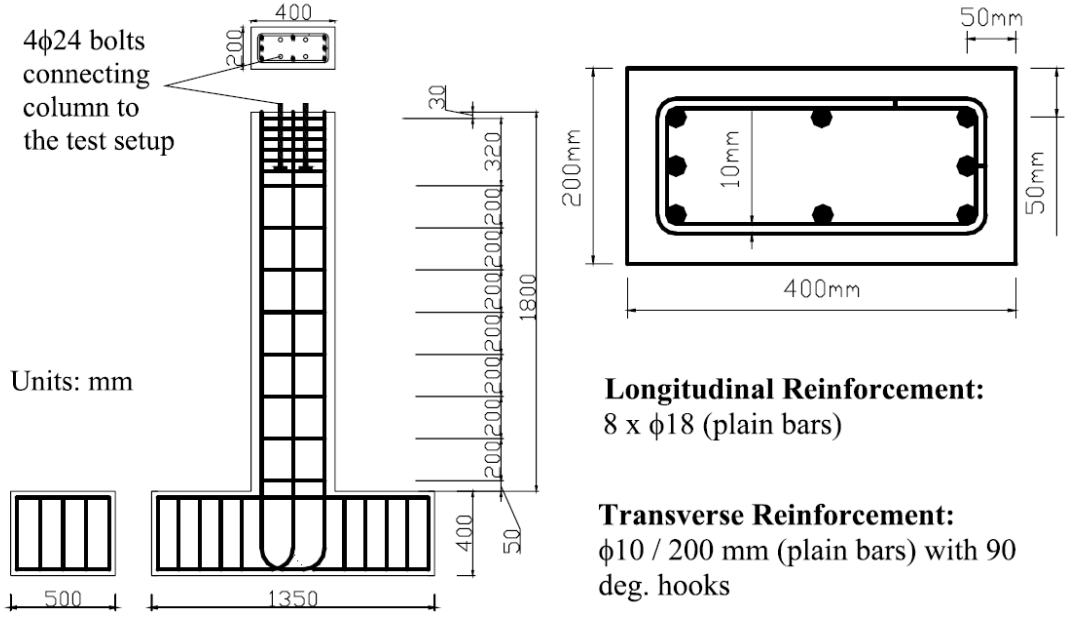

Figure 4.1: Specimen Details (Ozcan et al. 2010)

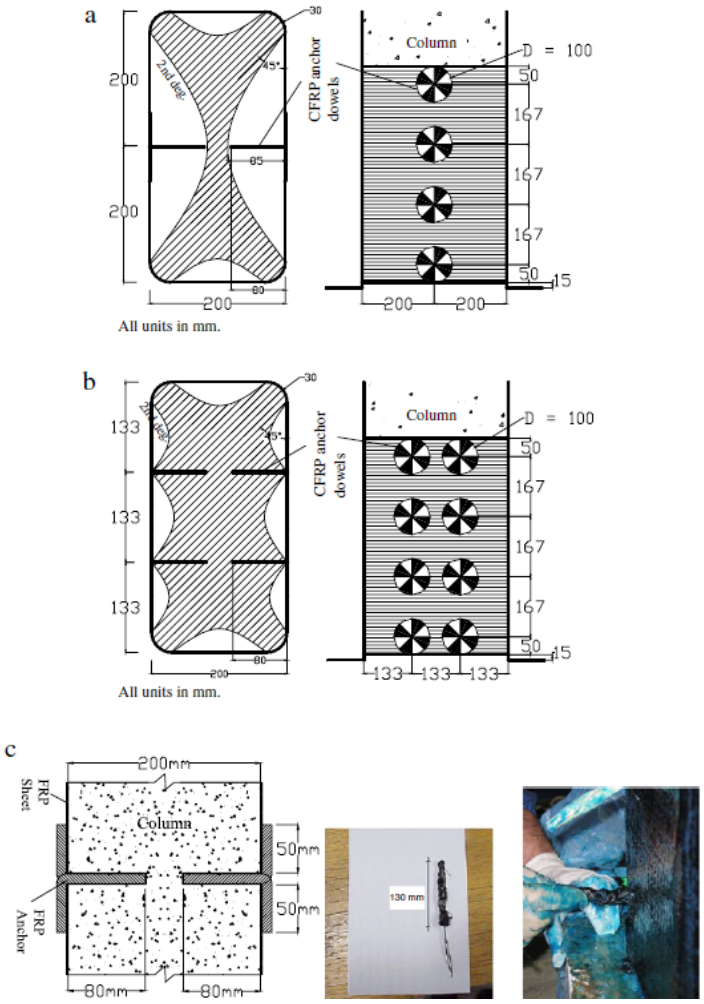

Figure 4.2: (a) CFRP anchorage configurations for 8-pinned and (b) 16-pinned type, (c) CFRP anchor dowel detailing (Ozcan et al. 2010)

Table 4.1: Specimen Details

Specimen name	f'_c (ksi)	f_y (ksi)	Steel reinforcement		Longitudinal steel ratio	Axial load		CFRP properties	
			Longitudinal	Transverse		Value (kips)	Ratio N/No $No=0.85f'_cA_g+A_sf_y$	Number of plies	Strengthening
S1	1.74	287	8x0.7" plain bars (18mm bars)	0.4" diameter bars @8" (10mm bars)	2.55%	110	35%	0	-
S2	1.45					99		1	16-pinned
S3	1.52					102		1	8-pinned
S4	1.31					94		1	No-pinned
S5	2.25					129		1	16-pinned

The specimens were tested under quasi-static cyclic lateral loading after the axial load was applied. The scheme of the cyclic loading is shown in Figure 4.3 and is the same that considered in the analyses.

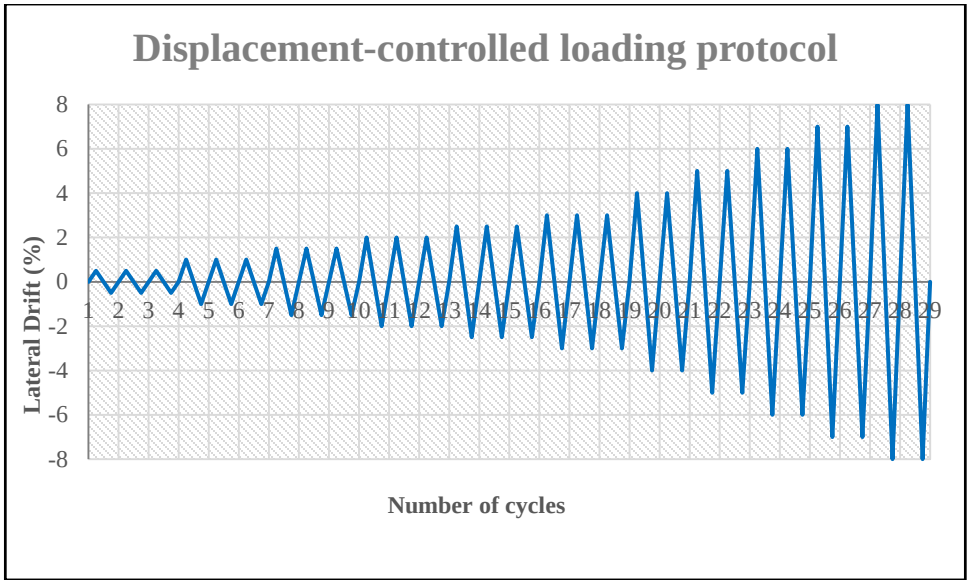

Figure 4.3: Displacement-controlled loading protocol

4.3.2 Concrete

4.3.2.1 Unconfined Concrete

The next graph shows the concrete compressive stress-strain relationship that was used for the analysis of each specimen. The model by Chang and Mander (1994) (*Concrete 07* in Opensees) was used for modeling the concrete constitutive response. The model takes the tensile strength of the concrete into account. As was expected, the higher the strength, the lower the ultimate strain. It is also useful to notice that even for the concrete with a maximum strength of 2.25 ksi, the strain at maximum stress is considerably lower than 0.002, which is the typical value for concrete commonly used in practice.

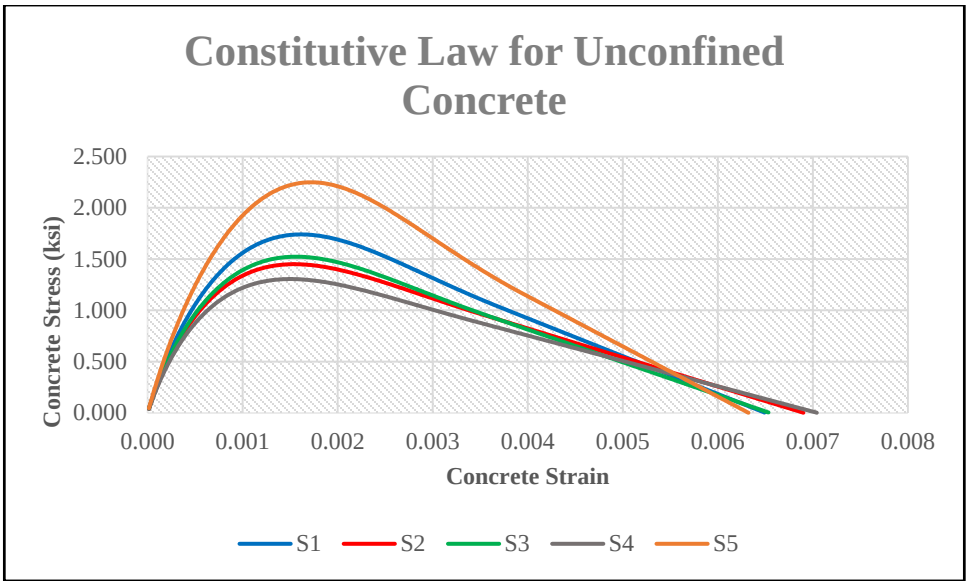

Figure 4.4: Constitutive law for unconfined concrete for all specimens

4.3.2.2 Confined Concrete

Figure 4.5 shows the steel-confined concrete behavior for each one of the five specimens. It is interesting to point out that the low transverse steel ratio provides almost no strength enhancement but increases deformation capacity because the original concrete strength is very low. Finally, the higher the concrete strength, the lower the ultimate strain of the confined concrete.

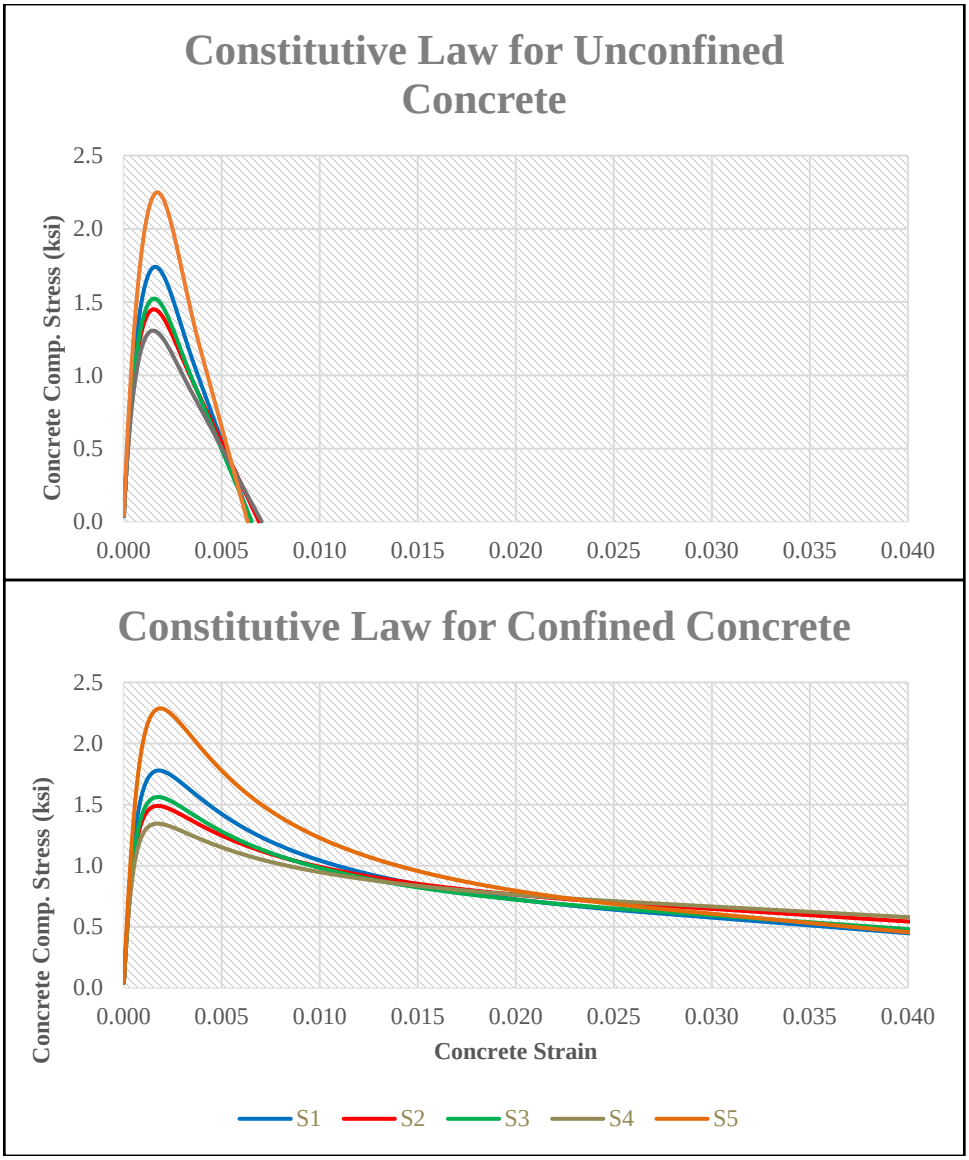

Figure 4.5: Constitutive law for steel-confined concrete for all specimens

4.3.3 FRP-Confined Concrete

The most interesting part of this study is the investigation and analysis of the FRP-confined concrete behavior. For this reason, the capabilities of a widely accepted model by Lam and Teng (2003) were used and will be explored. The selection of this model was

based on its ease of use and its inclusion in the ACI 440 guidelines. As for the parameters that were used, it should be noted that the authors suggest that the FRP rupture occurs at a strain equal to 75% of the rupture strain (0.015) provided by the manufacturer. Furthermore, the carbon fiber sheets used for strengthening had a thickness of 0.0065 in. and their elastic modulus was 33,350 ksi (stiffer than steel). It has to be noted that the fiber/epoxy matrix will have a lower elastic modulus, but this detail was not taken into consideration in the analysis.

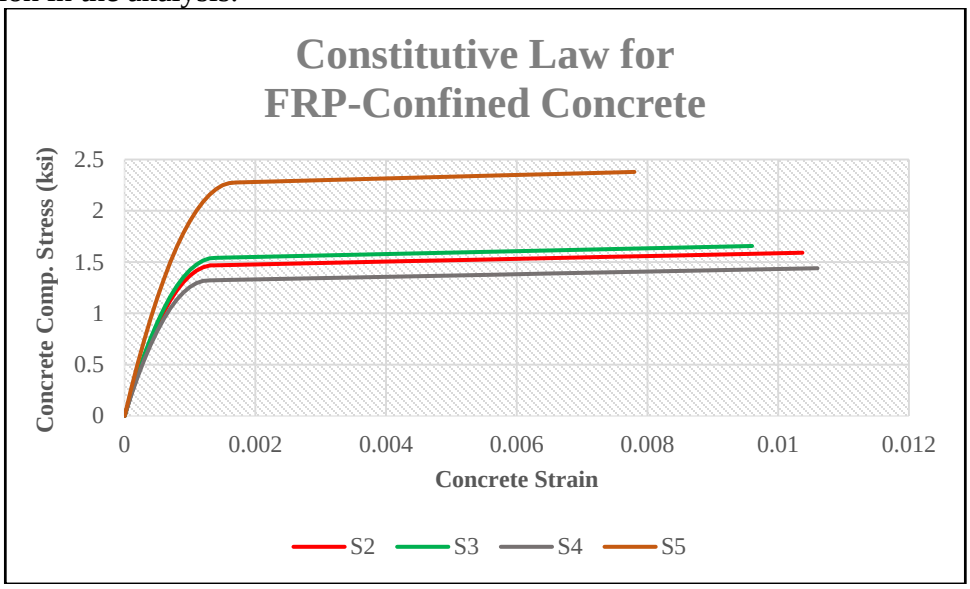

Figure 4.6: Constitutive law for CFRP-confined concrete for all specimens

As can be observed in Figure 4.6, the lower the original concrete strength, the higher the computed ultimate strain of the CFRP-confined concrete under uniaxial compression. It is also shown that ductility enhancement is not that significant, because of the low confinement ratio, which is dominated by the large aspect ratio of column section. The question that arises is how the transverse steel provides more ductility enhancement than the CFRP wraps. A similar trend is also observed in Figure 4.7. It is

shown that the computed post-peak branch of the CFRP-confined concrete is ascending compared to the steel-confined concrete that has a descending branch, but the computed post-peak branch of the CFRP-confined concrete is terminated considerably earlier. Again, these are the sectional analysis results. One possible reason for this response could be that the high dilatational properties of the low-strength concrete lead to high lateral strains that can be accommodated by the post-yielding behavior of the transverse steel but not by the CFRP that ruptures suddenly at a strain about 75% of the fracture strain. In general, the FRP rupture strain is usually the dominant parameter that controls the behavior, because after fracture of the FRP wrap, the previously confined concrete is free to spall. These hypotheses will be examined in the following sections. After comparing the analysis results with the experimental data, some conclusions are become apparent.

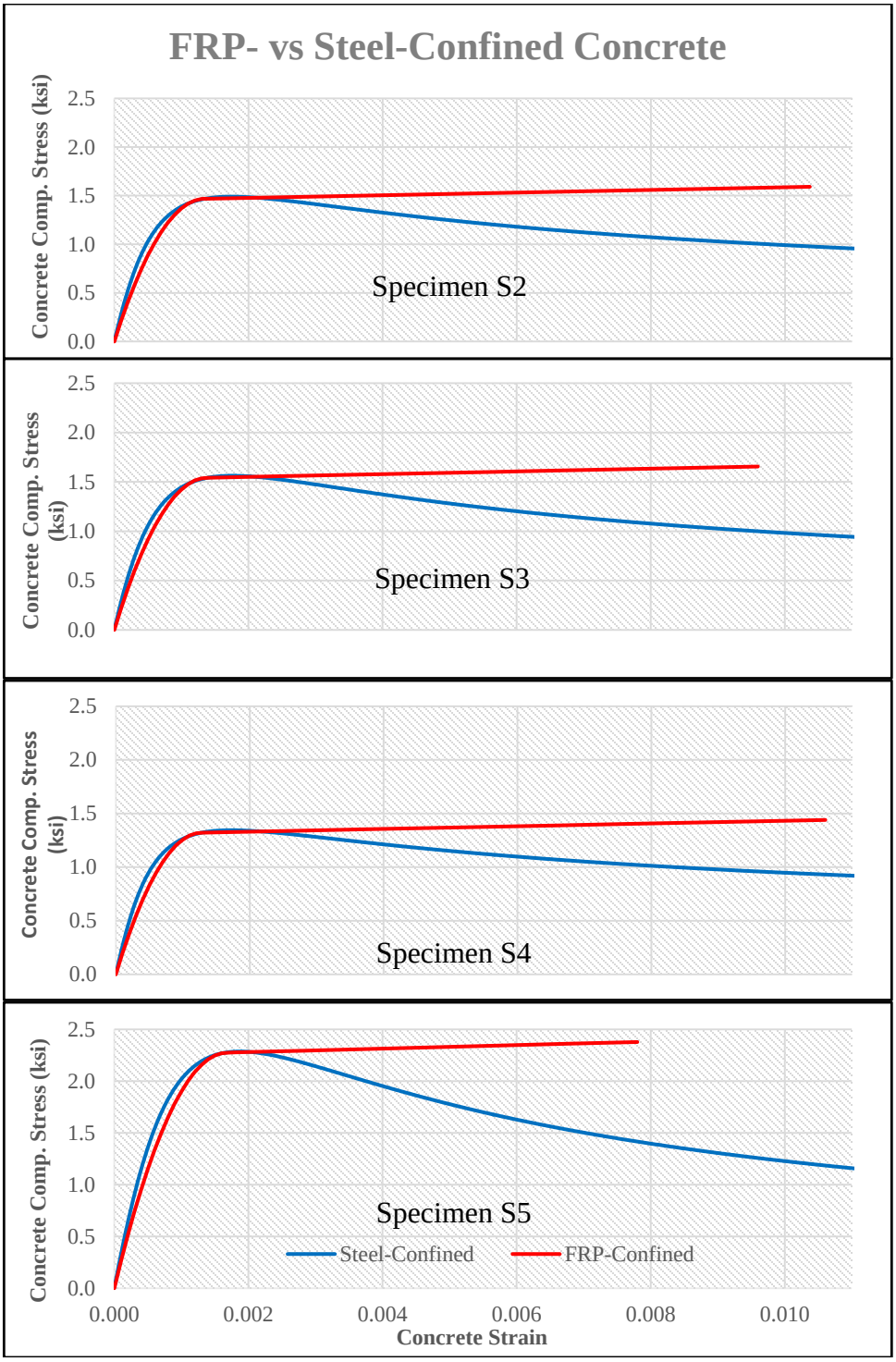

Figure 4.7: Comparison between FRP- and steel-confined concrete

4.3.4 Response Comparison of computed results and experimental response

In this section, the experimental and analytical results will be presented and compared. For each specimen the first graph presented shows the actual experimental or analysis response in imperial units (kips, inches). A normalized response will be shown in the graph that follows, where the load is divided by the peak load observed during the tests. For the analysis results, the load will be divided by the peak load observed in the analysis response, as shown in Table 4.2. The graphs with the *normalized response* are used to draw conclusions regarding the effect of the strengthening employed, a comparison that is more difficult to be made in the response graphs, because of the difference in the concrete strengths. Note that all the specimens failed because of longitudinal bar buckling. As shown earlier, there were only a few transverse steel ties provided, resulting in little confinement of the concrete. The FRP confinement delayed bar buckling, but did not prevent it. As a result, all the specimens failed suddenly and earlier than that predicted by the analysis. This finding is presented in section 4.3.5.

Table 4.2: Peak loads in experiment (average values) and analysis

Specimen name	Test P_{max} (kips)	Analysis P_{max} (kips)
S1	13.0	14.5
S2	10.7	14.0
S3	11.8	14.3
S4	11.0	13.5
S5	17.4	16.6

4.3.4.1 Test Results

In this section the experimental results of Ozcan et al. (2010) are presented. The comparisons are a) between specimens S1, S2 & S5, b) S1, S3 & S4, c) S1, S3 & S5 and d) S1, S2 & S3.

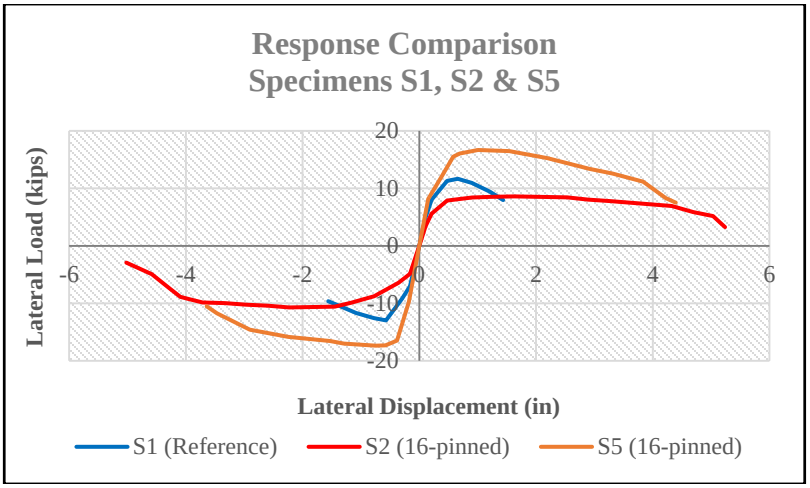

Figure 4.8: Experimental response comparison for specimens S1, S2 & S5

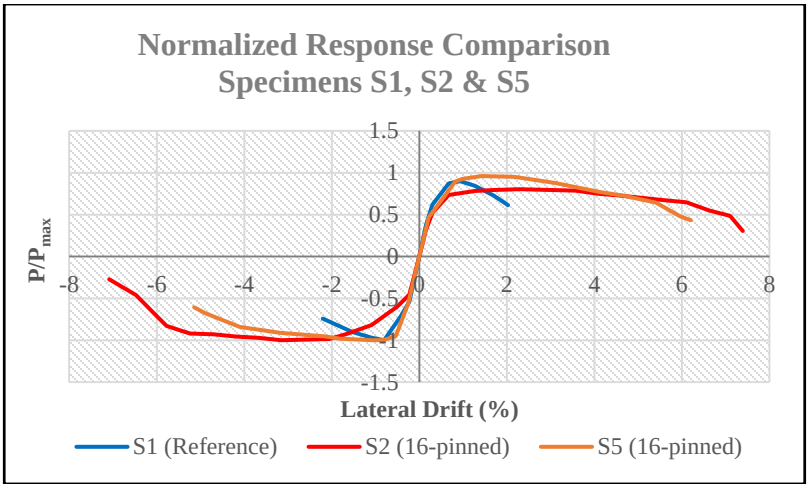

Figure 4.9: Experimental normalized response comparison for specimens S1, S2 & S5

Figure 4.8 and Figure 4.9 show the strength and ductility enhancement of S2 and S5 specimens due to the CFRP wraps and the anchor configuration of Figure 4.2b (16-pinned). The figures also show that for the same amount of CFRP material and anchors, the strength and ductility enhancement can be different due to the difference in the

unconfined concrete strength (1.45 ksi in S2 and 2.25 ksi in S5). This is likely a function of different axial load levels as well.

Results presented in Figure 4.10 and Figure 4.11 show that even though the strengthening configuration used for the specimens differed (8-pinned for S3 and no-pinned for S4), the response was shown to be quite similar. This could be attributed to failure of the CFRP anchors that strengthened the column more than the CFRP wrap. In other words, if the number and the configuration of the anchors used is not well designed then the behavior is similar to the one without any anchors. However, there is a small difference in the ductility enhancement (less than 1% drift).

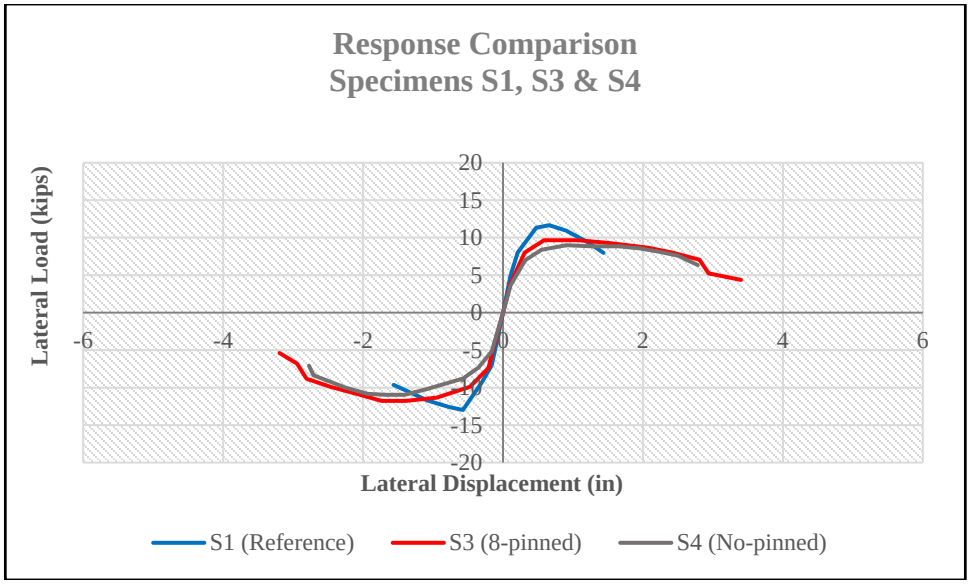

Figure 4.10: Experimental response comparison for specimens S1, S3 & S4

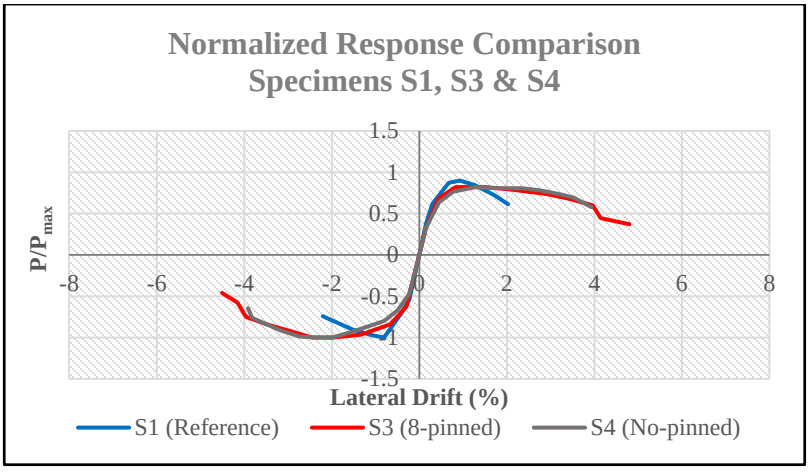

Figure 4.11: Experimental normalized response comparison for specimens S1, S3 & S4

It is obvious that the more anchors used in a column the better the confinement provided by the CFRP wrap. For columns with sectional aspect ratios of 2.0, the number of anchors is crucial, as shown in Figure 4.12 and Figure 4.13.

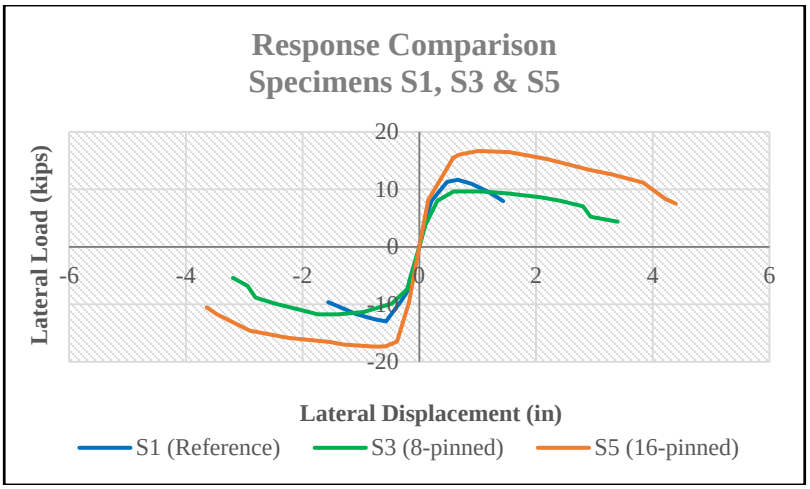

Figure 4.12: Experimental response comparison for specimens S1, S3 & S5

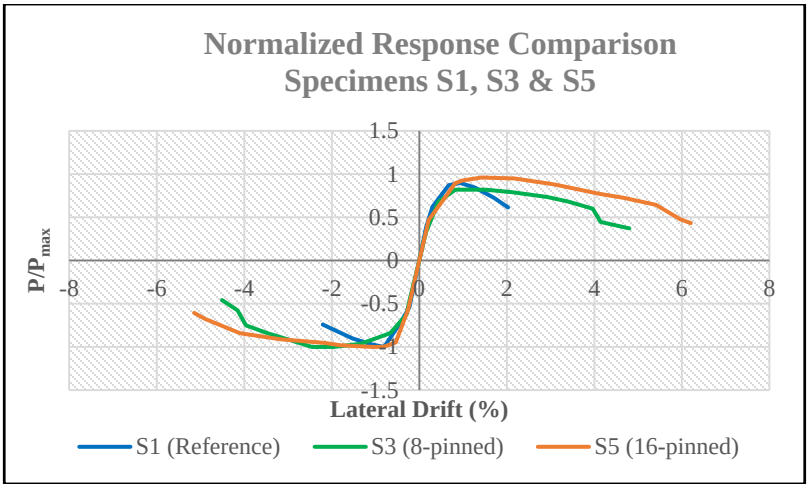

Figure 4.13: Experimental normalized response comparison for specimens S1, S3 & S5

Figure 4.14 and Figure 4.15 show the important effect of the number of anchors for columns with almost identical unconfined concrete strengths. Ductility enhancement is quite significant even though the strength is nearly the same.

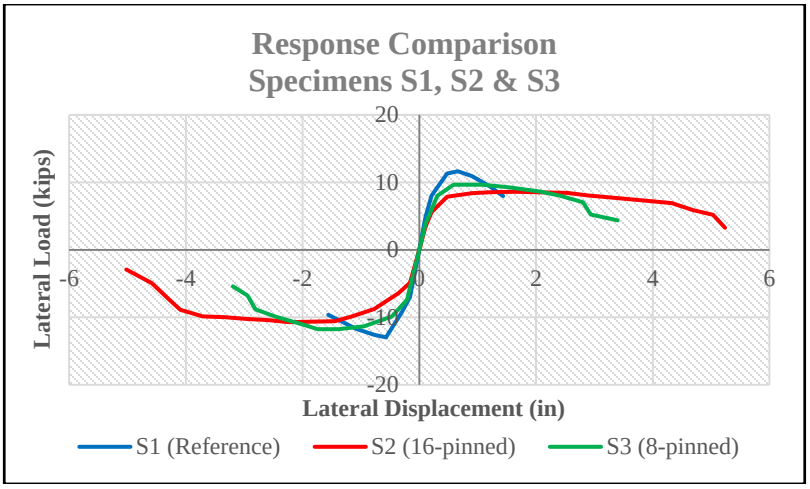

Figure 4.14: Experimental response comparison for specimens S1, S2 & S3

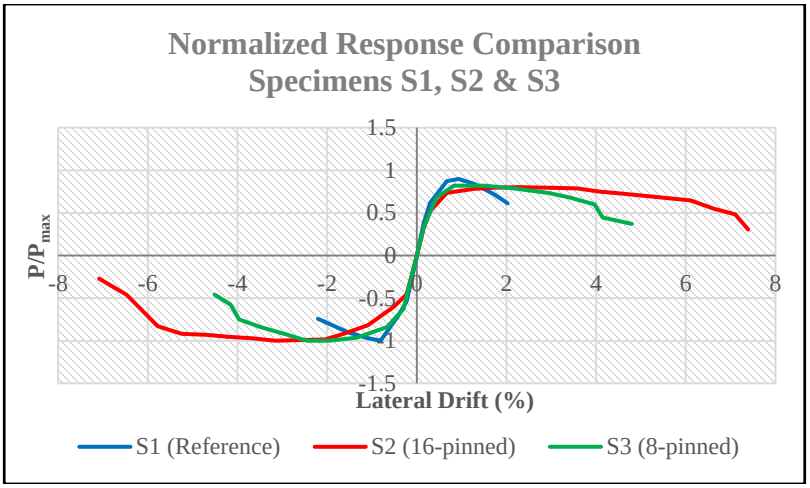

Figure 4.15: Experimental normalized response comparison for specimens S1, S2 & S3

4.3.4.2 Analysis Results

As in the comparison of experimental results, similar comparisons of the original and normalized response are illustrated.

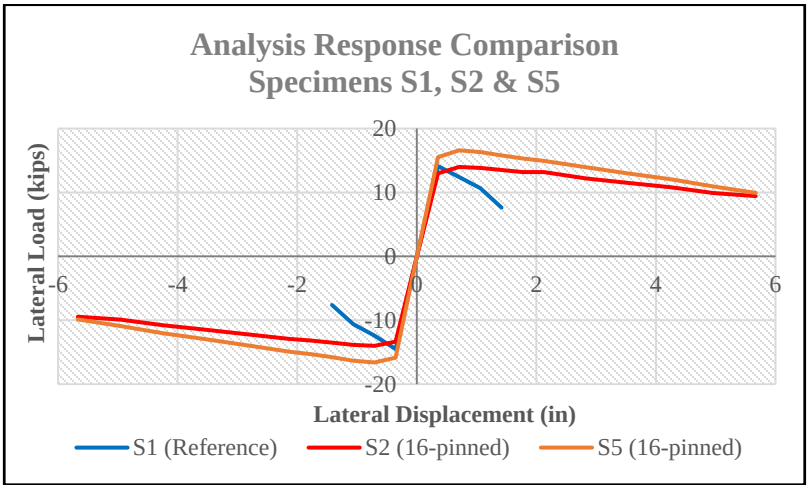

Figure 4.16: Analytical response comparison for specimens S1, S2 & S5

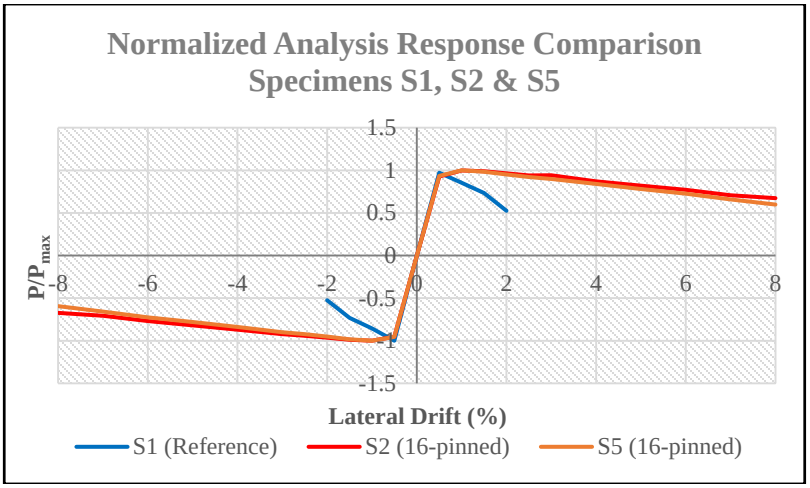

Figure 4.17: Analytical normalized response comparison for specimens S1, S2 & S5

The concrete strength and its effect on confinement provided by the FRP does not seem to affect significantly the analytical response, when the model of Lam and Teng (2003) is used. This is of a great interest because it agrees with the comments made in Chapter 2 about most of the design models used in practice; they cannot predict the behavior well if the concrete strength used is not in a certain range.

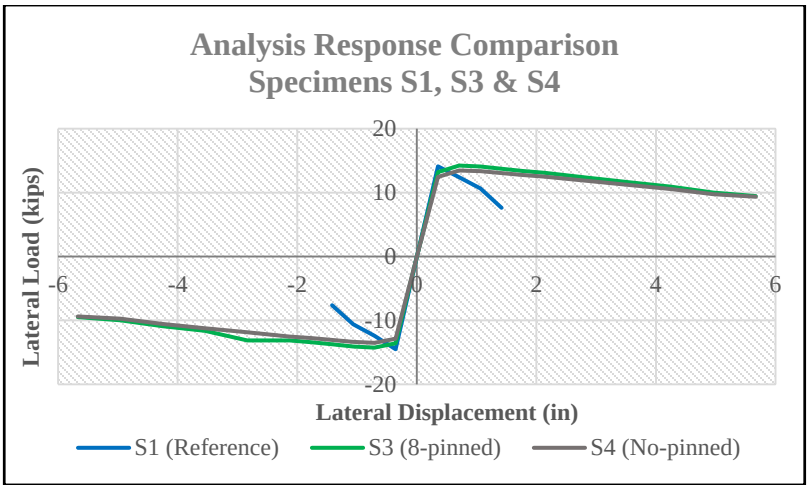

Figure 4.18: Analytical response comparison for specimens S1, S3 & S4

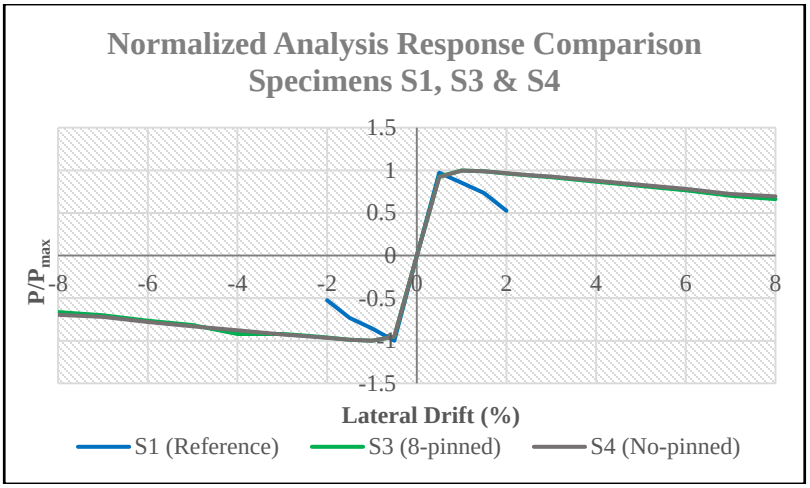

Figure 4.19: Analytical normalized response comparison for specimens S1, S3 & S4

The number of anchors is shown to highly affect the behavior (4.3.4.1) but this observation is not captured by the analysis. A modification to the current models seems reasonable and required. This becomes clearer in the figures with the normalized response.

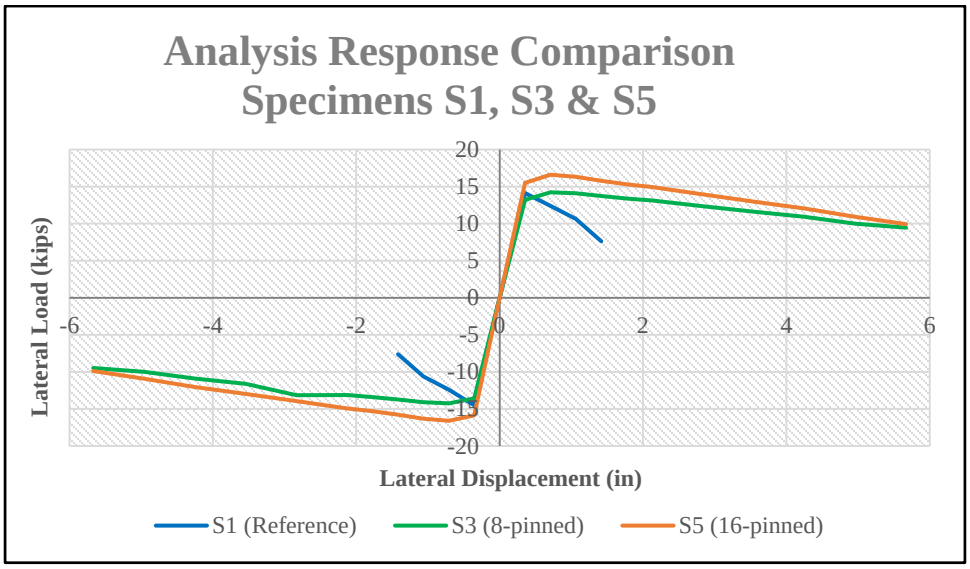

Figure 4.20: Analytical response comparison for specimens S1, S3 & S5

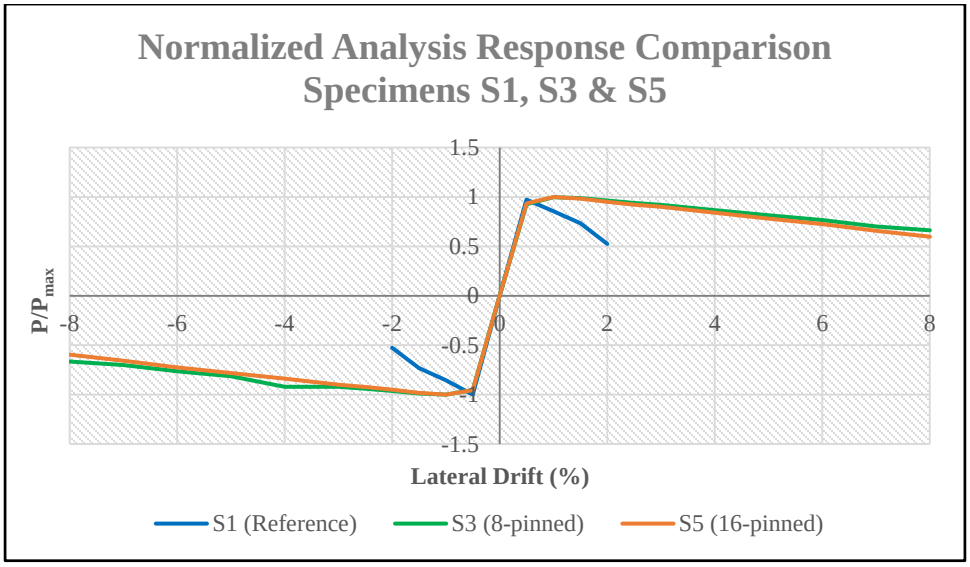

Figure 4.21: Analytical normalized response comparison for specimens S1, S3 & S5

Even though the anchors positively influenced the experimental response, the analytical model did not capture that influence.

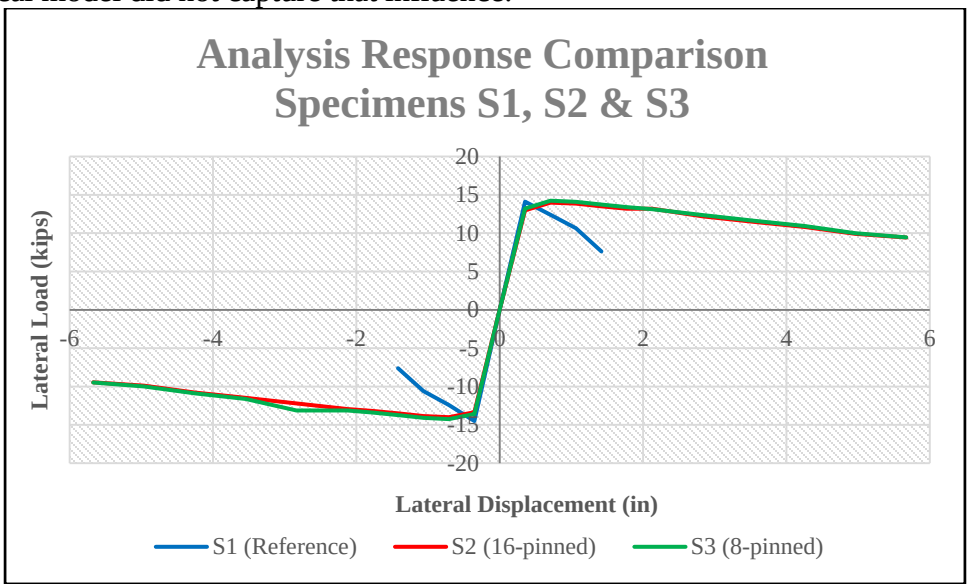

Figure 4.22: Analytical response comparison for specimens S1, S2 & S3

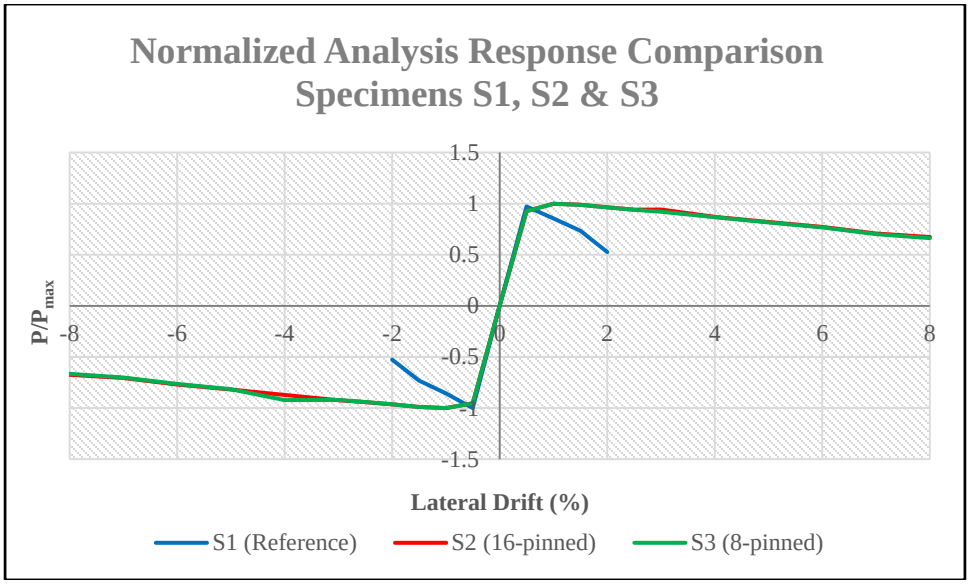

Figure 4.23: Analytical normalized response comparison for specimens S1, S2 & S3

4.3.4.3 Test-Analysis Response Comparison

This section includes the response comparisons for all the specimens. There are ten figures, each one of which compares the analytical with the experimental response (with and without normalization). It will be seen that the analysis overestimates the strength of the column in most of the cases. However, looking at the normalized responses one can realize that the analytical and the experimental responses are similar. This means that the post-peak behavior of the FRP material used was satisfactory. In addition, the experimental responses are terminated earlier than the analytical ones because the columns failed experimentally due to longitudinal bar buckling.

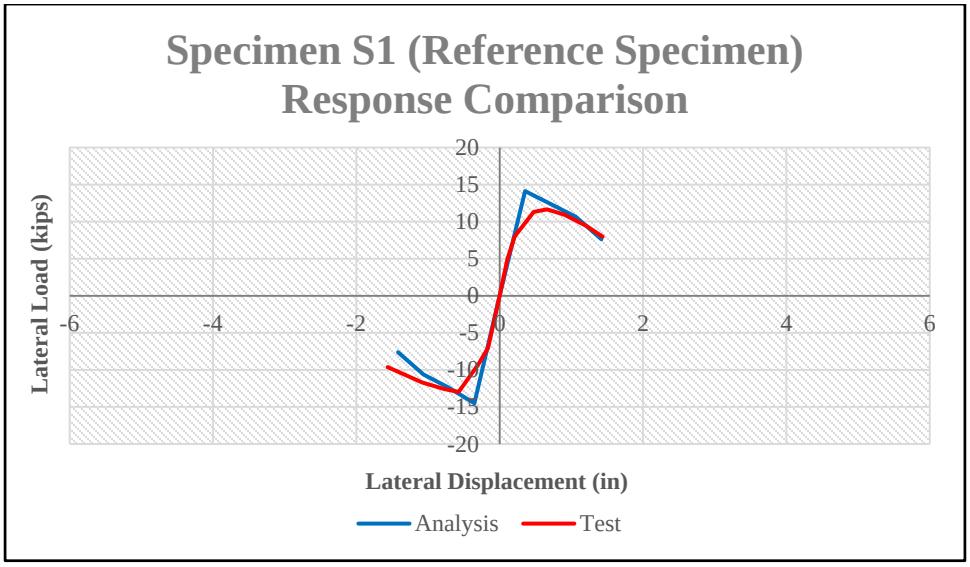

Figure 4.24: Test-Analysis response comparison for specimen S1

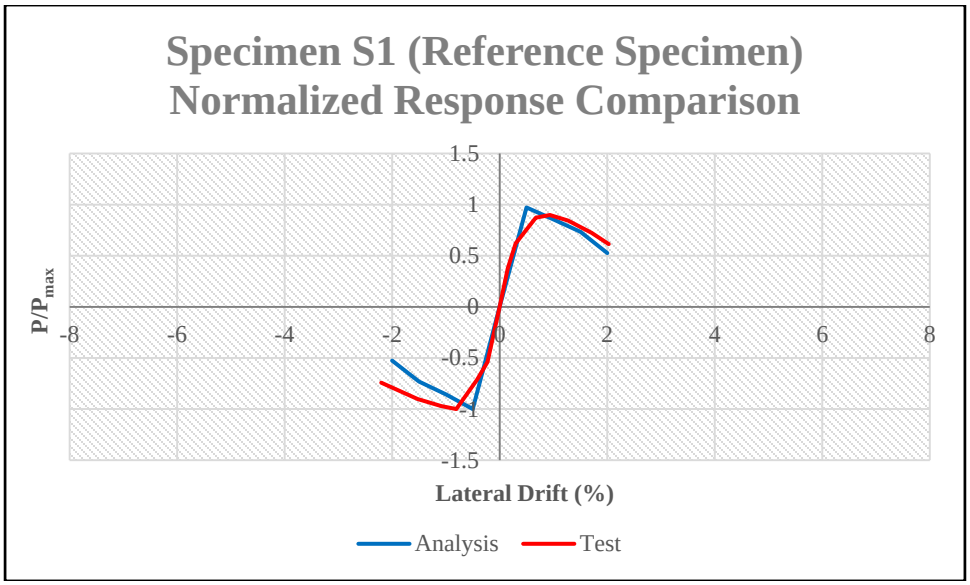

Figure 4.25: Test-Analysis normalized response comparison for specimen S1

Figure 4.26 and Figure 4.27 show the response of a 16-pinned column with concrete strength 1.45 ksi. Even though the normalized response comparison shows that

the post-peak curves are degrading in a similar manner, there is much difference in lateral load capacity.

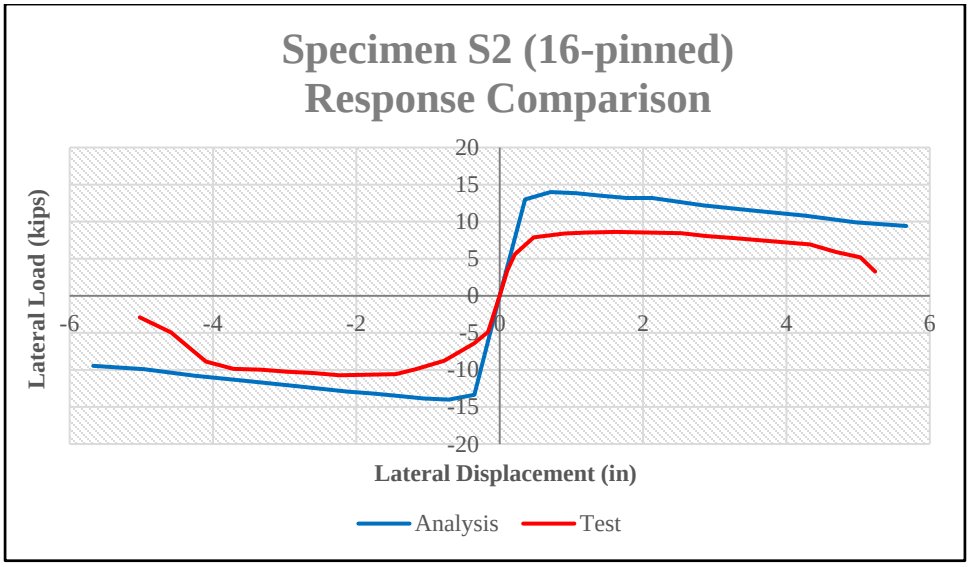

Figure 4.26: Test-Analysis response comparison for specimen S2

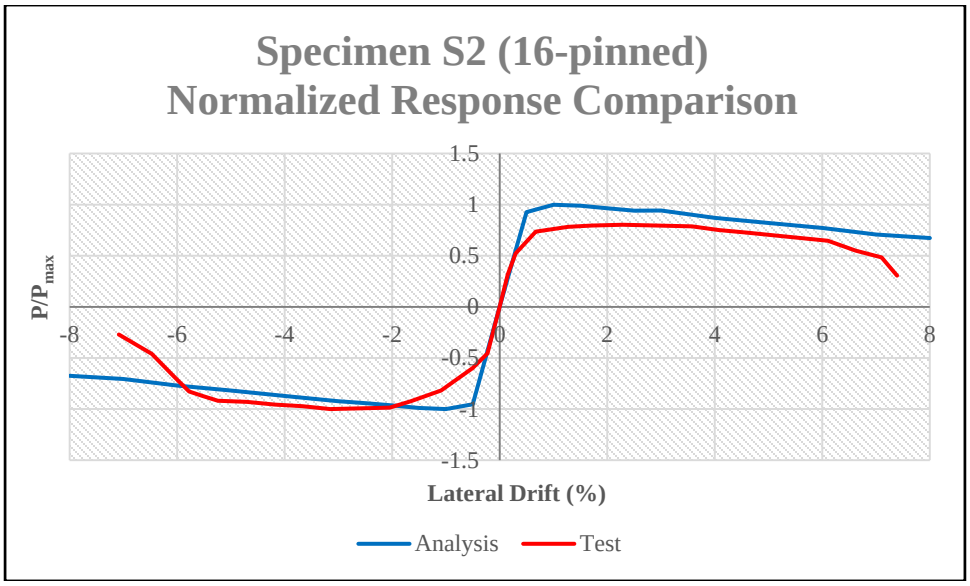

Figure 4.27: Test-Analysis normalized response comparison for specimen S2

Figure 4.28 and Figure 4.29 illustrate the premature failure of column S3 due to longitudinal bar buckling. Compared to column S2, the failure happened earlier and more suddenly.

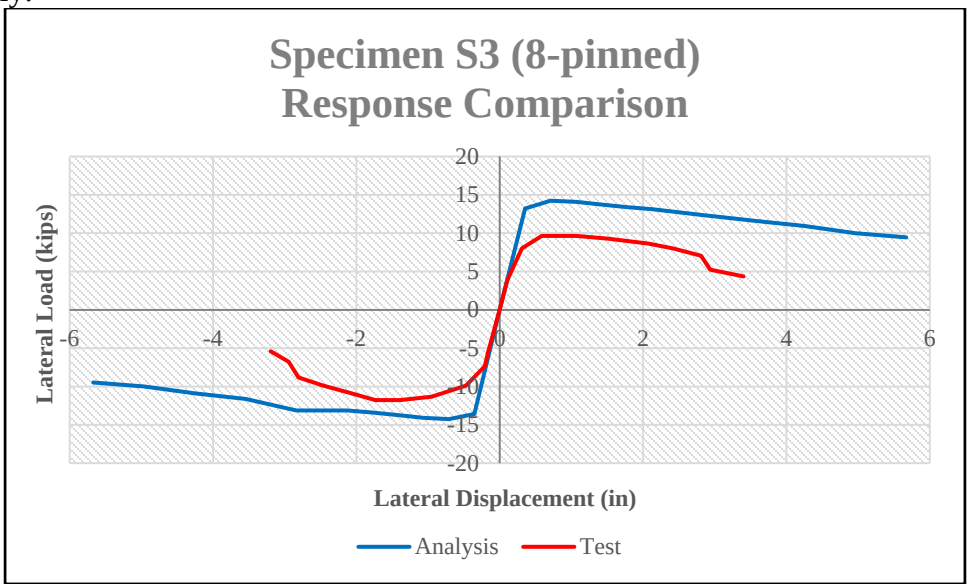

Figure 4.28: Test-Analysis response comparison for specimen S3

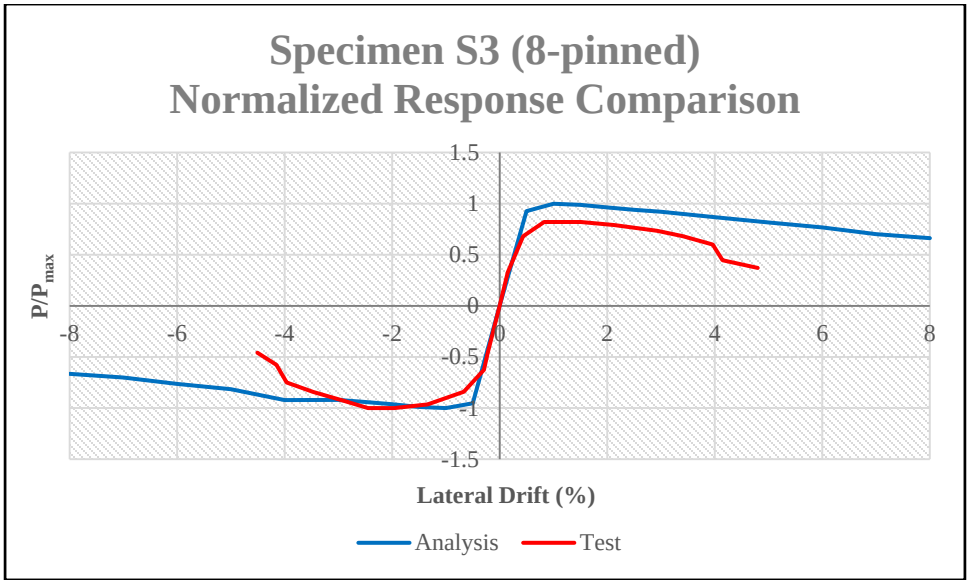

Figure 4.29: Test-Analysis normalized response comparison for specimen S3

Figure 4.30 and Figure 4.31 show that the specimen with no anchors experienced the poorest behavior in terms of ductility and ductility enhancement. However, the analysis model used (Lam and Teng 2003) does not take into account the anchors and shows no difference between the behavior prediction of an anchored and an unanchored column.

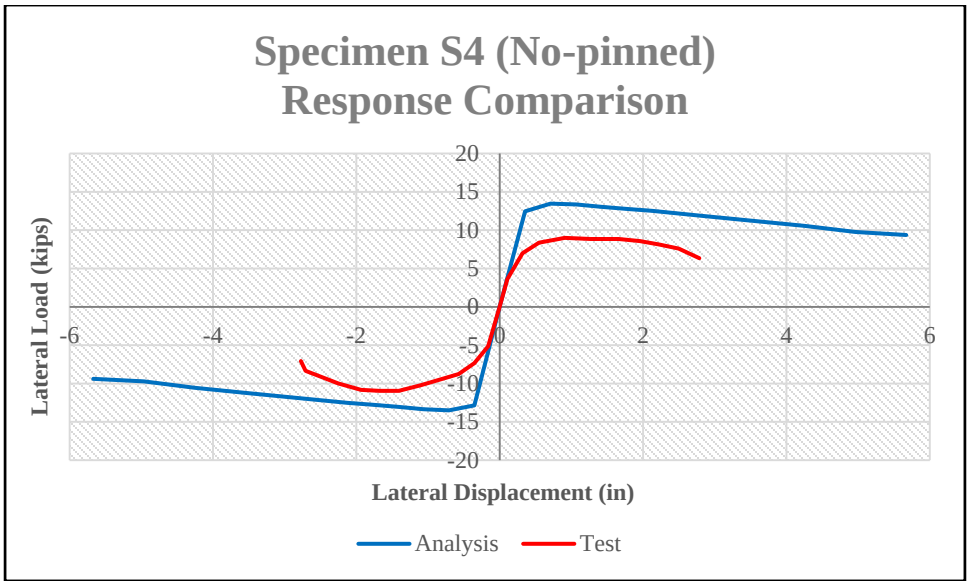

Figure 4.30: Test-Analysis response comparison for specimen S4

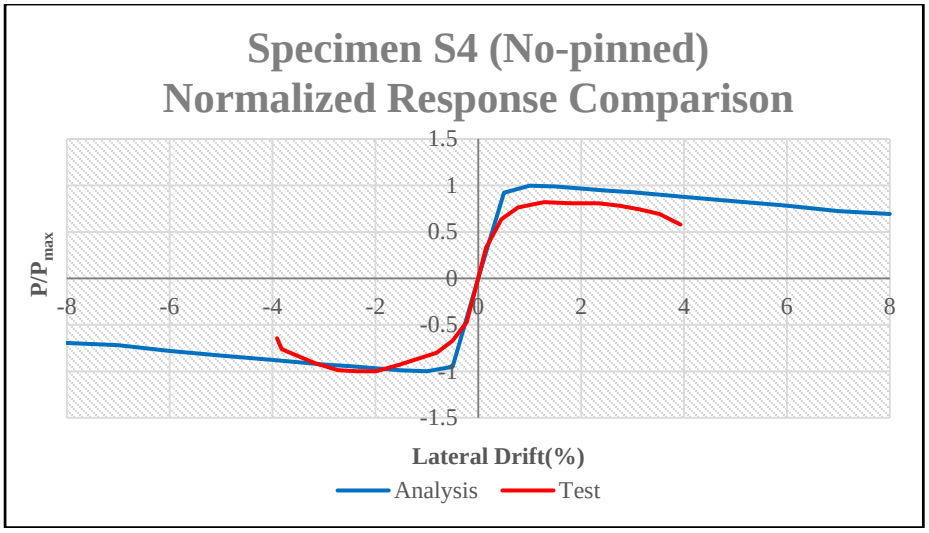

Figure 4.31: Test-Analysis normalized response comparison for specimen S4

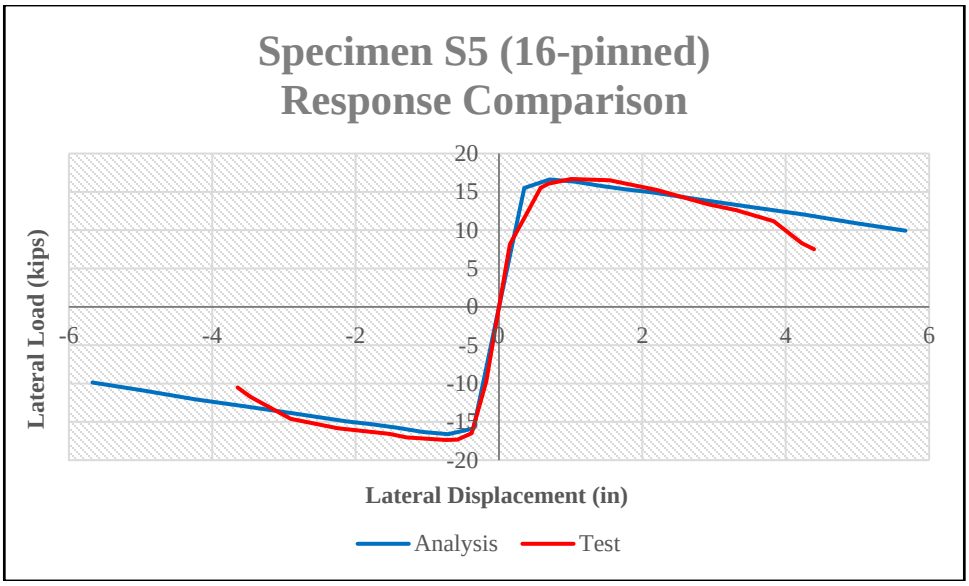

Figure 4.32: Test-Analysis response comparison for specimen S5

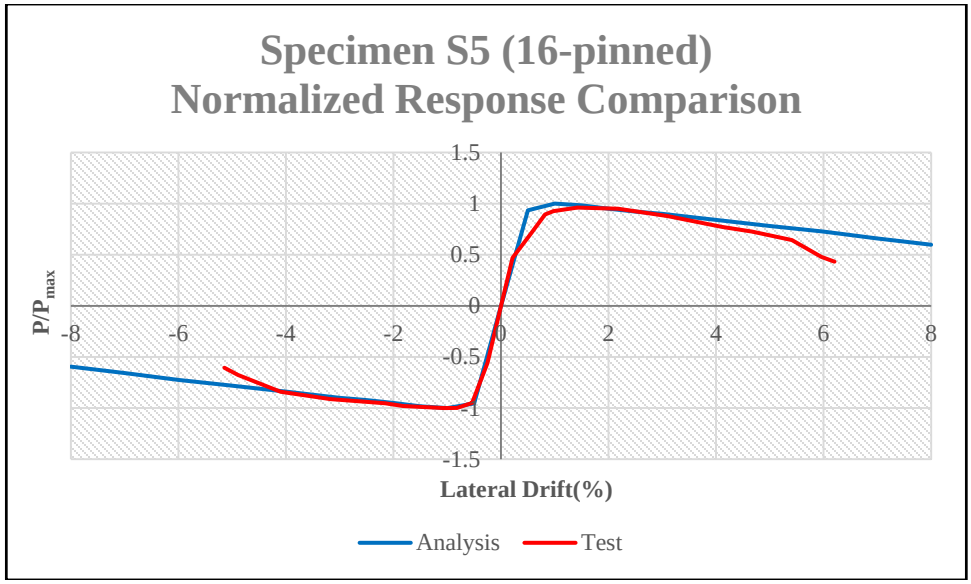

Figure 4.33: Test-Analysis normalized response comparison for specimen S5

The analysis overestimated the ductility and the lateral capacity of all the specimens except for specimen S5, the analysis response of which is acceptably close to the experimental one (Figure 4.32 and Figure 4.33). It should be noted that S5 is the only one that has a concrete strength close to the typical concrete used in practice, for which the models (for both unconfined and FRP-confined) were produced.

4.3.5 Type-2 Curves

The next figures show the FEMA 356 type-2 curves for the specimens of the experimental study of Ozcan et al. (2010). These curves provide typical force-deformation response for use in evaluation and rehabilitation of structures and are produced according to the information provided in Chapter 3. As explained before, similar curves should be produced for all the specimens with anchors found in the literature. Although the experimental data discussed in this study is limited, useful observations are made that agree with the suggestions of Kim (2008). More specifically, the observations in this study

strengthen the recommendations that a well-designed retrofitting system with both CFRP jackets and anchors proves to be sufficient to change the failure mode of the column and improve ductility.

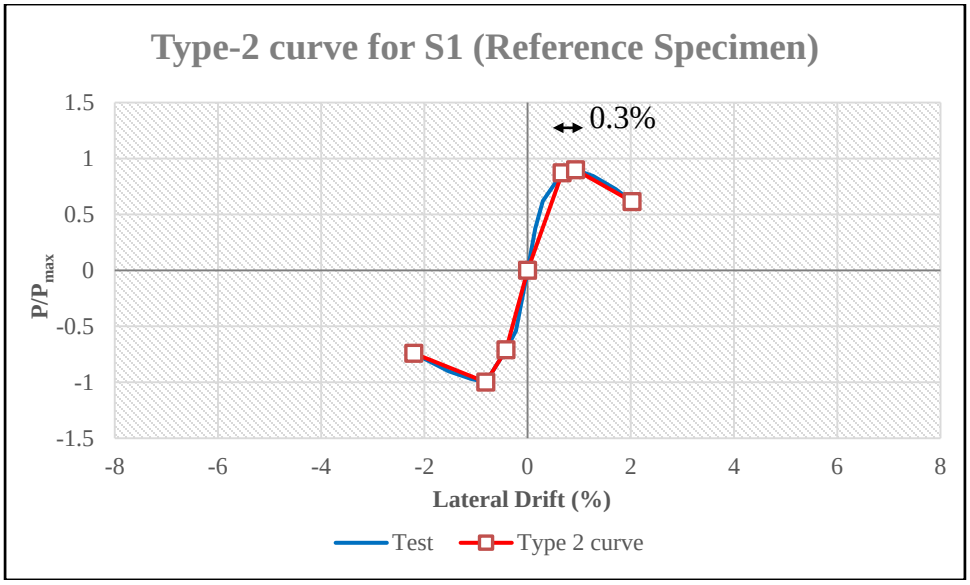

Figure 4.34: Type-2 curve for specimen S1 (Reference specimen)

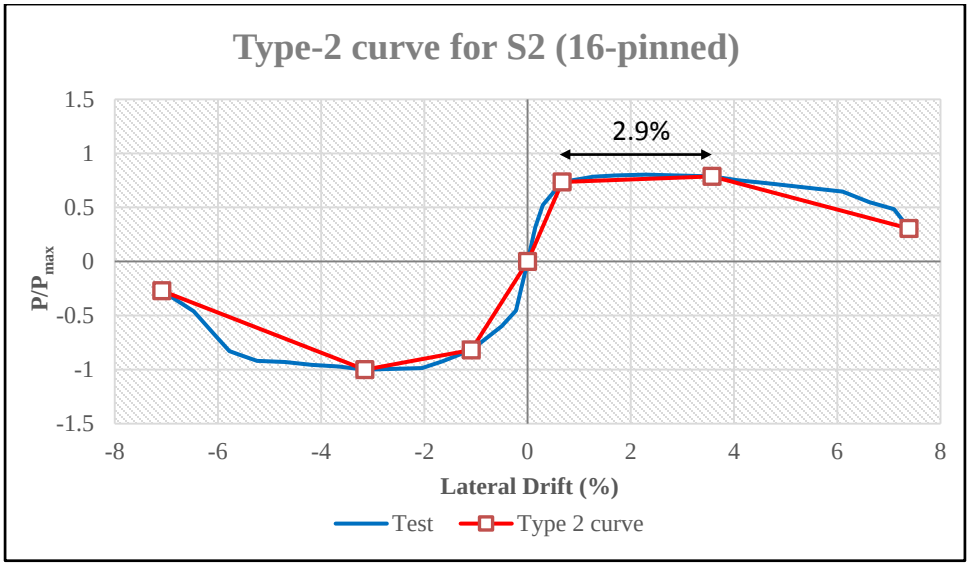

Figure 4.35: Type-2 curve for specimen S2 (16-pinned)

Figures from Figure 4.35 to Figure 4.38 show that the specimens with a few or no anchors (S3 and S4) exhibit less ductility than specimens with 16 anchors (S2 and S5). For all the curves the parameter “a” was calculated according to Figure 3.15, which for the 8-pinned and No-pinned specimens is around 1.0%.

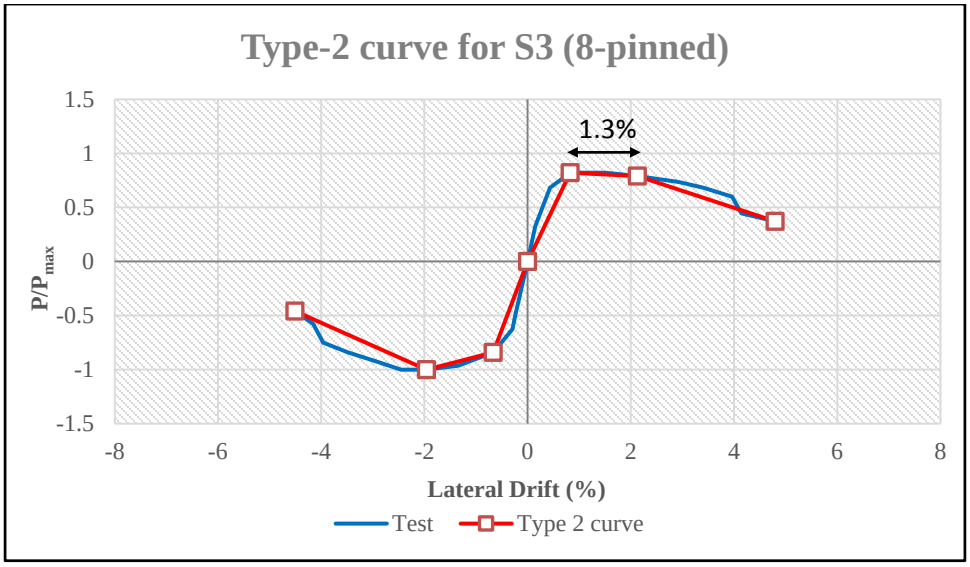

Figure 4.36: Type-2 curve for specimen S3 (8-pinned)

On the other hand, as shown in Figure 4.35 and Figure 4.38, the parameter “a” is from 2.0 to 3.0 % for the 16-pinned columns. This observation agrees well with Kim (2008), who reported that columns with adequate anchorage system can have behavior similar to well-confined as-built columns (with conforming transverse reinforcement according to FEMA 356). A component has conforming transverse reinforcement if hoops are spaced at not more than d/3 within the plastic hinge region (d is the depth of the cross-section).

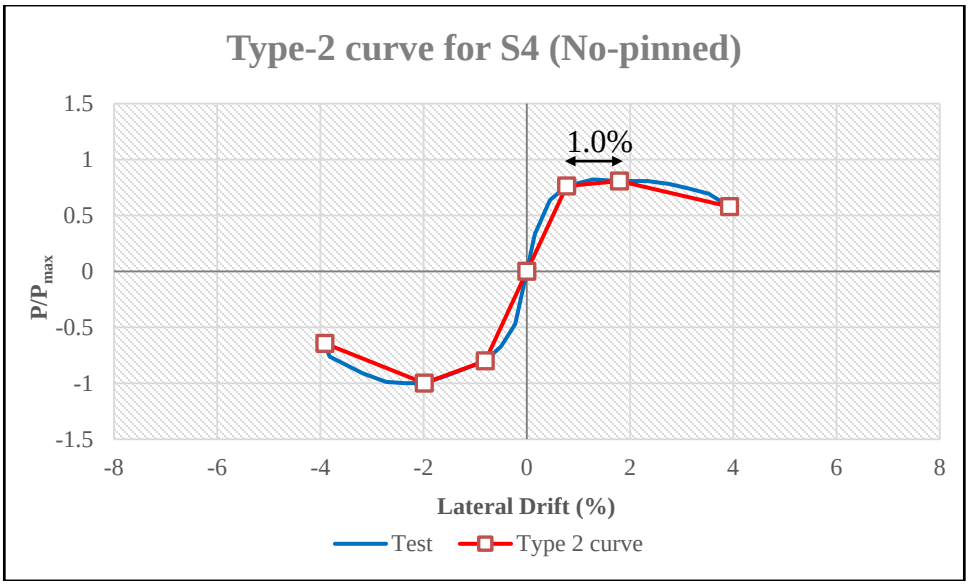

Figure 4.37: Type-2 curve for specimen S3 (No-pinned)

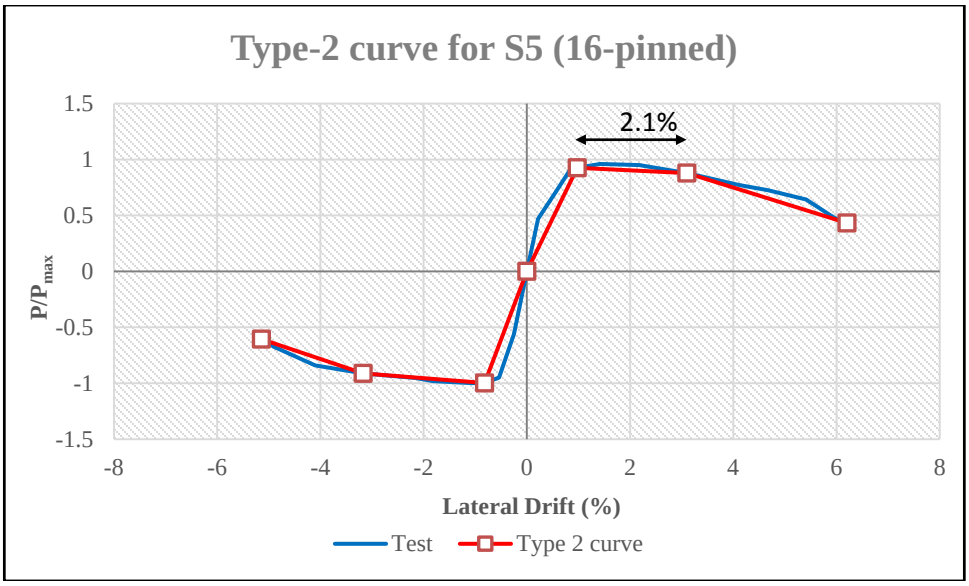

Figure 4.38: Type-2 curve for specimen S5 (16-pinned)

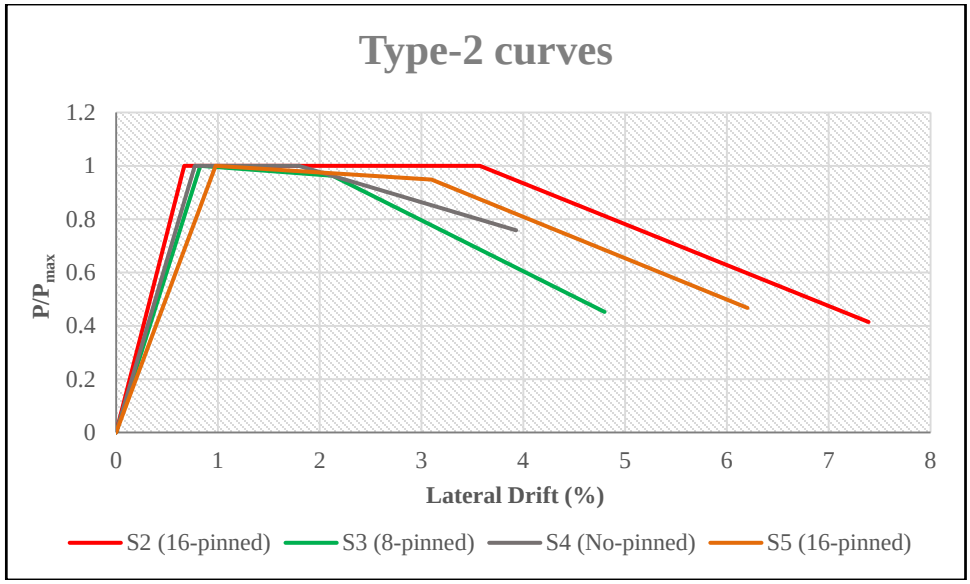

Figure 4.39: Type-2 curves for the retrofitted columns

Figure 4.39 shows that the inelastic region (plateau) before the start of the load degradation is larger for the columns with better anchorage system. In fact, the 16-pinned columns have about double the length of the plateau compared to the 8-pinned and No-pinned columns.

4.3.6 Discussion

The discussion of the results can be divided in three parts: the discussion of the experimental results, the comments on the analysis results and the comparison of the experimental and analytical results.

The main findings of the experimental study include the effect of confinement depending on the unconfined concrete strength and the configuration of the anchor dowels. It has been shown in the paper of Ozcan et al. (2010) that higher strength concrete columns dissipate less energy, because the ductility is decreased. This was one of the findings, presented in Chapter 2. However, poor concrete, as that used in the current study,

has a behavior that can be quite difficult to predict with current analytical procedures. It was shown that an adequate number of anchors can compensate for the negative effect of the large cross-sectional aspect ratio by delaying the rupture of the CFRP wrap and, consequently, the failure of the column. The anchors also have a positive effect on the strength enhancement. The strengthened specimens had better behavior than the reference specimen in terms of both strength and ductility. Finally, it is useful to note that the confinement ratio calculated by the authors for all the columns was above the limits that provide ascending post-peak response, or in other words sufficient confinement (see Chapter 2).

As described previously, the constitutive law used for the analysis of the FRP-confined concrete by Lam and Teng (2003) is commonly used. The analytical results, especially the normalized ones, show that the behavior of all the columns was estimated to be similar, even though different configurations of anchors were used and the concrete strength also varied. Thus, as stated in Chapter 2, current constitutive laws cannot successfully correlate column behavior with the concrete strength successfully. Judging by the results of Ozcan et al. (2010) and by other experimental results, one could say that the models should also be modified to account for the presence of anchor dowels. As explained in Chapter 3, many researchers agree that the behavior in such a case is very different.

The comparison between the test and analytical results showed that predicting the lateral load capacity of the first four specimens was difficult. For the reference specimen, the initial stiffness of both analytical and test response was the same and also the descending branch was almost identical. The difference was that the real specimen entered the inelastic region earlier than the analytical one. This could be attributed to the

unpredictable behavior of the poor concrete used. It is also worth noting that the poorest analytical response was for specimen S4, which had the lowest concrete strength and no anchors. However, if we compare the normalized responses (analytical and experimental), it can be seen that the analytical model reflects the degrading behavior very well, which means that the FRP-confined model has a post-peak ascending branch with a slope that agrees with the experimental results. Finally, the experimental response of specimen S5 was quite similar to the analytical one, which shows that the model by Lam and Teng (2003) could be applicable to typical concrete (2-6 ksi). Apart from that, all the specimens during the test failed because of longitudinal bar buckling at the base of the columns and this might be the reason why none of the columns agreed with the analytical results on the ultimate drift capacity. This is also indicated below. It is interesting that longitudinal bar buckling could be modeled in OpenSees using the *Reinforcing Steel* uniaxial material for the steel bars. This modeling procedure has been omitted as it exceeds the purpose of the present study.

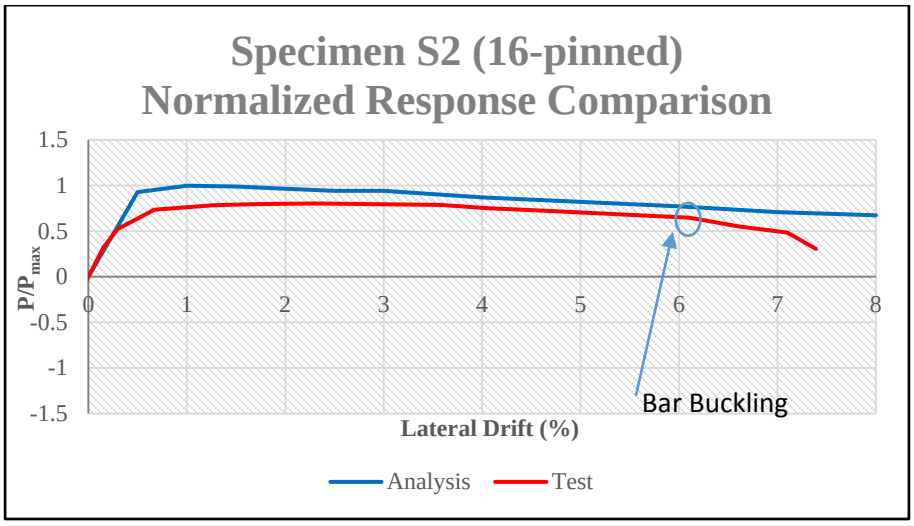

Figure 4.40: Test-Analysis normalized response comparison for specimen S2

In conclusion, this verification study produced some results that agree with the findings of Chapter 2, but more analytical results and comparisons with the respective experimental results are required. The analytical model that was used in this comparison (Lam and Teng 2003) exhibited deficiencies that are often encountered in most design models.

4.3.7 Example

4.3.7.1 Effect of Anchors on Confinement

It was shown before that the analytical response obtained with OpenSees was almost identical to the experimental response only for the specimen S5. For this reason, this specimen will be used as an example in this section. The effect of the anchors will be quantified according to Chapter 2, different solutions will be presented and the results will be discussed.

The use of anchors changes the effective confined area. For this reason the effective confined area will be calculated for several cases and the results will be compared. As explained by Wang and Restrepo (2001), the initial tangent slope in concrete arching θ has to be defined in order to calculate the effectively confined area, either steel or FRP as confining material is used. This angle relates to the concrete arching action onto the confined materials. In the model by Mander et al. (1988) for normal concrete confined by steel hoops, the arching angle (θ_s) is assumed equal to 45 degrees. Wang and

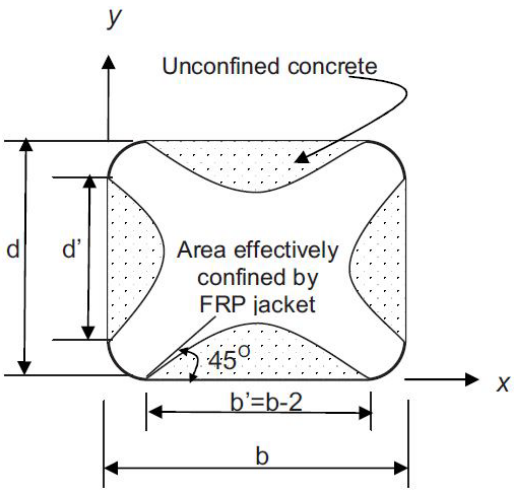

Figure 4.41: Arching action in square column

Restrepo (2001) proved experimentally that the arching angle for FRP jacketing is also 45 degrees, if the column is square.

Lam and Teng (2003) assumed that for rectangular columns, this angle (θ_j) increases when the length of a side decreases. This is the reason why they introduced the factors (h/b) and (b/h) in front of the ineffectively confined areas $w_i^2/6$, or similarly $(h-2r)^2/6$ and $(b-2r)^2/6$ in the following expression:

$$k_h = \frac{A_{eff}}{A_c} = \frac{1 - \frac{\left(\left(\frac{b}{h}\right)(h-2r)^2 + \left(\frac{h}{b}\right)(b-2r)^2\right)}{3A_g} - \rho_{sc}}{1-\rho_{sc}}$$

While this assumption seems reasonable, there is little experimental evidence to support that it is accurate. Furthermore, when the anchor dowels are added, concrete arching is completely different and thus the geometry is complicated further. For this reason, the results using both theories will be presented in this study and the actual difference will be illustrated with this example. Table 4.3 shows the increase in the effectively confined area, the strength and deformability enhancement, when anchors are implemented in the calculations. The number of anchors indicates the number of anchors used in the long side of the column. Again, the calculations are made for specimen S5, which is the reference specimen in this example, because of its accurate agreement with experimental results.

Table 4.3: Effect of anchor dowels in confinement of specimen S5

θ_j according to Lam&Teng						
Number of Anchors	A_{eff}/A_c	Relative Increase (%)	f'_{cc}/f'_c	Increase to f'_{cc}/f'_c (%)	$\varepsilon_{cu}/\varepsilon_{co}$	Increase to $\varepsilon_{cu}/\varepsilon_{co}$ (%)
0	0.58		1.06		4.58	
1	0.71	21.4	1.07	1.2	5.19	13.3
2	0.75	5.9	1.08	0.4	5.39	3.9
θ_j=45 degrees, as in Steel-Confined Concrete						
Number of Anchors	A_{eff}/A_c	Relative Increase (%)	f'_{cc}/f'_c	Increase to f'_{cc}/f'_c (%)	$\varepsilon_{cu}/\varepsilon_{co}$	Increase to $\varepsilon_{cu}/\varepsilon_{co}$ (%)
0	0.43		1.04		3.85	
1	0.67	56.4	1.07	2.4	5.03	30.7
2	0.76	12.0	1.08	0.8	5.43	7.8

When θ_j is taken as 45 degrees, the effectively confined area and, consequently, the strength and deformability enhancement, increases more rapidly. The sides of the unconfined areas are much shorter after the addition of the anchors. This is illustrated in Figure 4.42.

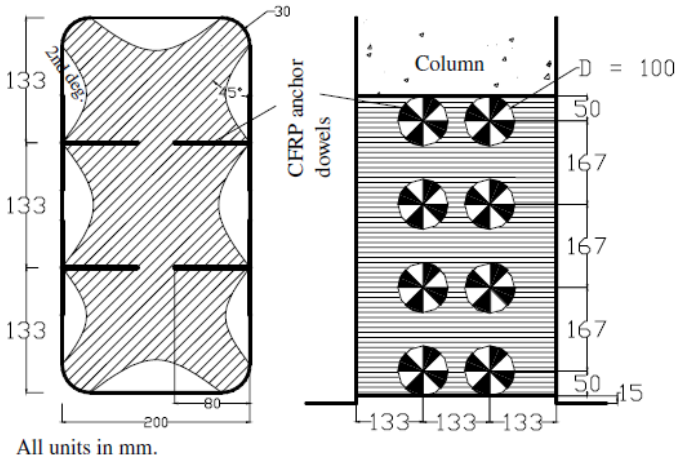

Figure 4.42: Concrete arching action for 16-pinned type anchor configuration

Additionally, it has been shown by way of experimental results that the increase in ductility is typically much more significant than the increase in strength. As was shown in the section 4.3.4.1 the specimens that had more anchors did not perform significantly better in terms of lateral load capacity than others, but were more ductile. This behavioral trend is shown in Figure 4.43, where S2 and S4 have similar concrete but S2 has anchors while S4 does not.

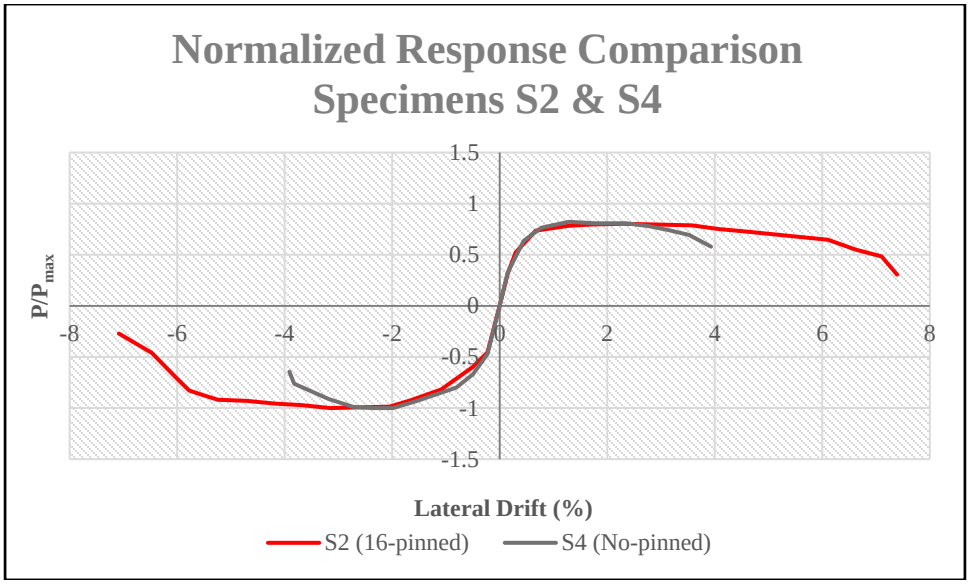

Figure 4.43: Experimental normalized response comparison for specimens S2 & S4

The question is whether the analytical model presented in the previous section can show the difference that was found in the experiments. The stress-strain model of Lam and Teng (2003) cannot be changed much to account for the presence of anchors, apart from changing f'_{cc} and ε_{cu}. In Figure 4.44, the constitutive laws for strengthened and unstrengthened, and anchored and unanchored, are compared. As a result, the envelope of

the analytical response with FRP confinement will not be much different with or without anchors.

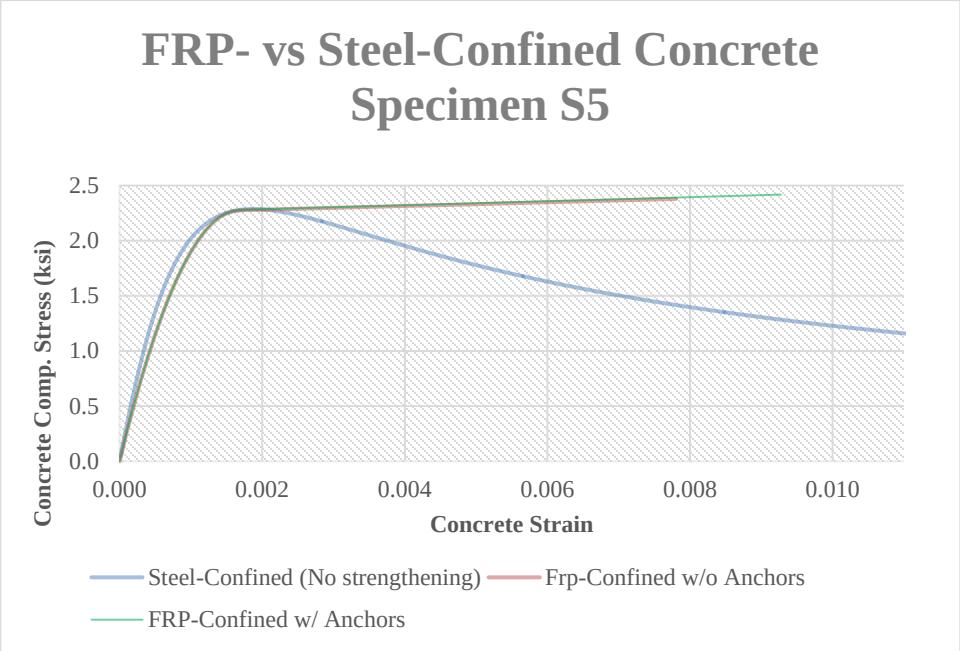

Figure 4.44: Constitutive law for FRP- and steel-confined concrete of specimen S5

Next, the analysis results are presented in Figure 4.45. As expected, the actual effect on the ductility cannot be examined here because the columns in the analysis did not fail before 8% drift was reached. That happens because of the low-strength concrete used, which has high deformability compared to higher-strength concrete and in the actual test the specimens failed due to longitudinal bar buckling which was not considered in the analysis.

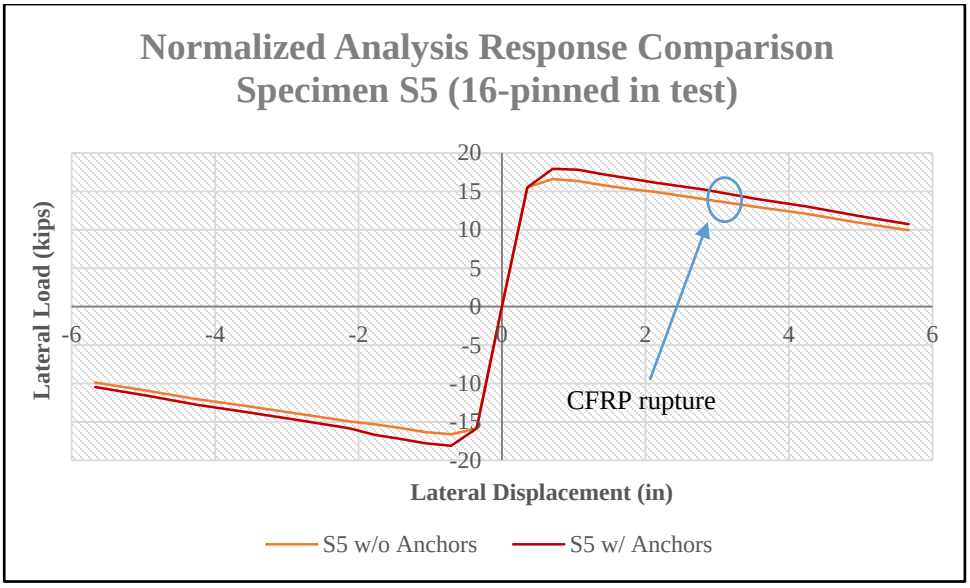

Figure 4.45: Analytical normalized response for S5 with and without anchors

Failure of FRP-wrapped columns initiates by way of column-base interface cracking and then the longitudinal bar yielding. Next, there is some debonding between the FRP wrap and the concrete column and, at some point, the FRP wrap ruptures. Post-peak response deterioration depends on the concrete. In the analysis of specimen S5, the failure of the CFRP occurred at around 4% drift, or 3 in. displacement (3.3% drift in the test). After this point it is estimated that the behavior of the anchored column and the one without anchors is quite similar.

4.3.7.2 Effect of Anchors on Minimum Required Thickness

As described in Chapter 2, the minimum FRP material needed to achieve sufficient confinement is of great interest. Table 4.4 shows the minimum CFRP thickness for specimen S5 according to each theory. Again, it has been shown that the criterion by Hu (2013) tends to be very accurate, especially for circular columns. However, as it is shown in the table, the criteria seem to be very conservative for this column (S5). In fact, this

column performed well in terms of both strength and ductility terms even though, according to some researchers, it should be designed with more CFRP material. It is clear that the cross-sectional aspect ratio is dominant in these equations and this is the reason why most of the criteria suggest that more CFRP layers should have been used. For example, the criterion by Hu (2013) suggests that 5 plies of the CFRP wrap should have been used. In summary, the positive effect of the presence of anchors should be included in these equations for more efficient design of the retrofit.

Table 4.4: Minimum thickness required for specimen S5

Criterion	**$t_{j,min}$ Expression**	**$t_{j,min}$**	**$t_{j,min}/t_{j,used}$ ($t_{j,used}$=0.0065'')***	**Parameters**
Mirmiran et al. (1998)	$0.15(D/2r)Df'_c/2f_{fu}$	0.059	9.08	r: corner radius D: equivalent diameter f_{fu}: effective tensile strength of FRP k_h: shape factor ρ_f: volumetric ratio of FRP to concrete λ: parameter to account for FRP stiffness
Lam & Teng (2003)	$0.07Df'_c/2f_{fu}k_h$	0.005	0.76	
Wu et al. (2007)	$\lambda Df'_c/2f_{fu}$	0.011	1.62	
Pantelides & Yan (2007)	$0.2Df'_c/2f_{fu}$	0.011	1.62	
Wei et al. (2008)	$0.1bhf'_c/(b+h)f_{fu}k_h$	0.004	0.65	
Hu (2013)	$0.11(D/2r)^{0.80}Df'_c/2f_{fu}$	0.029	4.45	

*Equivalent to how many plies should have been used.

Chapter 5: Summary, Conclusions and Recommendations

5.1 Summary and Conclusions

The review of the literature showed that all the parameters that affected the behavior of a strengthened column are not incorporated in any stress-strain model of confined concrete. Thus, the models found in the literature are useful for only a small category of specimens, as is usually specified in the respective paper. In addition, the review of the usefulness of FRP anchors in particular showed that such anchors are quite reliable. Anchorage systems seem to be essential for column retrofit, especially for columns with high cross-sectional aspect ratio.

A method was proposed for quantification of the benefits of anchors. This method seems to predict reasonably well the effectiveness of FRP anchors, as shown with extensive analysis of a column that was tested. There is a need for more specimens to be tested and studied in order to extend the conclusions.

The widely used model of Lam and Teng (2003) demonstrated certain deficiencies in predicting the behavior of most of the specimens of Ozcan et al. (2010). However, it predicted well the behavior of one of the specimens, a fact that strengthens the statement that the stress-strain models found in the literature are sufficiently precise only for a specific type of specimens. For example, some of the models are proper for square columns, some other only for concrete of a specific range of strength and so on. In addition, most of the criteria for selection of the thickness of the FRP jacket were found to be very conservative.

Last but not least, the statement of Kim (2008) was verified: If a rectangular column is strengthened with the appropriate FRP materials and anchorage system, its behavior can be classified as well-confined.

5.2 RECOMMENDATIONS

A method proposed for considering the presence of anchors gives reasonable results. The reasons why FRP anchors are useful was explained. A recommendation would be to use the current stress-strain models for assessment of the behavior of a rectangular column and modify the effectiveness of the jacket to reflect the presence of anchors.

In addition, the criterion of Hu (2013) seems to be reasonable for selecting the required thickness of the jacket and is on the conservative side. This criterion could be similarly modified to accommodate the inclusion of an anchorage system. Finally, the use of anchorage systems should be incorporated in the design guidelines as a mandatory addition to retrofitting columns with high aspect ratio or large columns. The specification of which aspect ratio is considered high and what size makes the column to be specified as large needs further investigation. In the present study, columns with aspect ratio up to 2.0 and face of the large side up to 16 in. were investigated.

5.3 FUTURE RESEARCH

- Further research is needed on the role of section aspect ratio and on the effect of column size. Such a study would require experimental work with several shapes and sizes with and without anchors.
- The response of all specimen reported in the literature should be classified according to the prevailing rules for modeling columns in evaluation or rehabilitation design of deficient structures.
- Design recommendations for FRP anchors should be revisited. Number of anchors, maximum spacing of anchors in the horizontal and vertical direction of the column are some of the parameters that should be investigated. This would probably

include both experimental and analytical work, as the current models should be developed to accommodate the presence of anchors in a more precise way.

Bibliography

Al-Salloum, Y. A. (2007). "Influence of edge sharpness on the strength of square concrete columns confined with FRP composite laminates." Composites Part B: Engineering **38**(5): 640-650.

Benzaid, R. and H. A. Mesbah (2013). Circular and Square Concrete Columns Externally Confined by CFRP Composite: Experimental Investigation and Effective Strength Models, INTECH.

Bisby, L., et al. (2012). "Effects of unconfined concrete strength on FRP confinement on concrete."

Brigante, D. (2013). NEW COMPOSITE MATERIALS, Springer.

Campione, G. and N. Miraglia (2003). "Strength and strain capacities of concrete compression members reinforced with FRP." Cement and concrete composites **25**(1): 31-41.

Chaallal, O., et al. (2003). "Confinement model for axially loaded short rectangular columns strengthened with fiber-reinforced polymer wrapping." ACI Structural Journal **100**(2).

Chaallal, O., et al. (2003). "Performance of axially loaded short rectangular columns strengthened with carbon fiber-reinforced polymer wrapping." Journal of Composites for Construction **7**(3): 200-208.

Chang, G. A. and J. B. Mander (1994). "Seismic energy based fatigue damage analysis of bridge columns: part 1-evaluation of seismic capacity."

Chen, J., et al. (2011). "FRP rupture strains in the split-disk test." Composites Part B: Engineering **42**(4): 962-972.

Council, B. S. S. (2000). "Prestandard and commentary for the seismic rehabilitation of buildings." Report FEMA-356, Washington, DC.

Csuka, B. and L. P. Kollár (2012). "Fiber-reinforced plastic-confined rectangular columns subjected to axial loading." Journal of Reinforced Plastics and Composites **31**(7): 481-493.

Fardis, M. N. and H. H. Khalili (1982). "FRP-encased concrete as a structural material." Magazine of Concrete Research **34**(121): 191-202.

Faustino, P., et al. (2014). "Design model for square RC columns under compression confined with CFRP." Composites Part B: Engineering **57**: 187-198.

Galal, K., et al. (2005). "Retrofit of RC square short columns." Engineering Structures **27**(5): 801-813.

GangaRao, H. V., et al. (2006). Reinforced concrete design with FRP composites, CRC press.

Ghobarah, A. and K. E. Galal (2004). "Seismic rehabilitation of short rectangular RC columns." Journal of earthquake engineering **8**(01): 45-68.

Harajli, M. H. (2006). "Axial stress–strain relationship for FRP confined circular and rectangular concrete columns." Cement and concrete composites **28**(10): 938-948.

Hassan, M. and O. Chaallal (2007). "Fiber-reinforced polymer confined rectangular columns: assessment of models and design guidelines." ACI Structural Journal **104**(6).

Hu, B. (2013). "An improved criterion for sufficiently/insufficiently FRP-confined concrete derived from ultimate axial stress." Engineering Structures **46**: 431-446.

Ilki, A., et al. (2008). "FRP retrofit of low and medium strength circular and rectangular reinforced concrete columns." Journal of Materials in Civil Engineering **20**(2): 169-188.

Kim, I. (2008). "Use of CFRP to provide continuity in existing reinforced concrete members subjected to extreme loads."

Kim, I., et al. (2011). "Use of carbon fiber-reinforced polymer anchors to repair and strengthen lap splices of reinforced concrete columns." ACI Structural Journal **108**(5).

Kim, S. and S. T. Smith (2009). "Behaviour of handmade FRP anchors under tensile load in uncracked concrete." Advances in Structural Engineering **12**(6): 845-865.

Koksal, H. O. and B. Doran (2011) Stress–strain model for fibre-reinforced polymer confined rectangular columns. Proceedings of the ICE - Structures and Buildings **164**, 391-408

Lam, L. and J. Teng (2003). "Design-oriented stress-strain model for FRP-confined concrete in rectangular columns." Journal of Reinforced Plastics and Composites **22**(13): 1149-1186.

Li, Y. (2004). Design of retrofitting FRP for concrete columns. Master Thesis at University of Toronto.

Lowes, L. N., et al. (2003). A beam-column joint model for simulating the earthquake response of reinforced concrete frames, Pacific Earthquake Engineering Research Center, College of Engineering, University of California.

Maalej, M., et al. (2003). "Modelling of rectangular RC columns strengthened with FRP." Cement and concrete composites **25**(2): 263-276.

Mandal, S., et al. (2005). "Influence of concrete strength on confinement effectiveness of fiber-reinforced polymer circular jackets." ACI Structural Journal **102**(3).

Mander, J. B., et al. (1988). "Theoretical stress-strain model for confined concrete." Journal of Structural Engineering **114**(8): 1804-1826.

Mazzoni, S., et al. (2006). "OpenSees command language manual." Pacific Earthquake Engineering Research (PEER) Center.

Mirmiran, A. and M. Shahawy (1997). "Behavior of concrete columns confined by fiber composites." Journal of Structural Engineering **123**(5): 583-590.

Mirmiran, A., et al. (1998). "Effect of column parameters on FRP-confined concrete." Journal of Composites for Construction **2**(4): 175-185.

Montuori, R., et al. (2012). "Comparative analysis and critical issues of the main constitutive laws for concrete elements confined with FRP." Composites Part B: Engineering **43**(8): 3219-3230.

Montuori, R., et al. (2013). "Ultimate behaviour of FRP wrapped sections under axial force and bending: Influence of stress–strain confinement model." Composites Part B: Engineering **54**: 85-96.

Ozcan, O., et al. (2010). "Seismic strengthening of rectangular reinforced concrete columns using fiber reinforced polymers." Engineering Structures **32**(4): 964-973.

Ozdemir, G. and U. Akyuz (2006). Tensile Capacities of CFRP Anchors. Advances in Earthquake Engineering for Urban Risk Reduction, Springer**:** 471-487.

Pantelides, C. P. and D. A. Moran (2012). "Design of FRP jackets for plastic hinge confinement of RC columns." Journal of Composites for Construction **17**(4): 433-442.

Pantelides, C. P. and Z. Yan (2007). "Confinement model of concrete with externally bonded FRP jackets or posttensioned FRP shells." Journal of Structural Engineering **133**(9): 1288-1296.

Pellegrino, C. and C. Modena (2010). "Analytical model for FRP confinement of concrete columns with and without internal steel reinforcement." Journal of Composites for Construction **14**(6): 693-705.

Pham, T. M. and M. N. Hadi (2013). "Stress prediction model for FRP confined rectangular concrete columns with rounded corners." Journal of Composites for Construction **18**(1).

Seible, F., et al. (1997). "Seismic retrofit of RC columns with continuous carbon fiber jackets." Journal of Composites for Construction **1**(2): 52-62.

Smith, S. T. (2009). "FRP anchors: recent advances in research and understanding." Proceedings of the 2nd APFIS: 35-44.

Spoelstra, M. and G. Monti (1999). "FRP-Confined Concrete Model." Journal of Composites for Construction **3**(3): 143-150.

Tahir, M. F., et al. (2013). "Design Guidelines Review for CFRP Confinement of Plain and Reinforced Concrete Square Columns." Life Science Journal **10**(12s).

Toutanji, H., et al. (2009). "Behavior of large-scale rectangular columns confined with FRP composites." Journal of Composites for Construction **14**(1): 62-71.

Wang, C. Y. and I. J. Restrepo (2001). "Investigation of Concentrically Loaded Reinforced Concrete Columns Confined with Glass Fiber-Reinforced Polymer Jackets." ACI Structural Journal **98**(3).

Wang, L.-M. and Y.-F. Wu (2008). "Effect of corner radius on the performance of CFRP-confined square concrete columns: Test." Engineering Structures **30**(2): 493-505.

Wei, Y., et al. (2008). "Study on the stress-strain relationship for insufficient FRP-confined rectangular concrete columns." China Civil Engineering Journal **3**.

Wu, G., et al. (2006). "Strength and ductility of concrete cylinders confined with FRP composites." Construction and building materials **20**(3): 134-148.

Wu, Y.-F., et al. (2006). "Fundamental principles that govern retrofitting of reinforced concrete columns by steel and FRP jacketing." Advances in Structural Engineering **9**(4): 507-533.

Wu, Y.-F., et al. (2008). "Experimental investigation on seismic retrofitting of square RC columns by carbon FRP sheet confinement combined with transverse short glass FRP bars in bored holes." Journal of Composites for Construction **12**(1): 53-60.

Wu, Y.-F. and Y.-Y. Wei (2010). "Effect of cross-sectional aspect ratio on the strength of CFRP-confined rectangular concrete columns." Engineering Structures **32**(1): 32-45.

Yang, X., et al. (2004). "Shape effect on the performance of carbon fiber reinforced polymer wraps." Journal of Composites for Construction **8**(5): 444-451.

Youssef, M. N. (2003). Stress-strain model for concrete confined by FRP composites. Ann Arbor, University of California, Irvine. **3078792:** 310-310 p.

Youssef, M. N., et al. (2007). "Stress–strain model for concrete confined by FRP composites." Composites Part B: Engineering **38**(5): 614-628.

Zhang, H. and S. T. Smith (2012). "FRP-to-concrete joint assemblages anchored with multiple FRP anchors." Composite Structures **94**(2): 403-414.

Zhang, H., et al. (2012). "Optimisation of carbon and glass FRP anchor design." Construction and building materials **32**: 1-12.

Vita

Apostolos Psaros Andriopoulos was born in Rhodes, Greece on December 19, 1990 to Filimon Psaros and Despoina Andriopoulou. After graduating from College of Rhodes, he attended University of Patras in Greece, receiving a Master of Engineering in July, 2013. In August, 2013, he entered the Graduate School at The University of Texas at Austin. He received his Master of Science in Structural Engineering degree in May, 2015.

Email address: afpsaros@gmail.com

This thesis was typed by the author.